ARIZONA DEPARTMENT OF TRANSPORTATION

REPORT NUMBER: FHWA-AZ91-349

HYDRAULIC MODELING OF ALLUVIAL FANS USING DAMBRK (NWS COMPUTER MODEL)

Final Report

Prepared by:
Hasan Mushtaq
L.W. Mays, Ph.D.
Department of Civil Engineering
College of Engineering and Applied Sciences
Arizona State University
Tempe, Arizona 85287-6306

February 1991

Prepared for:
Arizona Department of Transportation
206 South 17th Avenue
Phoenix, Arizona 85007
in cooperation with
U.S. Department of Transportation
Federal Highway Administration

The contents of this report reflect the views of the authors who are responsible for the facts and the accuracy of the data presented herein. The contents do not necessarily reflect the official views or policies of the Arizona Department of Transportation or the Federal Highways Administration. This report does not constitute a standard, specification, or regulation. Trade or manufacturer's names which may appear herein are cited only because they are considered essential to the objectives of the report. The U.S. Government and the State of Arizona do not endorse products or manufacturers.

Technical Report Documentation Page

1. Report No. FHWA-AZ91-349	2. Government Accession No.	3. Recipient's Catalog No.
4. Title and Subtitle Hydraulic Modeling of Alluvial Fans Using DAMBRK (NWS Computer Model)		5. Report Date February, 1991
		6. Performing Organization Code
7. Author (s) Hasan Mushtaq, Dr. L. W. Mays		8. Performing Organization Report No.
9. Performing Organization Name and Address Department of Civil Engineering, Arizona State University, Tempe, AZ 85287-5306		10. Work Unit No.
		11. Contract or Grant No. HPR-PL-1(37) ITEM 349
12. Sponsoring Agency Name and Address ARIZONA DEPARTMENT OF TRANSPORTATION, 206 S. 17TH AVENUE, PHOENIX, ARIZONA 85007		13. Type of Report & Period Covered Final Report
		14. Sponsoring Agency Code

15. Supplementary Notes

Prepared in cooperation with the U.S. Department of Transportation, Federal Highway Administration

16. Abstract

The design of hydraulic structures such as bridges on distributary flow areas and alluvial fans require methods that can adequately determine discharges at the structures. Flow conditions on distributary flow areas such as alluvial fans are quite complex and require an understanding of unsteady flow hydraulics and sometimes need multi-dimensional flow analysis. The primary objective of this report is to explore the use of the U.S. National Weather Service DAMBRK model, to describe the unsteady flow of floods on distributary flow areas.

The DAMBRK model was applied to several hypothetical situations to determine the capability of the program to describe unsteady flows. Three distributary flow areas below the McDowell Mountains in Scottsdale, Arizona, were modeled using the DAMBRK code. Lost Dog Wash, a relatively simple distributary flow area which has been referred to as an alluvial fan, was selected to develop an application procedure. After successfully modeling Lost Dog Wash, two of the six distributary flow areas (alluvial fans 4 and 5) in north Scottsdale were modeled.

Both fan 4 and fan 5 demonstrated subcritical and supercritical flows. The flood plains computed using DAMBRK are compared with the flood plains using the FEMA method. It is recommended that models describing erosion and sediment transport and transmission losses and infiltration be incorporated into the DAMBRK code. Similar studies using two-dimensional models are also recommended to determine the advantages and limitations of these approaches to model flood flows on alluvial fans.

23. Registrant's Seal

Registered Professional Engineer (Civil) CERTIFICATE NO 24414 LARRY W. MAYS ARIZONA, U.S.A.

17. Key Words: Alluvial Fan, flood plain, hydraulics, unsteady flow, hydraulic structures.	18. Distribution Statement: Document is available to the U.S. public through the National Technical Information Service, Springfield, Virginia 22161		
19. Security Classification (of this report): Unclassified	20. Security Classification (of this page): Unclassified	21. No. of Pages: 133	22. Price

PREFACE

This project was funded by the Arizona Transportation Research Center, Arizona Department of Transportation, at Arizona State University. The author is grateful to the project committee members, who helped in preparing the report by technically reviewing and criticizing throughout the project duration.

ABSTRACT

Distributary flow areas such as alluvial fans, bajadas, alluvial slopes, and alluvial plains occur quite frequently along mountain bases. The design of hydraulic structures and highway crossing structures such as bridges and culverts on distributary flow areas and downstream of these structures require methods that can adequately determine discharges at the structures. The FEMA method is only a very approximate method that ignores the fundamental hydraulics. The traditional state-of-the-art engineering methods for the design and analysis mostly depend on typical one-dimensional, steady, gradually varied flow approaches. Unfortunately, flow conditions on distributary flow areas such as alluvial fans are quite complex and require an understanding of unsteady flow hydraulics and frequently need multi-dimensional flow analysis. The primary objective of this report is to explore the use of the U.S. National Weather Service DAMBRK model, to describe the unsteady flow of flood waves on distributary flow areas. Through use of such a model, more accurate definition of flood plains can be made and more accurate hydraulics can be determined for the design of hydraulic structures such as highway drainage structures.

The DAMBRK model is based upon a four-point, implicit, finite difference solution of the Saint-Venant equations for one-dimensional unsteady flows. The model was applied to several hypothetical situations in order to determine the capability of the program to describe unsteady flows (flood waves). Three distributary flow areas near the McDowell mountain in Scottsdale, Arizona, were also modeled using the DAMBRK code. Lost Dog Wash, a relatively simple distributary flow area, which has been referred to as an alluvial fan, was selected to develop an application procedure. After successfully modeling Lost Dog Wash, two of the six distributary flow areas

(alluvial fans) in north Scottsdale were modeled. Modeling of both fan 4 and fan 5 demonstrated both subcritical and supercritical flows. The flood plains computed using DAMBRK are compared with the flood plains computed using the FEMA method.

TABLE OF CONTENTS

Page

PREFACE ii

ABSTRACT iii

TABLE OF CONTENTS v

LIST OF TABLES vii

LIST OF FIGURES viii

CHAPTER

1 INTRODUCTION 1

1.1 Research Objectives 1

1.2 Alluvial Fans - Distributary Flow Areas 1

1.3 Debris Flows on Alluvial Fans 2

2 STATE OF THE ART IN EVALUATING FLOOD HAZARDS ON ALLUVIAL FANS (HYDROLOGY/ HYDRAULICS ASPECTS) 6

2.1 General Description of Hydrologic/ Hydraulic Processes 6

2.2 HEC-1 8

2.3 Other Methods 11

2.4 Two-Dimensional Models 20

3 HYPOTHETICAL CASES 22

3.1 Methodology and Assumptions in DAMBRK 22

3.2 Description of Hypothetical Channel 22

3.3 Application 29

3.4 Summary 32

4 APPLICATION TO LOST DOG WASH 35

4.1 Description of the Area 35

4.2 Defining Cross-Sections 39

CHAPTER Page

4.3 Modeling the Fan 41

5 APPLICATION TO FANS 4 AND 5 IN NORTH SCOTTSDALE 48

5.1 General 48

5.2 Hydrology of the Area 48

5.3 Description of Fan 4 50

5.4 Description of Fan 5 54

5.5 Hydrology of Fan 4 and Fan 5 56

5.6 Approaches 56

5.7 Flows from the Sub-Basins 60

5.8 Results 60

6 SUMMARY AND CONCLUSIONS 72

6.1 Summary 72

6.2 Limitations of using DAMBRK 73

6.3 Recommendations 74

APPENDIX

A DESCRIPTION OF THE THEORETICAL ASPECTS AND LIMITATIONS OF THE DAMBRK MODEL A-1

B SUMMARY OF SIMULATED RUNS IN TABLES B-1

C SAMPLE INPUT DATA C-1

D INPUT AND OUTPUT FILES FOR THE LOST DOG WASH D-1

E BRIEF DESCRIPTION OF FEMA METHOD E-1

F METHOD FOR HAND CALCULATION F-1

GLOSSARY 118

REFERENCES 121

LIST OF TABLES

Table		Page
3.1	Elevation-Top Width Data for Cross Sections	27
4.1	Initial Condition at Different Peak Flow, with n=0.05	43
4.2	Initial Condition at Different Peak Flow, with n=0.04	44
4.3	Initial Condition at Different Peak Flow, with n=0.03	45
4.4	Percentage Change in Flow Depth and Velocity with Change in n Values	47
5.1	Rainfall Amount for 24-Hour Duration for Different Return Periods	51
5.2	Rainfall Distribution for SCS Type IIA	53
5.3	Discharge Hydrographs at the Apexes	58
5.4	Inflow Hydrograph for Lateral 1	61
5.5	Inflow Hydrograph for Lateral 2	63
5.6	Inflow Hydrograph for Lateral 3	65
5.7	Comparison of Velocity and Depth between DAMBRK and FEMA Method for Fan 4 (Inflow at the Apex only)	68
5.8	Comparison of Velocity and Depth between DAMBRK and FEMA Method for Fan 4 (Addition of Lateral Inflow)	68
5.9	Comparison of Velocity and Depth between DAMBRK and FEMA Method for Fan 5 (Inflow at the Apex only) with n=0.050	69
5.10	Comparison of Velocity and Depth between DAMBRK and FEMA Method for Fan 5 (Inflow at the Apex only) with n=0.052	70
5.11	Comparison of Velocity and Depth between DAMBRK and FEMA Method for Fan 5 (Inflow at the Apex only) with n=0.055	71

LIST OF FIGURES

Figure		Page
1.1	Basic desert profile	3
1.2	Intersection of entrenched channel and alluvial fan surface	4
2.1	Basic structuring components of the HEC-1 model	9
2.2	Typical depth-width relationship for incised channel	17
2.3	Typical depth-width relationship for overland flow condition	18
3.1	Typical layout of the hypothetical channel	23
3.2	Different types of cross-sections	25
3.3	Typical channel section	26
3.4	Variable peak inflow hydrograph	28
3.5	Hypothetical channel with multiple slope	33
4.1	Location of the Lost Dog Wash	37
4.2	Detailed topography of the Lost Dog Wash	38
4.3	Typical cross-section across alluvial fans	40
4.4	Radially defined cross-sections	42
5.1	Approximate location of the six fans	49
5.2	SCS type IIA rainfall characteristics	52
5.3	Boundaries of alluvial Fan 4 with the cross sections	55
5.4	Boundaries of alluvial Fan 5 with the cross sections	57
5.5	Discharge hydrographs at the apexes	59
5.6	Lateral inflow 1 with sub-basin outflows	62
5.7	Lateral inflow 2 with sub-basin outflows	64
5.8	Lateral inflow 3 with sub-basin outflows	66
A-1	The x-t solution plane	A-5

Figure | Page

E-1 Ralationship between length of a single channel and ratio of canyon slope to fan slope E-3

F-1 Graphical representation of Newton's-method F-4

CHAPTER 1

INTRODUCTION

1.1 Research Objectives

The primary objective of this research is to determine whether the US National Weather Service DAMBRK model can be used to adequately model the unsteady flows of distributary flow areas such as alluvial fans, bajadas (Glossary), alluvial slopes, and alluvial plains. Demonstration projects are performed in this research to better understand the usefulness of DAMBRK in determining the extent of flooding in distributary flow areas. Several hypothetical cases were studied to determine the limitations of DAMBRK for modeling distributary flow areas, with respect to slopes of the channel, flare angles of the fan, lengths of the fan, etc. The DAMBRK model was also used to model three actual alluvial fans in Scottsdale, Arizona.

1.2 Alluvial Fans-Distributary Flow Areas

The definition of the alluvial fan is given in the Federal Register (1989, p. 9528) as "a geomorphic feature characterized by a cone or fan-shaped deposit of boulders, gravel, and fine sediments that have been eroded from mountain slopes, transported by flood flows, and then deposited on the valley floors, and debris flows, erosion, sediment movement and deposition, and channel migration."

Bull (1977, p. 222) defined alluvial fans in a simpler manner. He described it as a deposit whose surface forms a segment of a cone that radiates downslope from the point where the stream leaves the source area (see Glossary). Even though "alluvial fan" is the more common name, yet, sometimes it has been defined as "distributary flow areas." Kemna (1990, p. 166) defined distributary flow areas as "the area (in square miles) on the piedmont plain downstream from the primary diffluence and bounded by the

potential limits of major floods. The stream channels are separated by a wide variety of interfluves that range from high ridges well above large floods to low indistinct ridges (as found on many actively aggrading alluvial fans)." Figure 1.1 depicts a basic desert profile.

It is easily understood that alluvial fans cannot be described by one single criteria. Some pediments approximate a segment of a cone and many alluvial fans are not fan-shaped because they are restricted by adjacent larger fans. Drew first used the term "alluvial fan" in his work and subsequent researchers have continued to use the term "alluvial fan" in the same context as described above (Bull, 1977, p. 222). An alluvial fan that lacks the form of coalescing alluvial fans is best called an "alluvial slope" (Hawley and Wilson, 1965). Bull (1977, p. 225) described the stream as the link between erosional (pediment) and depositional (fan) parts of the system. Figure 1.2 shows a typical channel profile where a channel intersects an alluvial fan surface.

1.3 Debris Flows on Alluvial Fans

It is very obvious that the alluvial fans are typically subject to some kind of debris flows or mud flows along with the flooding events. The U.S. National Weather Service DAMBRK model has the capability to model mud flows as well. But this debris or mud flow option will not be used in this research as discussed below.

First of all, Bull (1977, p. 236) explained the factors that govern debris flow which are "abundant water (intense rainfall) over short periods of time at regular intervals, steep slopes having insufficient vegetative cover to prevent rapid erosion, and a source material that provides a readily available and abundant source of detritus and matrix of mud." Again, Melton (1965, p. 17) also described debris flow as a very rare event for the state of Arizona.

Secondly, Innes (1983, p. 474) described steep slopes, suitable regolith

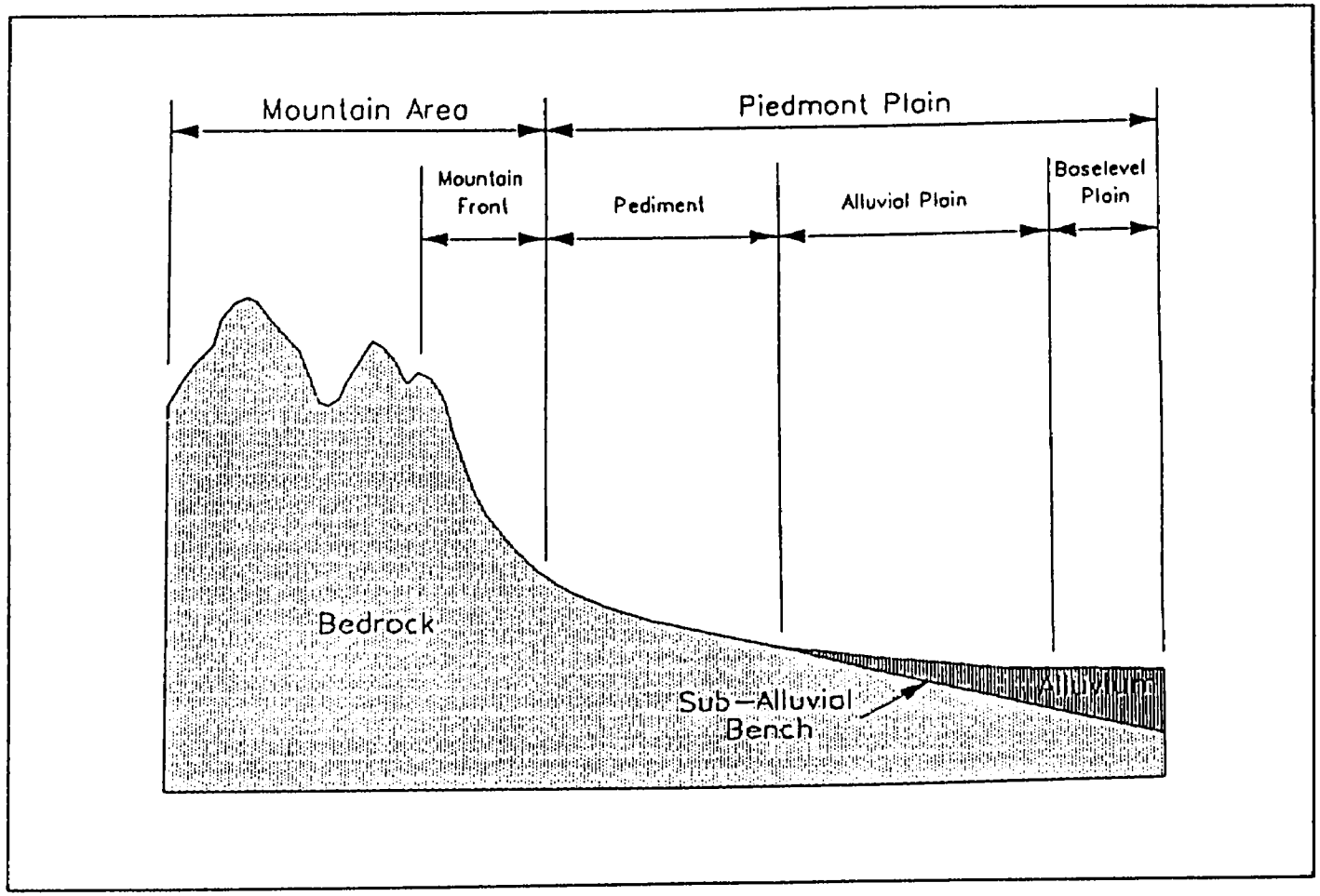

Figure 1.1 Basic Desert Profile (After Ward, 1988, p. 9)

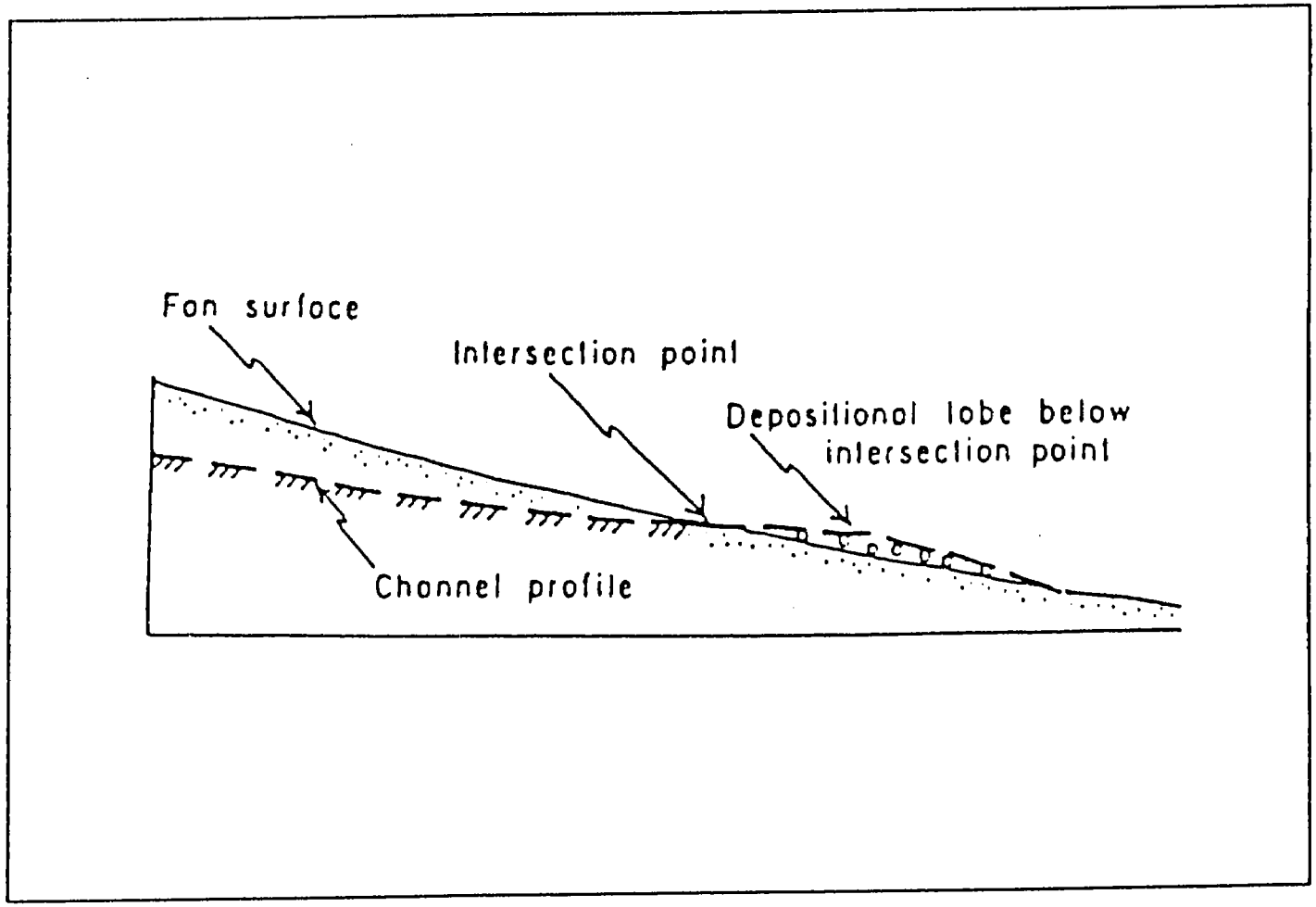

Figure 1.2 Intersection of Entrenched channel and alluvial fan surface (After, Hooke, 1967, p. 450)

(see Glossary), and high pore pressure as the basic requirements for debris flow activity. According to Innes, from the works of Brunsden and Ballantyne, it appears that the minimum slope required for hillslope debris flow is 30°. Innes also stated that Rapp and Nyberg recorded debris flows on slopes of 25.5^{o}; and Owens recorded debris flows on slopes as low as 20°. The later two, however, are exceptional, and it is possible that they may be partly valley-confined (one of the three debris flow categories) in origin (Innes, 1983, p. 474). Now, for the hypothetical cases, the maximum slope that was dealt with was less than 12°. And the slopes of the of the alluvial fans in the area of interest do not even exceed 4°.

Therefore, in view of the above facts, the complexity of the debris flow modeling is excluded from this research.

CHAPTER 2

STATE OF THE ART IN EVALUATING FLOOD HAZARDS ON ALLUVIAL FANS (HYDROLOGY/HYDRAULIC ASPECTS)

2.1 General Description of Hydrologic/Hydraulic Processes

In the Southwestern part of the United States, highways are often crossed by alluvial fans, which quite frequently occur at the mountain bases. Crossings of highways and alluvial fans, such as a bridge crossing, may present complexity in the method of designing structures, if proper hydrologic as well as hydraulic analysis of the alluvial fan is not available. Specific design requirements for various highway crossings on alluvial fans are satisfied by using lumped hydrologic approaches such as HEC-1 with the simplified kinematic wave model or one-dimensional, steady, gradually varied flow approaches such as HEC-2. Flows on the distributary flow areas are complex in nature and the hydraulic design often requires an understanding of unsteady hydraulics and frequently even need multi-dimensional flow analysis. An improved approach for alluvial fan hydraulic analysis would be to use the runoff hydrographs from the hydrological computer model(s) at the apex of the alluvial fan determined through a model such as HEC-1 and route these hydrographs through the alluvial fan using an unsteady flow model such as the U.S. National Weather Service DAMBRK model.

The power of the flood events and the risk associated with the flooding in alluvial fans in arid and semi-arid regions should never be underestimated. Unless a better understanding of hydraulic processes on alluvial fans is developed and rational, equitable, and cost-effective flood plain management schemes are implemented, there is every reason to believe that flooding on developed alluvial fans will become both more

serious and costly (French, 1987, p. 14). The arid and semi-arid regions, of the United States, are considered by many to be ideal locations for the storage and/or disposal of hazardous and radioactive wastes. For example, there is a low level waste burial site for commercially generated wastes, and a similar burial site for defense related low level radioactive wastes in Nevada (French, 1987, p. 15). Another reason for examining the hydraulic processes on alluvial fans is that in many of the arid and semi-arid regions of the United States are considered to be primary sources of potable water. For example, Tucson, Arizona is currently totally dependent on ground water for its potable water supply, and much of the ground water available to Tucson derives from an alluvial fan deposit of late Cenozoic age (Bull, 1977). From the engineering point of view, the primary important fact in a floodplain is the inundation of the area in case of a flooding event.

These flooding events are unsteady flow events, rapidly varied in nature; and they are usually analyzed by either some mathematical or analytical models. The currently available flood routing models vary in complexity from simple hydrologic methods such as the Muskingum model to complex one and two dimensional finite difference and finite element models. These models can broadly be classified into process-type models, often called "hydraulic models," and models using a conceptual or systems approach, commonly referred to as "hydrologic models" (Weinmann, 1979, p. 1521). Chow, et al (1988) use the distinction of "lumped" and distributed models from the hydrologic and hydraulic models

Within hydraulic routing models, the one dimensional kinematic, diffusion, and full dynamic wave models are being applied in engineering practice. The major assumption in the kinematic wave approach is that the inertia and pressure terms are negligible as compared with the friction and

gravity terms. On the other hand, the diffusion model assumes that the inertia terms in the equation of motion are negligible as compared with the pressure, friction, and gravity terms (Ponce, 1978, p. 353). The full dynamic wave model considers all the terms in the Saint-Venant equation (Appendix A).

2.2 HEC-1

The HEC-1 computer program was developed to simulate the surface runoff responses or hydrologic processes of flood events on river basins varying in sizes and complexity. The whole basin is represented as an interconnected system of hydrologic and hydraulic components. Each component models an aspect of the precipitation-runoff process within a portion of the basin, commonly referred to as subbasin. The components may be defined as runoff, stream channel, or a reservoir. Representation of a component requires a set of parameters which specify the particular characteristics of the component and mathematical relations which describe the physical process (Hydrologic Engineering Center, 1981, p. 1). The three basic structuring components of the HEC-1 model, a subbasin runoff component, a routing component, and a hydrograph combining component, are described in Fig 2.1.

Modeling Capabilities and Options

The HEC-1 model uses a simplified linear kinematic wave routing approach in its simulation procedure. Basically, the HEC-1 program has the capability to simulate the precipitation-runoff process and compute flood hydrographs at the desired locations in the basin (Hoggan, 1989, p. 96). The basin boundaries are delineated and the whole area is subdivided into subbasins depending on the hydrologic characteristics. There are a number of featuring options in addition to the basic precipitation-runoff simulation

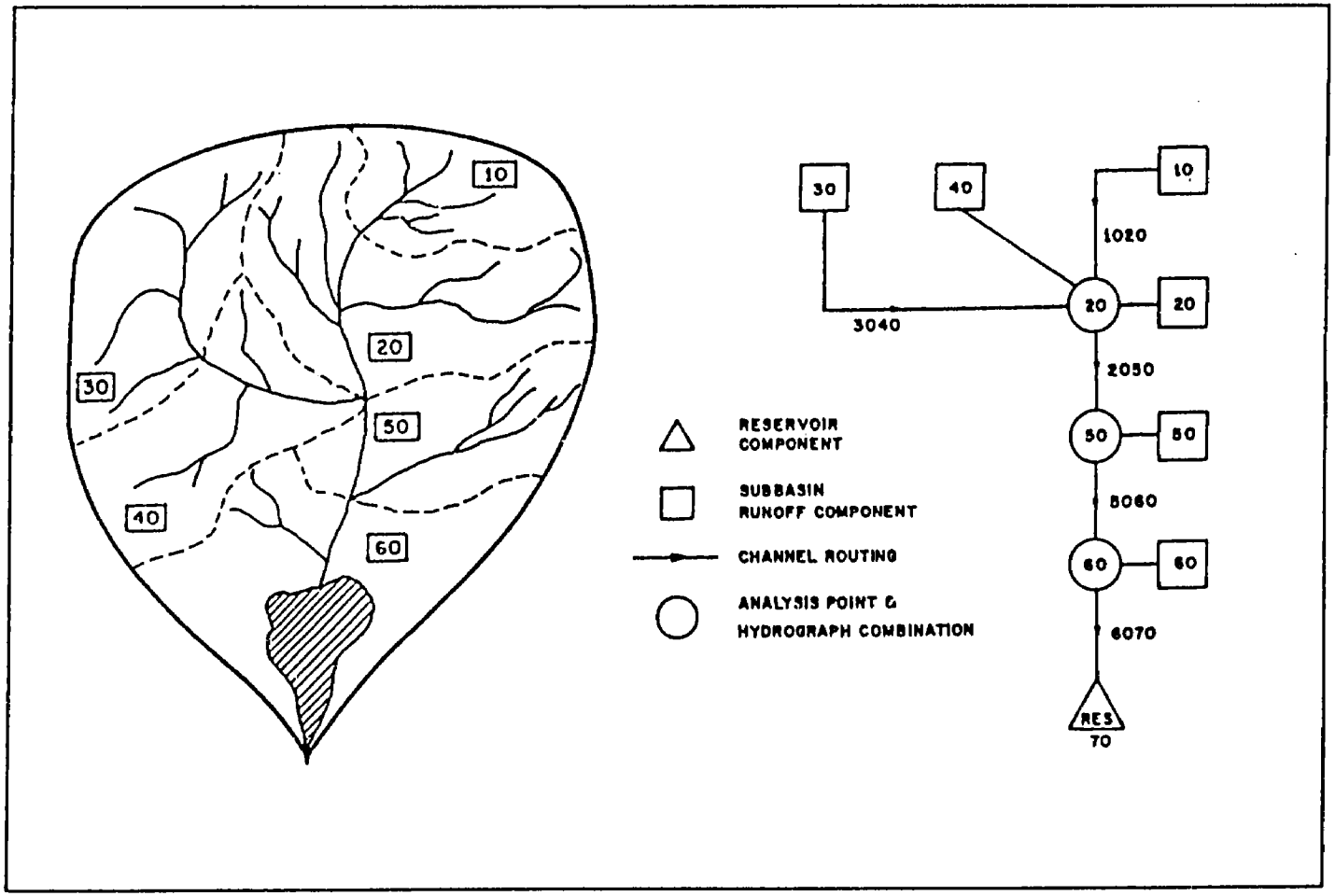

Figure 2.1 Basic structuring components of the HEC-1 model (After Hydrologic Engineering Center, 1981, p. 1)

capability of the HEC-1 computer code. Hoggan (1989, p. 97) listed the additional capabilities of the HEC-1 model as following : snowfall and snowmelt simulation, dam safety analysis, pumping and diversion schemes, parameter estimation, multiple-flood and multiple-plan analyses, and simulation of precipitation depth-area relationships.

Assumptions and Limitations

The primary assumption that is made is the parameters, which define the hydrologic processes, reflect average conditions within the subarea; but if such averages are not appropriate for the subarea, then it is necessary to consider smaller subareas within which the average parameters do apply.

Among several limitations of the model, the following are important : (1) single storm simulation; because there is no provision for soil moisture recovery during periods of no precipitation, (2) model results are in terms of discharges not stages (a hydraulic computer program HEC-2, for example, can be used in conjunction with HEC-1 to obtain stages), (3) streamflow routing is performed by either hydrologic routing or a linear explicit kinematic wave method. These models do not reflect the full Saint-Venant equations which are required for flat rivers (Hydrologic Engineering Center, 1981, p. 2)

Discussions

The use of kinematic wave technique is a popular method among some models. Because the kinematic wave model ignores the local and convective acceleration term and the pressure term in the momentum equation of the Saint-Venant equation, the mechanism to describe back water effects does not exist in such a model. Theoretically, the kinematic wave model only describes a pure translation of a flood wave. The attenuation that does result from use of the kinematic wave is a direct result of numerical error. Hromadka (1988, p. 208) said that "the literature contains several

examples of kinematic wave channel routing performance that indicate that this procedure may be of limited value in comparison to other methods." He also added that Akan and Yen (1981, p. 729) showed that the kinematic wave peak flow-rate estimates and hydrograph timing differ from the other comparable modeling results. From the experimental data of Hromadka (1988, p. 209), for steep slopes or peaked hydrographs, the errors were significant; but the errors reported were due to computational error, e.g., numerical-diffusion, and not due to the model's underlying assumptions as to hydraulics of flow.

Katopodes (1983, p. 711) found out that as long as the channel remains prismatic and the roughness is independent of distance, the characteristics are straight lines, then an extremely simple, inexpensive model can be constructed.

2.3 Other Methods

Edwards and Thielmann Procedure, Cabazon, California

A scattered residential development, Cabazon, located northwest of Palm Springs in Riverside County, California, was lacking enough flood plain delineation information for the community officials, to make any land use decisions or to develop design criteria for proper flood-proofing measures (Ward, 1988, p. 87). In order to develop land use guidelines and recommended flood-proofing criteria, an extensive engineering study was performed by Edwards and Thielmann (1982). The result of that study is the following methodology.

Methodology

The methodology followed by Edwards and Thielmann is basically the same as Dawdy's method, which is adopted by Federal Emergency Management Agency. They revised Dawdy's method in order to more

realistically analyze engineering problems.

Edwards and Thielmann stated that Dawdy's assumption, "as an alluvial fan widens, the probability of flooding of a given magnitude at a given point should, in general, decrease." (Dawdy, 1979, p. 1407) acknowledges the fact that the downslope widening introduces greater area for a channel of given width to occur; and the possibility of the location of a channel of given geometry and discharge could be a random event. So, they suggested to remove the statistical component from the Federal Emergency Management Agency method, showing the justification that, "By eliminating the statistical component from the Dawdy (FEMA) method, the resulting flow characteristics represent conditions on the cone resulting from the 100-year peak discharges as determined at the apex, rather than conditions that would occur at any given point on the cone from an event which has one percent probability of occurring annually at that point."

Realizing the potential for supercritical flows on these alluvial fans, Edwards and Thielmann suggested the second revision as to assume normal depth, to uphold a more realistic scenario, instead of critical depth (as assumed by Dawdy). In support of this assumption, they also added that development of critical depth would not occur until sometime into the runoff hydrograph and until the critical depth is established, supercritical flow will probably be the predominant regime.

In view of the above stated assumptions, Edwards and Thielmann presented a revised set of equations for computing flood depths, widths, and velocities on the alluvial fan. Depending on Manning's equation, with an assumption of a wide, rectangular channel, these equations also incorporate the stabilizing criteria suggested by Dawdy, which is, "a decrease in depth creates a two hundred-fold increase in width, i.e., $dD/dW = -0.005$." The set of

new, revised equations proposed by Edwards and Thielmann are as following :

$$D = \left\{ \frac{Q_n}{178.8\, S^{\frac{1}{2}}} \right\}^{\frac{3}{8}} \quad \ldots\ldots\ldots\ldots\ldots\ldots \quad (2.7)$$

$$W = \left\{ \frac{17.16\, (Q_n)^{\frac{3}{8}}}{S^{\frac{3}{16}}} \right\} \quad \ldots\ldots\ldots\ldots\ldots\ldots \quad (2.8)$$

$$V = 0.41\, Q^{\frac{1}{4}}\, S^{\frac{3}{8}}\, n^{\frac{-3}{4}} \quad \ldots\ldots\ldots\ldots\ldots\ldots \quad (2.9)$$

where, Q = depth of flow (ft.)

W = width of channel (ft.)

V = velocity of flow (fps.)

Q = discharge (cfs.)

S = channel slope (ft/ft)

n = Manning's roughness value.

After applying these equations to the Cabazon study, depths of 1 to 3 feet, velocities of 10 to 25 feet per second, and widths of 100 to 500 feet were reported for 100-year peak discharge values ranging from 5,000 cfs. to 30,000 cfs., and the slopes ranging from 2 percent to 18 percent. The computed values were reportedly supported by indirect field measurements (by the USGS) of flooding on alluvial fans (Ward, 1988, p.89)

Federal Insurance Administration, 1980 Experimental Procedure

Before Federal Emergency Management Agency adopted the Dawdy

method, the Federal Insurance Administration (FIA) had experimented with a special flood insurance zone designated as "AF" (for alluvial fans). The procedure was developed based on the unpublished works by Lare and Esyter of the Albuquerque District of the Corps of Engineers (Ward, 1988, p. 91).

Methodology

The basic difference between this procedure and Dawdy's method is the absence of a statistical parameter that is responsible for reduced flooding probability in the downfan direction. The Federal Insurance Administration procedure emphasizes on dividing the fan into separate reaches that exhibit similar flow characteristics. For example, possible reach limits can be identified as : 1) the fan apex, 2) intersection points with main valley and canyon sides, 3) points of substantial change from an entrenched channel to a braided channel, 4) a change in overbank encroachments (structures), and 5) points of substantial change in grading (Ward, 1988, p. 91)

Hydraulic analysis of an alluvial fan, following this procedure utilizes the same two assumptions used in Dawdy's method : 1) critical flow will be the dominant regime on the fan surface, and 2) channel geometry will stabilize when a depth decrease creates a two hundred-fold increase in flow width. The critical flow assumption is utilized in developing a set of curves relating overbank flow depth to a total flow path width. Ward (1988, p. 92) has stated the following steps to follow in order to accomplish the task :

1. To determine the most representative channel geometry for the different reaches of the fan, field inspections are required.
2. Using the representative channel geometry determined from the previous step, a water surface profile model (HEC-2 for example) is used to develop hydraulic data for a range of discharge values and total

flow widths. While using this procedure, the bottomwidth for a given channel is kept constant and the overbank widths are varied, both of which are included in the total flow width. Using the critical depth assumption, the model is then run for different combinations of discharge and total flow width. The model result will produce depth of flow and velocity data for the different elements of the cross-section.

Figures 2.2 and 2.3 are the typical representation of depth-width curves that will result from applying the procedure described in steps 1 and 2. These figures also identify the cross-section variables that are used in the analysis. Figure 2.3 depicts a typical sheetflow on an alluvial fan where there are no well-entrenched or defined channels..

The Federal Insurance Administration provides some guidelines on how the different reaches might be analyzed in order to be able to use their recommended method. The guidelines (Ward, 1988, p. 94) are as following :

1. Areas within a canyon, or areas on the fan surface where a deeply entrenched channel exists can be investigated with conventional procedures such as HEC-2. Caution is required, however, to insure that the channel has sufficient conveyance and stability to preclude the possibility of an avulsion.
2. Areas on an alluvial fan protected by structural works (channels, diversion structures, debris basins, etc.) should be analyzed with a very critical evaluation of the performance capability of such structures.
3. Majority of the areas where natural fan processes, such as trenching, natural migration of channels, and sediment deposition are free to take place, should be analyzed under the two following categories :

   a. Entrenched Fans : This condition is recommended for "those

cases where an unbroken flow path exists which conveys up-canyon flow down-fan to a point where sediment deposition takes place." Based on field data and/or topographic maps, a typical cross-section is developed for this reach. A depth-width relationship is developed, similar to that illustrated in Figure 2.2, and a flood depth (for the selected discharge) is determined in accordance with the dD/dW = -0.005 criteria. The computed depth associated velocity parameters are assumed to apply at any point across the fan contained within this reach. Whenever a noticeable change in channel geometry or slope is encountered, a new reach, new depth-width curves should be developed, and new depth-velocity characteristics should be determined.

b. Untrenched fans : A critical depth analysis for a shallow sheetflow condition (figure 2.3) is employed in this situation. The depth of flow to be used in this area is based on the previously cited assumption that the lateral widening of the channel will terminate when the reduction in depth results in a two hundred fold increase in flow width. From a similar figure as in figure 2.3 the ratios of dD/dW can be computed for a given discharge until a ratio of 0.005 is found. The depth and flow velocity associated with this depth-width combination would then be considered representative for this reach of the fan. Based on the logical assumption that this is a random flow pattern that could, at some time, occur at any point across this reach of the fan, the computed depth-velocity parameters are applied to all areas of the fan within this reach.

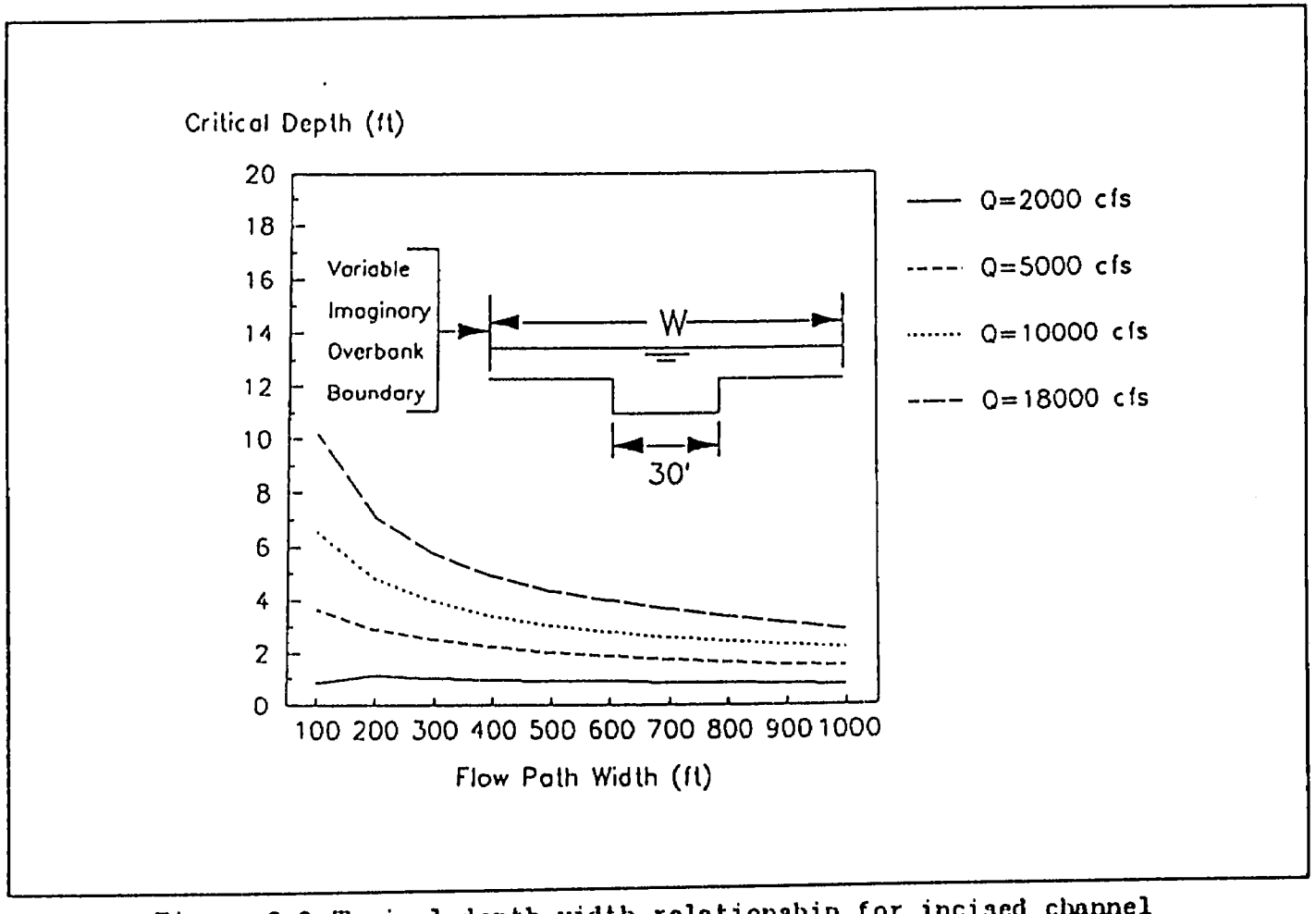

Figure 2.2 Typical depth-width relationship for incised channel (After Ward, 1988, p. 94).

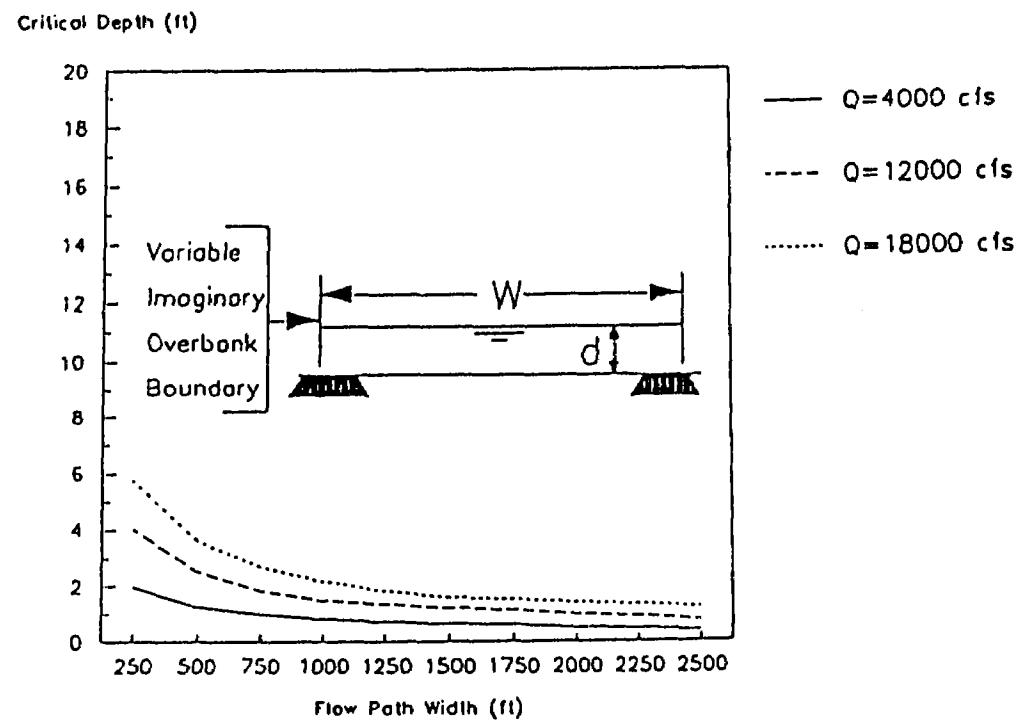

Figure 2.3 Typical depth-width relationship for overland flow condition (After Ward, 1988, p. 94).

Soil Conservation Procedure

More than 19 years ago, James Malone (Hydraulic Engineer, SCS) developed a computer program to analyze the hydraulics of fan flooding and to quantify the financial damage that would occur as a result of such flooding events.

Methodology

The lateral (overbank) flooding that would initiate on an alluvial fan as a result of flows exceeding the bankful capacity of an incised channel is the prime concern of this procedure. The method requires a runoff hydrograph at the apex of the fan and a typical cross-section to define the channel reach that extends downstream from the fan apex.

First of all, the procedure routes the apex hydrograph through the channel section to determine at what point in the hydrograph the bankful capacity will be exceeded. After the program identifies that the bankful capacity is exceeded, it starts calculating velocity, depth, and volume of water that will spread laterally from the channel bank during the current time interval. The code can compute infiltration losses for the laterally flowing water that escapes from the defined channel. Ward (1988, p. 98) has a more detailed description of the method where he described seven sequential steps to perform this procedure on the alluvial fans.

The ability of the code to transform the overbank hydraulic data into a predicted summary of financial damage is a unique one. To use this option, the user has to develop some sort of a rating curve, which will relate the overbank flow depth and velocity with the dollars of flood damage.

The requirement of a stable, non-erodable channel cross-section acts as a limitation of the program. It also confines the analysis to a single cross-section location. This approach may be suitably applicable in projects where

there are stabilized, man-made constant cross-sections (Ward, 1988, p. 102).

2.4 Two-Dimensional Models

One of the problems in modeling the alluvial fans is when flows on a distributary area no longer remain one-dimensional. A lot of times water starts flowing across those portions of the fan surface, where there are no entrenched channels to carry such flows. The conventional way of modeling these flows is to neglect the existence of these flows; which is not a very realistic approach. The only alternative procedure may be is to use two-dimensional flow models. There are advantages and disadvantages in using a two-dimensional flow routing model. These include, first of all, the ability to consider the effect of complex topography and variable hydraulic roughness over the alluvial fan; secondly, attenuation or bulking of the hydrograph across the fan; thirdly, the effect of varying sediment concentration on the hydraulics of flow; fourthly, the hydraulic capacity of channels and overland areas; and finally, the effects of natural or man-made flow paths on the floodplain (Grindeland et al., 1990, p. 271). There are several 2-D models available, two of which, FESWMS and FLO-2D, will be discussed below in brief.

A computer model known as FESWMS (Finite Element Surface Water Modeling System), is available for solving multi-dimensional hydraulics problems. The hydrodynamic model, RMA-2, which has gone through several modifications, is used as the core program to develop the FESWMS. The model allows steady and time dependent solutions. Also, Preprocessor and Postprocessor have been developed to simplify network preparation and allow automatic plotting of networks, velocity vectors, and contours of water depth (Brion and Mays, 1987, p. 2)

Another computer model, FLO-2D (originally named MUDFLOW),

exists which can route water floods or hyperconcentrated water-sediment flows in two dimensions. The model uses a central, finite difference routing scheme and uniform grid elements to apply the continuity and momentum equation. The two-dimensional modeling of alluvial fans permits the evaluation of site-specific physical influences on the magnitude and extent of flooding. Potential flood scenarios can also be efficiently analyzed by computer models (Grindeland et al., 1990, p. 273).

CHAPTER 3

HYPOTHETICAL CASES

3.1 Methodology and Assumptions in DAMBRK

This part of the research deals with several hypothetical situations. The application of the DAMBRK computer model to several hypothetical examples helped determine the capability of the program to describe unsteady flows (flood waves) propagating down a fan shaped channel at relatively shallow depths for both subcritical and supercritical flows and the transition between these flows. Appendix A provides a description of the theoretical aspects and limitations of the model.

3.2 Description of the Hypothetical Channel

Application of DAMBRK was made to simple hypothetical channels, to determine the sensitivity and response of the DAMBRK model to different slopes, peak inflows, and flare angles. Figure 3.1 shows the typical layout of the hypothetical channel. The length of the hypothetical channel is 21,600 ft. (approximately 4.09 miles) with almost half of the channel fan-shaped. Cross-sections are used to describe the geometry of the channel. A maximum of 200 (two hundred) cross-sections, can be used in the DAMBRK model. Each cross-section is defined by a set of elevation-top widths. A maximum of eight elevations along with the same number of widths can be used. It is also possible to specify any off-channel storage on the flood plain associated with any cross-section. There is an option to generate (interpolate) additional cross-sections in between specified sections. This linear interpolation property is valid for both active and inactive (off-channel storage) portions of the sections. The generation of the additional sections enables the distance steps (Δx_i), used to solve the Saint-Venant equations, to be smaller than the distance steps separating the original specified cross-sections (Fread, 1988, p.

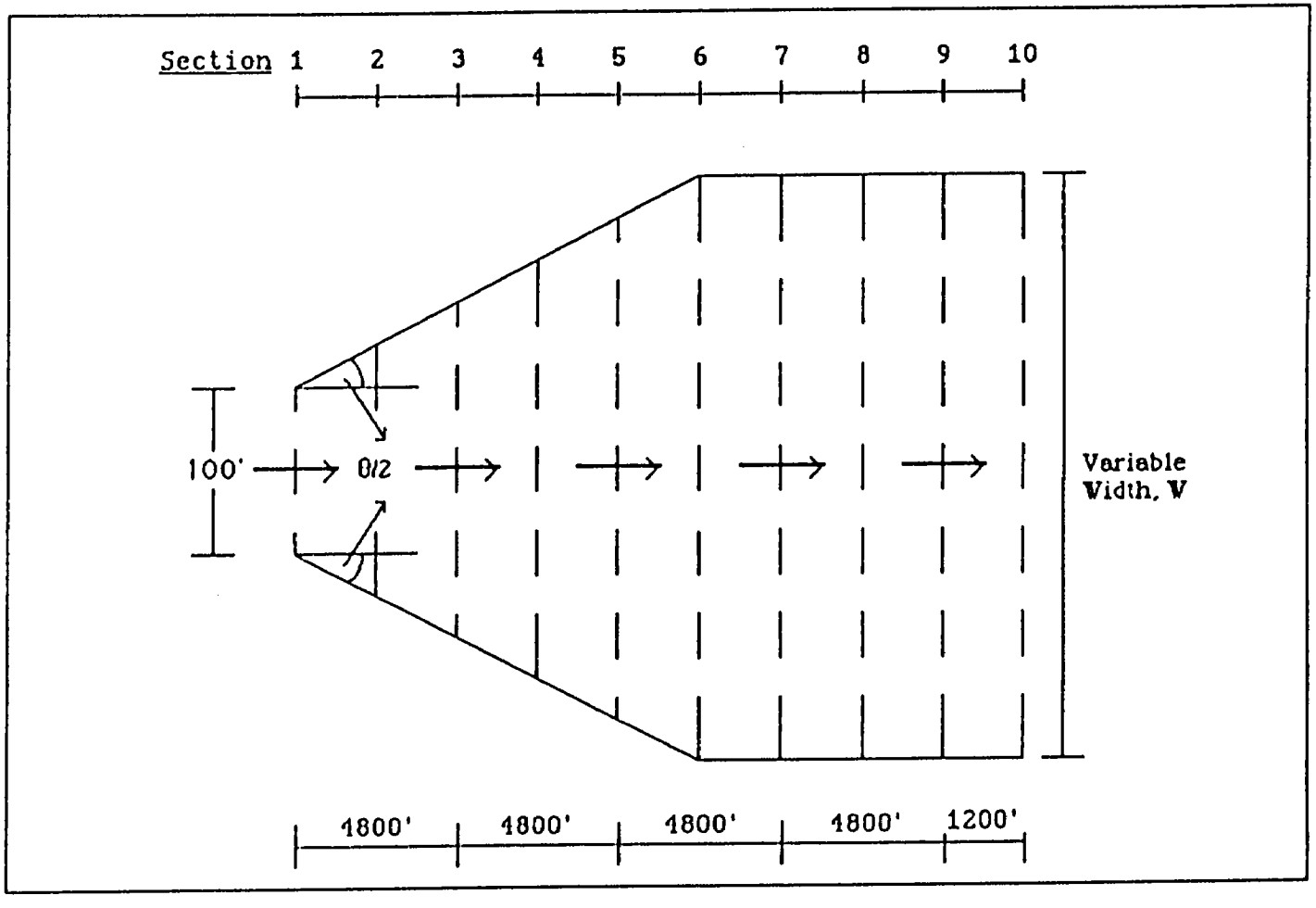

Figure 3.1 Typical layout of the Hypothetical Channel.

55). For the purposes of this research the hypothetical channel is defined by ten cross-sections and each cross-section is defined by six elevations and widths. No off-channel storage is defined with these sections. However, this could be an additional option to model alluvial fans. Figure 3.2 shows different types of cross-sections, which are used to model the alluvial fan for all the hypothetical case studies.

Figure 3.3 illustrates a single channel approach. In this method the original cross-sections are defined by an equivalent simple section (FEMA, 1985, p. A5-2). The elevation-top widths for each cross-section are presented in Table 3.1.

Inflow

In order to model the alluvial fans an inflow hydrograph at the apex of the fan is required. This can be determined by performing a hydrologic study of the watershed that contributes to the apex of the fan in consideration and to various drainage points downstream of the apex. An inflow hydrograph, which attains a very high magnitude within a very short time, is selected. Figure 3.4 is the typical shape of the inflow hydrograph. The initial steady, nonuniform flow is chosen as 400 cfs., so that at time t=0 the entire channel has a steady state flow of 400 cfs. Within two hours the hydrograph reaches its peak, starting from the initial steady, nonuniform flow of 400 cfs., and recedes back to 400 cfs. again after a total time of four hrs. The magnitude of the peak flow varies depending upon the case.

Routing Option

The DAMBRK model has the capability to deal with 12 (twelve) different options (Fread, 1988, p. A-21). For modeling the alluvial fans, the following two options are used :

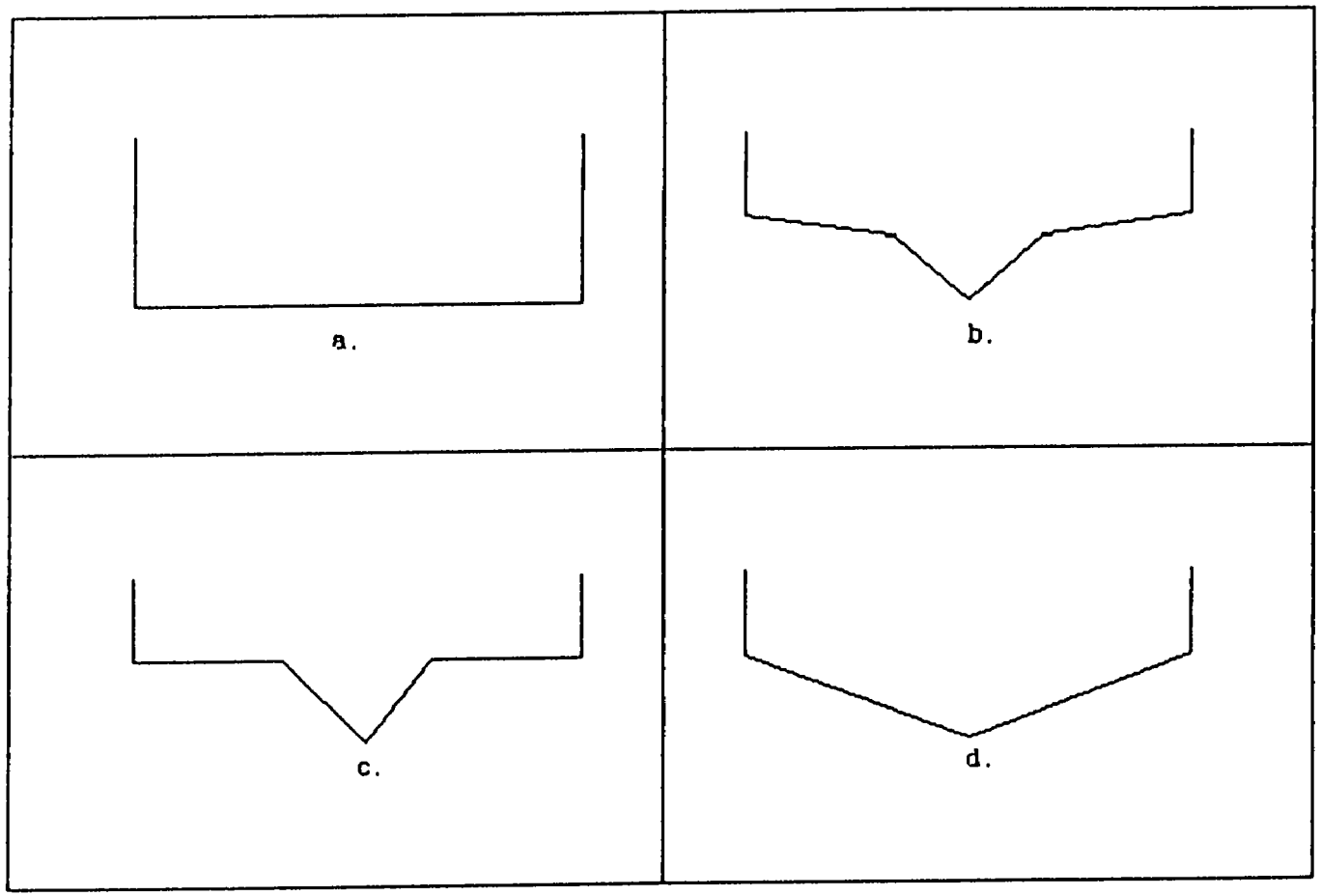

Figure 3.2 Different types of cross-sections.

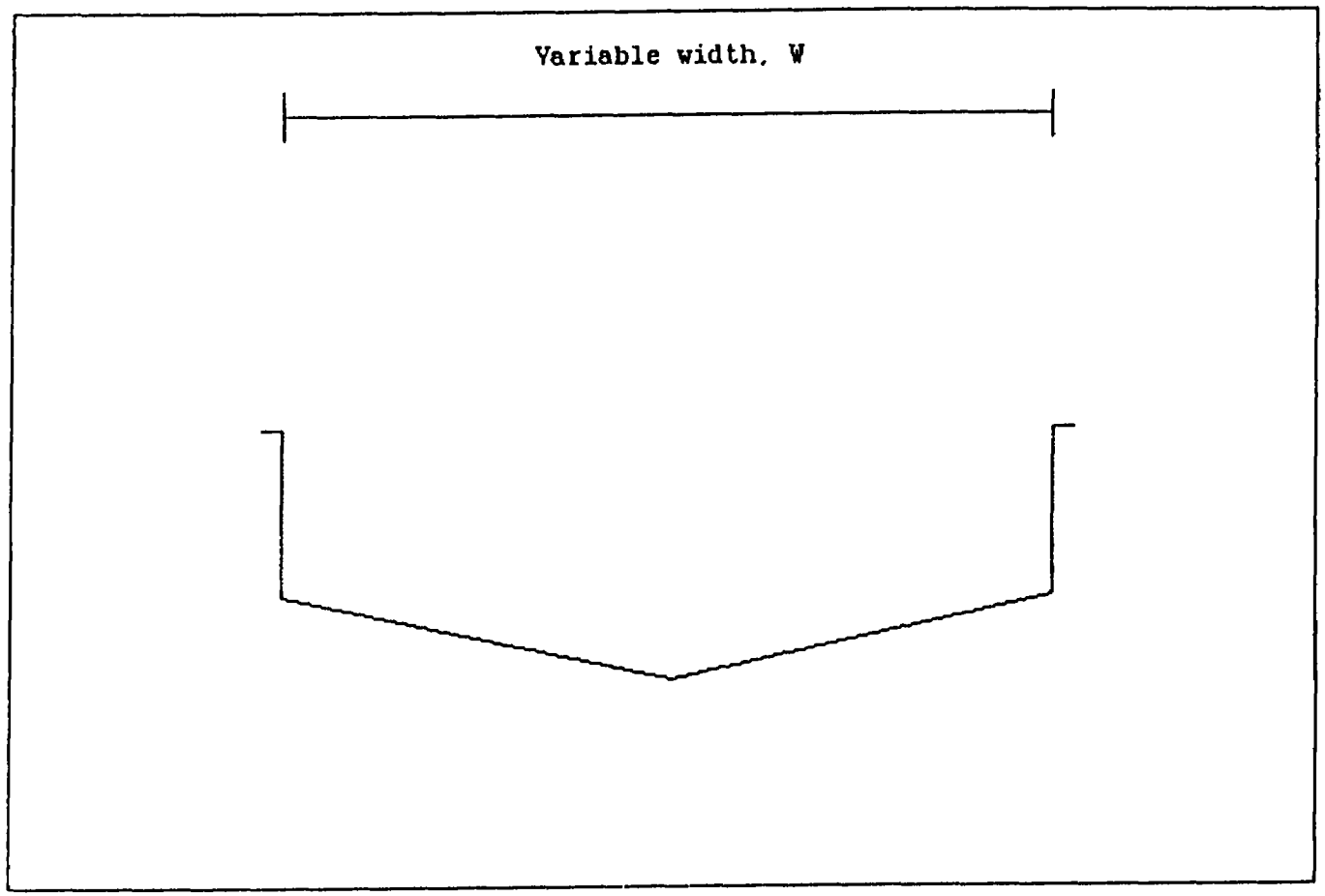

Figure 3.3 Typical channel section.

Table 3.1 Elevation-Top Width Data for Cross-Sections.

Channel Section	(All numbers are in ft. unless otherwise mentioned)					
1						
Elev.	6150.0	6153.0	6155.0	6155.01	6158.0	6162.0
Width	0.0	60.0	100.0	100.0	100.0	100.0
2						
Elev.	5650.0	5653.0	5655.0	5655.01	5658.0	5660.0
Width	0.0	1860.0	3100.0	3100.0	3100.0	3100.0
3						
Elev.	5225.0	5228.0	5230.0	5230.01	5233.0	5235.0
Width	0.0	3660.0	6100.0	6100.0	6100.0	6100.0
4						
Elev.	4875.0	4878.0	4880.0	4880.01	4883.0	4885.0
Width	0.0	5460.0	9100.0	9100.0	9100.0	9100.0
5						
Elev.	4575.0	4578.0	4580.0	4580.01	4583.0	4585.0
Width	0.0	7260.0	12100.0	12100.0	12100.0	12100.0
6						
Elev.	4325.0	4328.0	4330.0	4330.01	4333.0	4335.0
Width	0.0	9060.0	15100.0	15100.0	15100.0	15100.0
7						
Elev.	4307.0	4310.0	4312.0	4312.01	4315.0	4317.0
Width	0.0	9060.0	15100	15100.0	15100.0	15100.0
8						
Elev.	4295.0	4298.0	4300.0	4300.01	4303.0	4305.0
Width	0.0	9060.0	15100.0	15100.0	15100.0	15100.0
9						
Elev.	4290.0	4293.0	4295.0	4295.01	4298.0	4300.0
Width	0.0	9060.0	15100.0	15100.0	15100.0	15100.0
10						
Elev.	4289.0	4292.0	4294.0	4294.01	4297.0	4299.0
Width	0.0	9060.0	15100.0	15100.0	15100.0	15100.0

Note :

Channel Length : 21,600 ft. (or approx. 4.09 miles).

Flare Angle : 64.01 degrees.

Peak Inflow : 15,000 cfs.

Combination of Subcritical and Supercritical Flow.

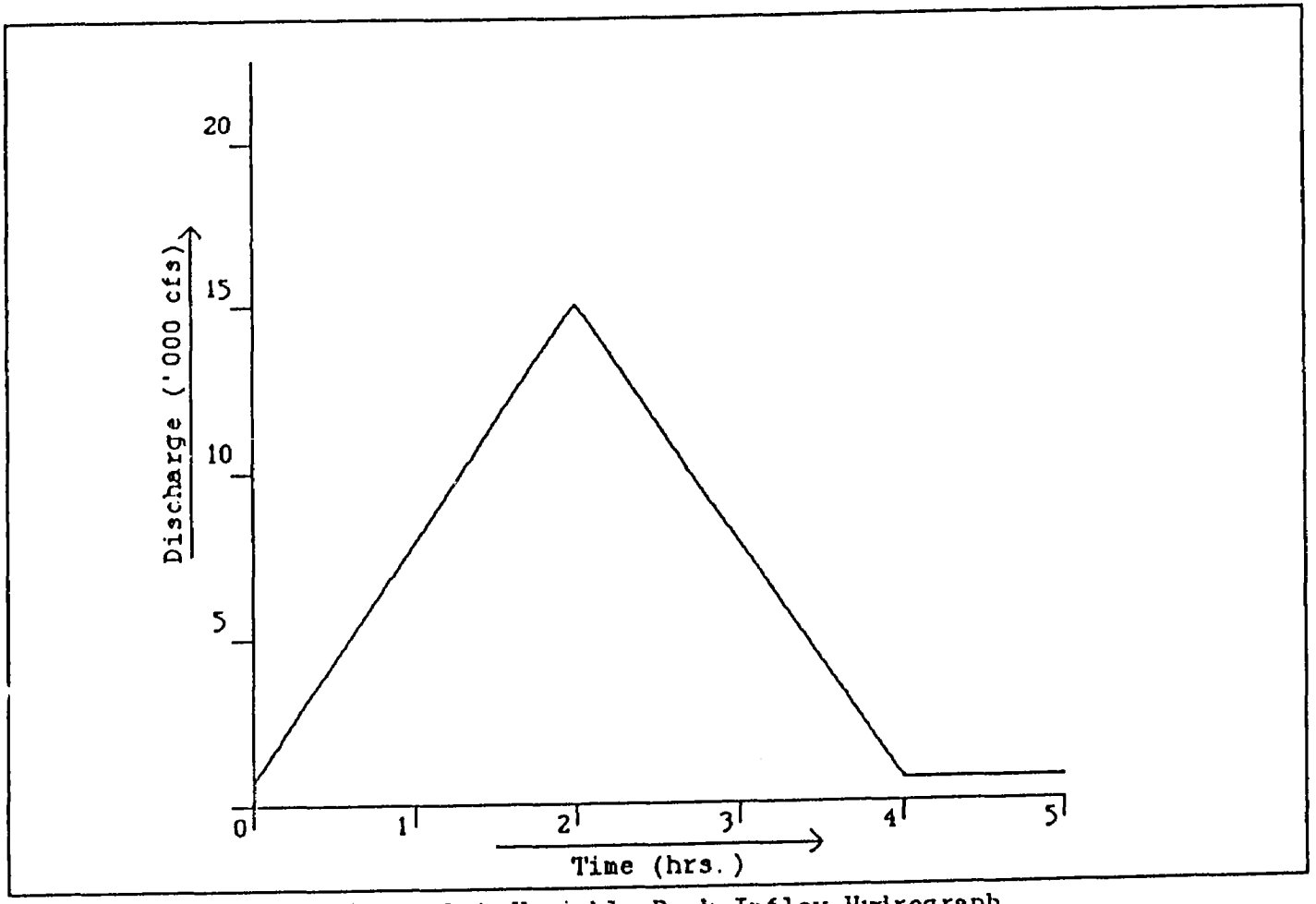

Figure 3.4 Variable Peak Inflow Hydrograph.

1. Subcritical dynamic routing of an input hydrograph through a downstream channel/valley.

2. Supercritical dynamic routing of an input hydrograph through a downstream channel/valley.

Both of these options are applied to the hypothetical cases. The recent model by Fread (1988) has the capability to handle mixed conditions (both subcritical and supercritical).

The hypothetical channel described previously is modeled with different flow conditions. In different cases the peak inflow was varied from 5,000 cfs. to 15,000 cfs. The slope was varied from 2.2 ft/mi. to 1100 ft/mi. The flare angle, θ was varied from 4.77 degrees to 87.56 degrees. All these variations and the resulting peak flows and depths are described in the following section.

3.3 Application

The application considers five different cases with ten different hypothetical situations (e.g. ten different slopes or flare angle for each case). A total of over 50 computer runs (simulations) are summarized in Tables in Appendix B. A sample input description for DAMBRK is presented in Appendix C. This particular sample input is one of the many set-ups for the five hypothetical cases.

Case One (Subcritical flow)

Slope limitation

The first attempt was made to determine the limitations on slope to maintain subcritical flow. The peak inflow of the hydrograph was selected as 15,000 cfs. and a flare angle of 11.42 degrees was used. The slope of the channel was varied keeping everything else the same. The maximum slope, that can be attained, was found to be approximately 40 ft/mi (< 1%). At this slope,

elevations at some of the sections in the channel started to have supercritical flows. The maximum slope at which all flows would become supercritical was found to be approximately 211 ft/mi which is about 4%. Table B.1 lists the discharges, depths, velocities, and time to peak discharge, and elevation for different bottom slopes of the hypothetical channel.

Case Two (Subcritical flow)

Flare angle limitation

This case was used to determine the limits of the flare angle. Two different studies were made under this case. The first one was conducted with a very flat slope of 2.2 ft/mi. And the second was performed with a slope of 39.6 ft/mi; which is the limit for the flow to remain subcritical. It was found that the slope does not affect the variation of the flare angles. Because in both the studies the maximum flare angle that the model could handle was 11.42 degrees. The peak inflow for the case was 15,000 cfs. Tables B.2.1 and B.2.2 list the discharges, depths, velocities, time to peak discharge, and elevation for different flare angles of the hypothetical channel.

Case Three (Subcritical flow)

Increasing flare angle with decreasing inflow

In the previous case the maximum flare angle of the hypothetical channel was found to be only 11.42 degrees with a peak inflow of 15,000 cfs. In case three, attempts were made to increase the flare angle. It was found that the flare angle can be increased as high as almost 90.0 degrees but with lesser peak inflows. This shows that the carrying capacity of the channel reduces as the flare angle increases. Again two different studies were conducted with bottom slopes of 2.2 ft/mi and 39.6 ft/mi. The conclusion that the bottom slope does not have any influence on the flare angle was evident once again in the cases that subcritical flow was maintained. For both bottom slopes, the

maximum flare angle that could be attained was about 87.56 degrees. Tables B.3.1 and B.3.2 list the discharges, depths, velocities and time to peak discharge, and elevation for different flare angles, and peak inflows.

Case Four (Supercritical flow)

Flare angle limitation

From the results of case one it was found that with a slope of more than 211 ft/mi. the flow is supercritical for all elevations at all the sections. In this case study the bottom slope of the hypothetical channel was made as high as 22% (1100 ft/mi). With the steep slope of 1100 ft/mi., attempts were made to the limit the flare angle. The maximum flare angle that was possible was found to be 64.01 degrees. Now, with the same peak inflow of 15,000 cfs. for subcritical conditions, the model was not able to handle more than 11.42 degrees. This shows that the flow condition (subcritical/supercritical) certainly has a direct influence on the maximum flare angle. The study was carried on with three different peak inflows of 5,000, 10,000, 15,000 cfs, respectively. In the supercritical state increasing or decreasing the peak inflow resulted in about the same maximum flare angle of 64.01 degrees for all peak discharges. Tables B.4.1, B.4.2, and B.4.3 list the discharges, depths, velocities, time to peak discharge, and elevation for different flare angles having a steep slope of 1100.0 ft/mi.

Case Five (Combination of Subcritical and Supercritical flow)

Flare angle limitation

In case five, attempts were made to model the hypothetical channel with multiple slopes, i.e., with both subcritical and supercritical slopes. The slopes for the hypothetical channel, in case five, were varied from 2.2 ft/mi to 1100 ft/mi. All elevations in all the sections remained subcritical for slopes less than 39.6 ft/mi. In this case the maximum flare angle that could be

achieved was about 64.01 degrees which is the same as found in case three. The latest version of DAMBRK (Fread, 1988), allows the model to perform the routing procedure for a mix of slopes of the subcritical and supercritical state. Fig 3.5 shows the distribution of slopes along the length of the channel. The discharges, depths, velocities, and time to peak discharge, and maximum elevation for different flare angles in this hypothetical channel are listed in Table B.5.1.

3.4 Summary

All the major findings that have been identified in the research study, so far, will be summarized in the following section.

Subcritical state

The maximum slope that can be dealt with in the DAMBRK model was found to be 39.6 ft/mi. (<1%). Elevations in some sections started having supercritical flows for slopes greater than 39.6 ft/mi. This situation can be handled in the DAMBRK model. The maximum flare angle, with a peak inflow of 15,000 cfs.,was found to be only 11.42 degrees; but with a substantial decrease of the peak inflow to 5,000 cfs., it was possible to increase the flare angle to 87.56 degrees.

Supercritical state

The model results showed that at slopes greater than 211 ft/mi., the flow will become supercritical. With a peak inflow of 15,000 cfs., the maximum flare angle was found to be 64.01 degrees, which is less than that found for the subcritical state.

Critical state

According to the DAMBRK model, flows with Froude numbers less than or equal to 0.95 are grouped as subcritical flows, while flows having Froude numbers of greater than or equal to 1.05 are grouped as supercritical flows.

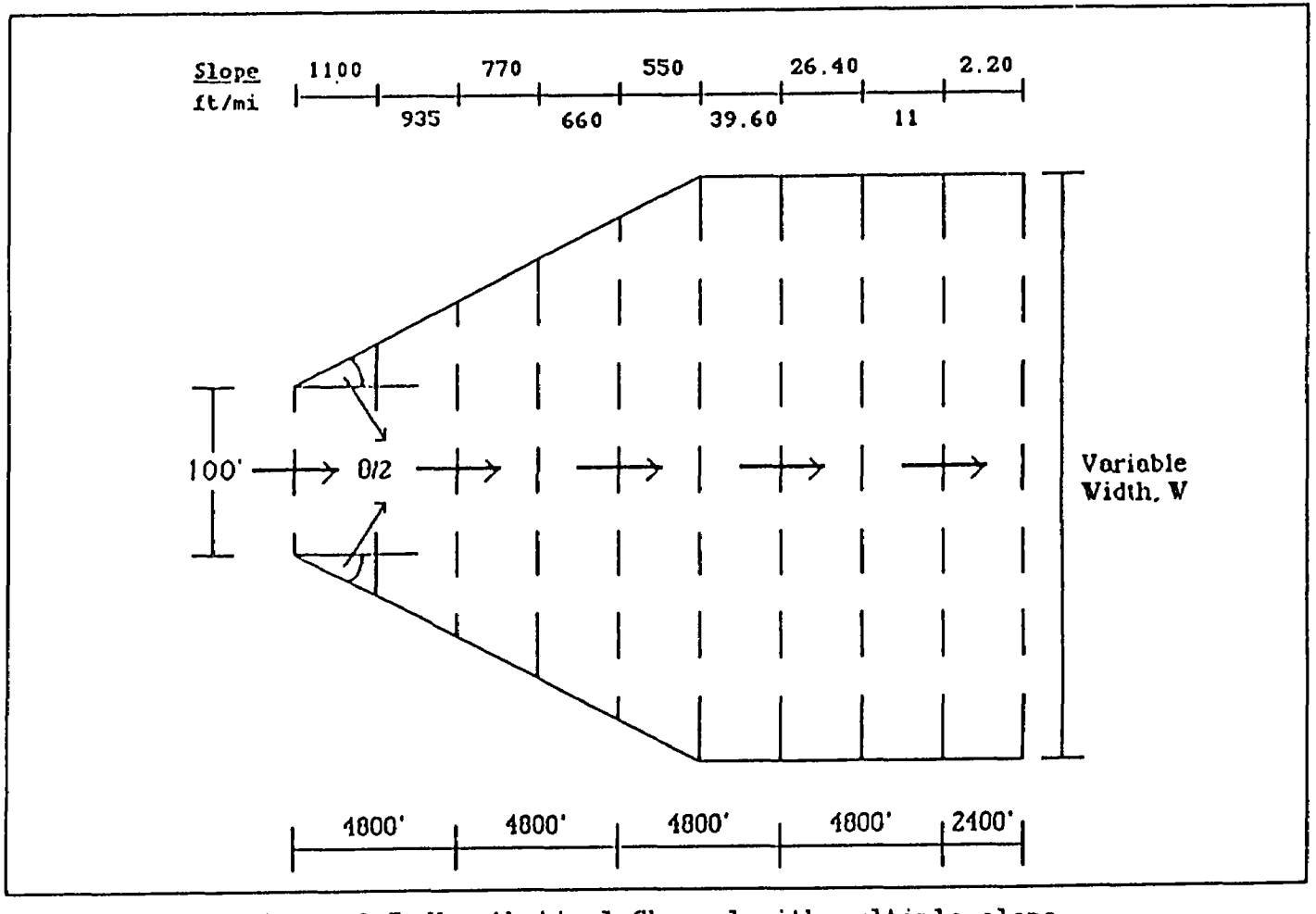

Figure 3.5 Hypothetical Channel with multiple slope.

In between the slopes of 39.6 ft/mi and 211 ft/mi., the flow remained in the transition state and the Froude numbers also varied within the range.

Other possible ways to model alluvial fans will also be tested with the actual application are the following:

1. For very large flare angles use cross-sections that are defined radially.
2. In defining the cross-sections consider the portions of flow on the outer part of the fan as dead storage areas.

CHAPTER 4

LOST DOG WASH APPLICATION

4.1 Description of the Area

Among all the available alluvial fans here in Arizona, it is not an easy task to select one site for modeling purposes. The selection of an alluvial fan primarily depended on the following set of criteria.

- Available detail topography,
- Hydrology of the area,
- Relatively easy drainage pattern.

After carefully considering the criteria described above, the alluvial fan known as "Lost Dog Wash" also referred to as "Dead Dog Wash" (Pearthree, 1988, p. 1) was selected for the modeling purpose. The alluvial fan is located on the southern piedmont of the McDowell Mountains (see Figure 4.1). The intent behind selecting this particular alluvial fan is to develop a modeling procedure; so that the DAMBRK model can be applied to much more complex situations depending on the procedure developed. Maps at a scale of 1"=100' with a 2 ft. contour interval were available for this site from the City of Scottsdale, Scottsdale, Arizona (see Figure 4.2). The hydrology of the area was also available from the same source. Finally, the drainage pattern depicts an easier form in comparison with other available alluvial fan information.

In addition to the work done on the hypothetical channels, a major portion of the study was performed on Lost Dog Wash. The geomorphic units are delineated to show how recently they have been active. The criteria set to delineate these units are topography, surface characteristics, and the amount of soil-profile development associated with the units (Pearthree, 1988,p. 1). Figure 4.1 shows the location of Lost Dog Wash along with the other

geomorphic units. Figure 4.2 shows the detailed topographic features of the Lost Dog Wash alluvial fan. Figure 4.2 shows the 2 ft. interval contour map for the Lost Dog Wash.

The southern piedmont of the McDowell Mountains was divided into four units (Figure 4.1). The geomorphology of the area is better described by Pearthree (1988, p. 2) of the Arizona State Geological Society as follows:

> The geomorphology of the McDowell Mountains in the vicinity of Dead Dog Wash is fairly typical of piedmonts of central and southern Arizona. Piedmonts that are not associated with active fault zones commonly are composed of alluvial fan deposits of a wide variety of ages. Because active faulting is not important in southern and central Arizona (Menges and Pearthree, 1983; Pearthree and Scarborough, 1985), fan deposition has been controlled by climatic changes that have occured periodically during the past 2 million years (the Quarternary period). The past 10,000 years (the Holocene period) have been an interval of extensive alluvial fan-deposition in the southwestern U.S. (Bull, 1988); hence, much of the piedmont in the Dead Dog Wash area is composed of fans that are younger than 10,000 years old (units 2, 3, and 4; Figure 4.1). At present, Dead Dog Wash is confined to a fairly well defined channel for about 1 km (1/2 miles) out onto the piedmont, at which point it spreads out into a distributary flow system (unit 4). However, in the geologically recent past (sometime in the past 10,000 years), Dead Dog Wash was depositing alluvial fans near the mountain front (units 2 and 3). The extensive alluvial fan deposits mapped as unit 1 probably record a much older interval of fan deposition similar to that

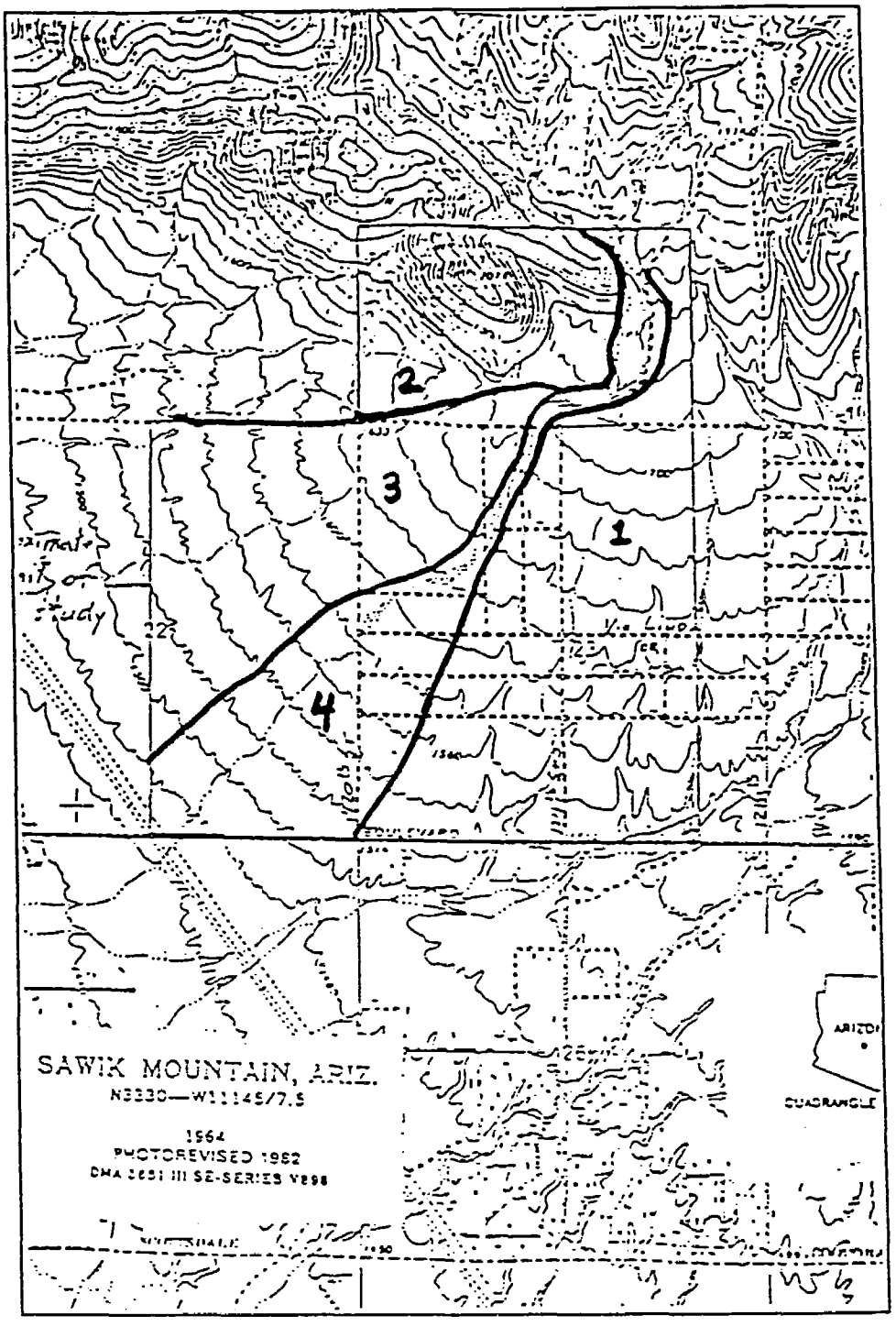

Figure 4.1 Location of the Lost Dog Wash.
(After Pearthree, 1988, p.2)

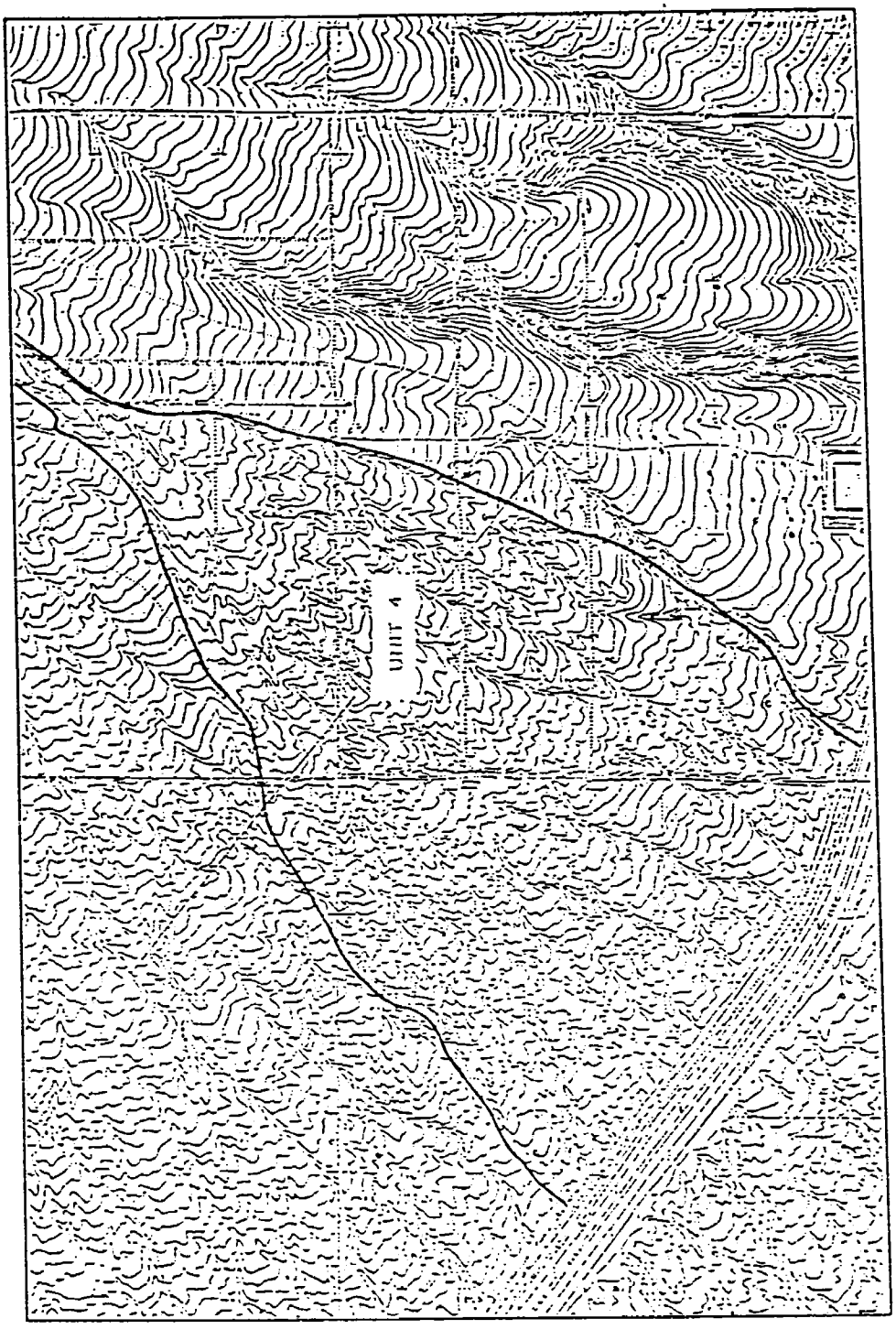

Figure 4.2 Detailed topography of the Lost Dog Wash.

which has occured in the past 10,000 years.

The channel which contributes flow to these units, forms after two other streams are combined in the upper part of the selected site (shown in Figure 4.1.). The combined stream then flows around the McDowell Mountains and forms the flow system. The Lost Dog Wash fan (unit 4) was modeled from a point where the narrow stream starts to spread out. The average width of the channel at the mouth was about 90 ft. The width of the fan varied in the downstream direction; and the maximum width was 1040 ft. The length of the fan (unit 4) was 0.33 miles (about 1750 ft.). The measured flare angle is 31.11 degrees on the average.

4.2 Defining Cross-Sections

The geomorphology of the area changes with distance from the mountain and offers a fairly complex situation. The major complexity arises while defining the cross-sections of these fans for the purpose of modeling. The 0.33 mile long alluvial fan was defined by ten cross-sections. A straight line cross-section taken across the fan presents a view as in Figure 4.3.; which clearly shows that the fan surface appears to have an upward convex shape, if cross-sections are taken as a straight line. This particular finding supports the statement that the cross alluvial fan sections are of convex shape (Bull, 1977, p.222). This offers a great difficulty in modeling fan systems like this. In order to get around this problem, it is proposed to take the cross-sections along the contour intervals. The widths of the sections would be the average lengths of the contours. To make the cross-sections perpendicular to the flow direction, sometimes the cross-sections are divided and taken radially as shown in Figure 4.4. The very first cross-section at the mouth of the fan was taken as the apex of the fan. The distances between the cross-sections varied from 0.03 miles (about 160 ft.) to 0.04 miles (about 211 ft.). And the average slopes for

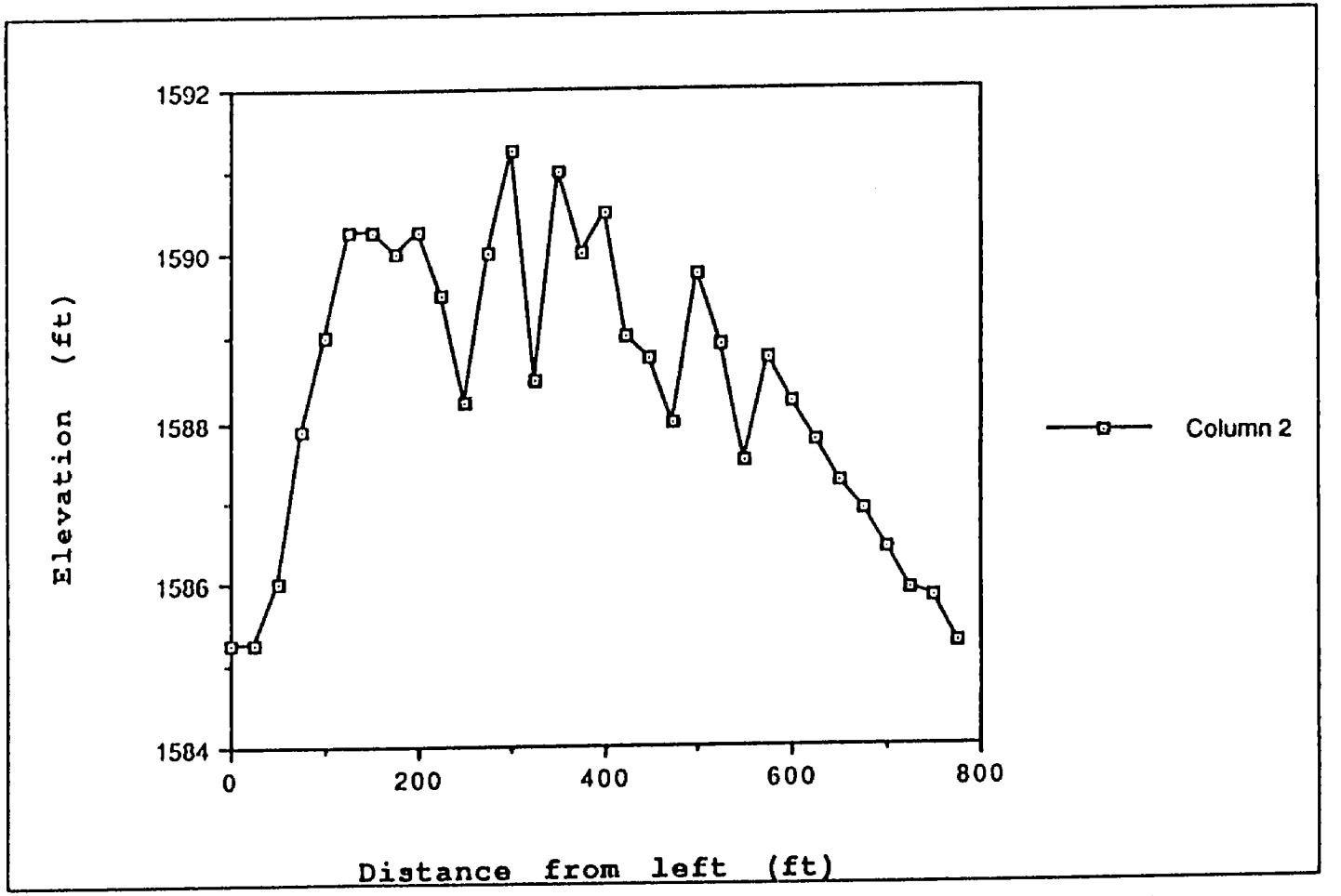

Figure 4.3 Typical cross-section across alluvial fans.

different reaches varied from 293 ft/mi to 396 ft/mi.

4.3 Modeling the Fan

As found in the previous section the actual slopes for the fan varied from 293 ft/mi to 396 ft/mi. Referring back to case one study of this report, it is clearly seen that the flow ocurring in this fan is going to be supercritical; because about 40 ft/mi slope was the limit for subcritical flows found in the case one study. The second routing option described in routing option, chapter three, was chosen to model the fan. The option is as follows:

> "Supercritical dynamic routing of an input hydrograph through the downstream channel/valley."

The "Lost Dog Wash" fan was modeled in various approaches. To determine the minimum flow required to use DAMBRK, different peak inflows were used, which ranged from 5,000 cfs. to 15,000 cfs. The initial steady, nonuniform flow for the model was varied to determine the minimum flow to keep DAMBRK running. Tables 4.1, 4.2, and 4.3 list minimum flow, initial depth, peak outflow, etc. for three different Manning's roughness coefficients.

The minimum flow required to run the model does not have any direct correlation with the peak inflow, except for the first case in Table 4.3.; where the minimum flow required was 345 cfs. instead of 310 cfs., when peak inflow was increased from 12,500 cfs. to 15,000 cfs. As the Manning's roughness coefficients (n values) decreased, the minimum flow required to run the model also decreased from 1520 cfs. for n=0.05 to 310 cfs. for n=0.03.

Initial depth and the depth of flow kept decreasing with decreasing n values; but the peak outflow and velocity of flow was increasing at the same time. The peak outflow increment was not of any substantial magnitude. A 20% decrease (from 0.05 to 0.04) in n value decreases the depth of flow by 10%

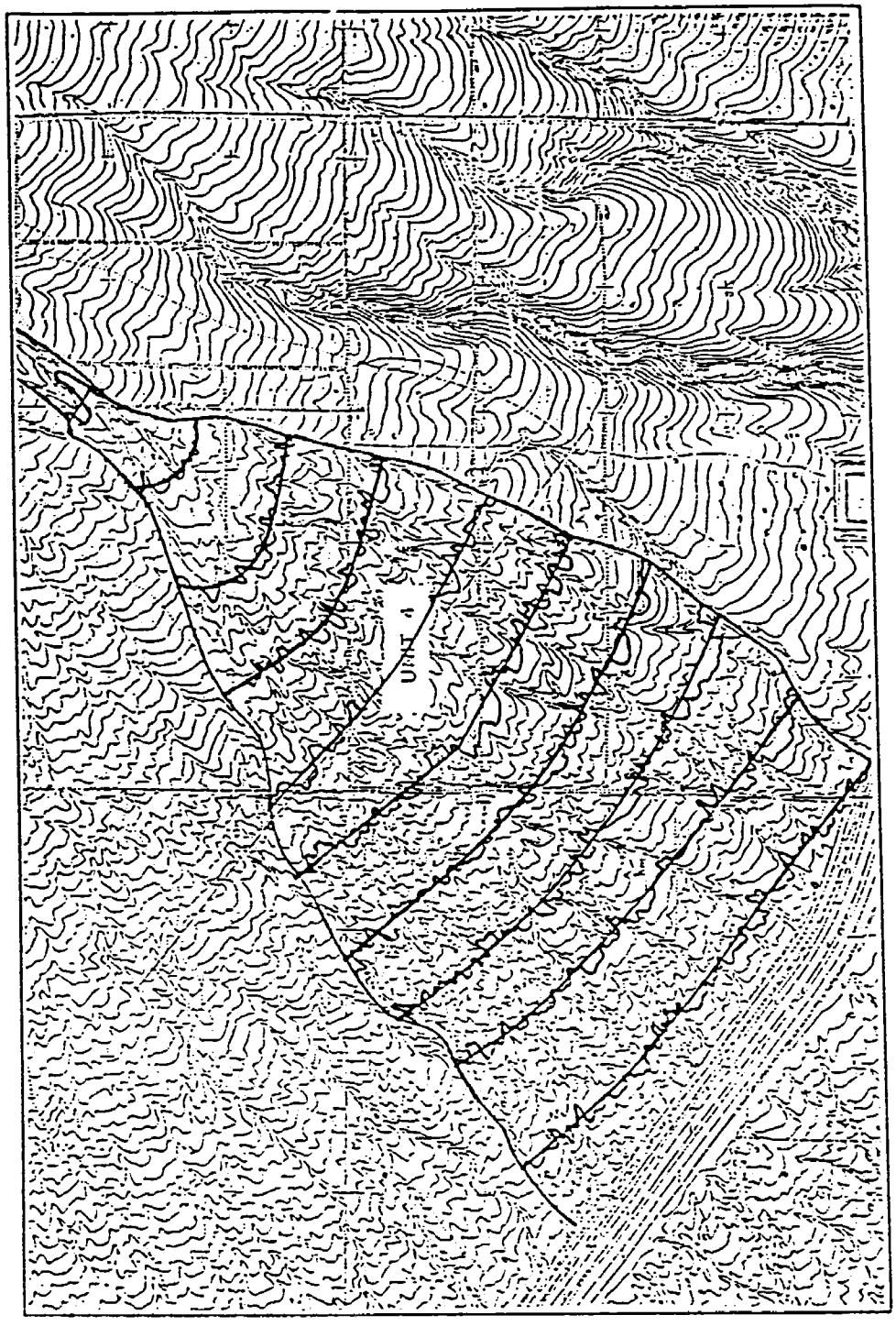

Figure 4.4 Radially defined cross-sections.

Table 4.1.- Initial Condition at Different Peak Flow with n=0.05.

Section	Peak Inflow	Min^m Flow	Initial Depth	Depth of Flow	Peak Outflow	Time	Max^m Velocity
	(cfs)	(cfs)	(ft)	(ft)	(cfs)	(hrs)	(ft/sec)
	(1)	(2)	(3)	(4)	(5)	(6)	(7)
6	15,000	1,520	0.38	1.48	14,927	2.0	11.42
	12,500	1,520	0.38	1.33	12,435	2.0	10.63
	10,000	1,520	0.38	1.16	9,945	2.0	9.73
	7,500	1,520	0.38	0.98	7,455	2.0	8.67
	5,000	1,520	0.38	0.77	4,969	2.0	7.38
10	15,000	1,520	0.36	1.49	14,845	2.0	9.57
	12,500	1,520	0.36	1.33	12,363	2.0	8.95
	10,000	1,520	0.36	1.15	9,884	2.0	8.23
	7,500	1,520	0.36	0.96	7,407	2.0	7.39
	5,000	1,520	0.36	0.75	4,936	2.0	6.34

Note :

Avg. Slope : varies from 293 ft/mi to 396 ft/mi

Flare Angle : 31.11 degrees.

Table 4.2.- Initial Condition at Different Peak Flow, with n=0.04.

Section	Peak Inflow	Min^m Flow	Initial Depth	Depth of Flow	Peak Outflow	Time	Max^m Velocity
	(cfs)	(cfs)	(ft)	(ft)	(cfs)	(hrs)	(ft/sec)
	(1)	(2)	(3)	(4)	(5)	(6)	(7)
6	15,000	728	0.22	1.31	14,934	2.0	13.00
	12,500	728	0.22	1.17	12,441	2.0	12.10
	10,000	728	0.22	1.02	9,948	2.0	11.08
	7,500	728	0.22	0.86	7,457	2.0	9.88
	5,000	728	0.22	0.67	4,967	2.0	8.42
10	15,000	728	0.21	1.33	14,858	2.0	10.77
	12,500	728	0.21	1.18	12,373	2.0	10.06
	10,000	728	0.21	1.03	9,890	2.0	9.25
	7,500	728	0.21	0.86	7,409	2.0	8.31
	5,000	728	0.21	0.66	4,932	2.0	7.13

Note :

Avg. Slope : varies from 293 ft/mi to 396 ft/mi

Flare Angle : 31.11 degrees.

Table 4.3.- Initial Condition at Different Peak Flow, with n=0.03.

Section	Peak Inflow	Min^m Flow	Initial Depth	Depth of Flow	Peak Outflow	Time	Max^m Velocity
	(cfs)	(cfs)	(ft)	(ft)	(cfs)	(hrs)	(ft/sec)
	(1)	(2)	(3)	(4)	(5)	(6)	(7)
6	15000	345	0.12	1.11	14945	2.0	15.36
	12500	310	0.11	0.99	12449	2.0	14.30
	10000	310	0.11	0.86	9955	2.0	13.10
	7500	310	0.11	0.73	7462	2.0	11.69
	5000	310	0.11	0.57	4970	2.0	9.96
10	15000	345	0.11	1.13	14880	2.0	12.64
	12500	310	0.08	1.01	12391	2.0	11.78
	10000	310	0.08	0.88	9904	2.0	10.82
	7500	310	0.08	0.74	7419	2.0	9.70
	5000	310	0.08	0.57	4937	2.0	8.33

Note:

Avg. Slope : varies from 293 ft/mi to 396 ft/mi

Flare Angle : 31.11 degrees.

to 13% and increases the flow velocity by about the same amount, whereas a decrease of 25% (from 0.04 to 0.03) in n value produces a decrease of 13% to 16% for the depth of flow and increases the flow velocity by about the same percentage. These results are shown in Table 4.4.

Appendix D provides the input for one single set up of the model Lost Dog Wash. The corresponding output follows the input.

Table 4.4.- Percentage Change in Flow Depth and Velocity with Change of n Values.

		n value Reduction of 20%		n value Reduction of 25%	
Section	Peak Inflow (cfs)	Depth of flow, % Reduction	Velocity % Increase	Depth of flow, % Reduction	Velocity % Increase
6	15000	11.49	12.15	15.27	15.36
	12500	12.03	12.15	15.38	15.38
	10000	12.07	12.18	15.69	15.42
	7500	12.25	12.25	15.12	15.48
	5000	12.99	12.35	14.95	15.46
10	15000	10.74	11.14	15.04	14.79
	12500	11.28	11.03	14.41	14.60
	10000	10.43	11.02	14.56	14.51
	7500	10.42	11.07	13.95	14.33
	5000	12.00	11.08	13.64	14.41

CHAPTER 5

APPLICATION TO FAN 4 AND FAN 5 IN NORTH SCOTTSDALE

5.1 General

There is an urgency of flood-hazard management and planning, in an area, north of Scottsdale city limits, because of increasing development in the area. The Federal Emergency Management Agency (FEMA) has identified six alluvial fans in north Scottsdale. The underlying reason for interest in these six fans is the proposed Outer Loop Freeway, located to the north of Central Arizona Project aqueduct(CAP). It is important to know the impacts of the alluvial natured drainage area, and also to determine the impacts of the anticipated developments in the area, on the freeway. This is beyond the scope of this study.

The six fans cover approximately 120 square miles, which starts from the Tonto National Forest to the north to the Central Arizona Project (CAP) canal to the south. McDowell Mountain and Paradise Valley are the east and west boundaries of the area respectively. Figure 5.1 shows the approximate location of the six fans.

5.2 Hydrology of the Area

Two of these six fans (4 and 5) are chosen for the purpose of this research. Cella Barr Associates (1988) has done a complete hydrology on the area of interest, where they modelled the entire drainage basin using the United States Army Corps of Engineers' HEC-1 computer model. Several updates in the hydrology of the area resulted in an addendum report by Cella Barr Associates (1989).

Three rainfall zones were identified. The first zone, drained by alluvial fan 1, has an average 100-year 24-hour rainfall of 4.3 inches. Zones 2, 3, and 4, has an average 100-year 24-hour rainfall of 4.4 inches. And the third zone,

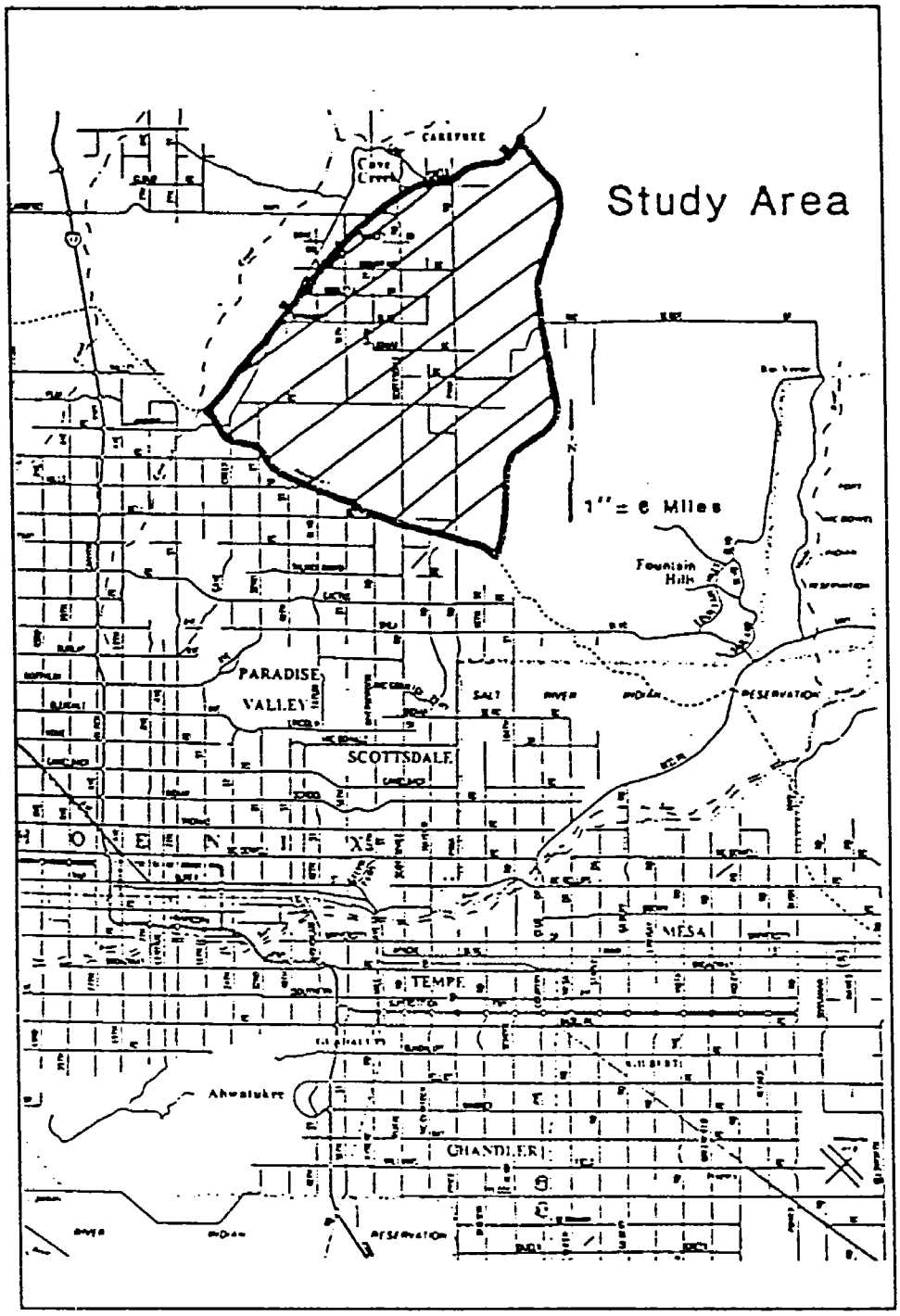

Figure 5.1 Approximate location of the study area (After SLA, 1987, p. 2).

drained by alluvial fans 5, and 6 has an average 4.8 inches of rainfall. Table 5.1 lists the different zones with different rainfall averages with several return periods (CBA, 1988, p. 11). The 24-hour 100-year average basin precipitation was prepared from the National Oceanic, and Administration Atlas (NOAA) 2, Volume VIII, Arizona, for input into the HEC-1 model. SCS Type IIA distribution was used to simulate the high-intensity rainfall characteristics of summer convective thunderstorms. Figure 5.2 shows the SCS Type IIA rainfall characteristics while Table 5.2 lists the cumulative rainfall amounts for SCS Type IIA distribution.

There was a disagreement between the CBA's drainage area division and the SCS drainage area division. This difference resulted in apexes of the alluvial fans to be in different locations in the two methods. In the addendum report CBA has relocated the apexes of the alluvial fans, with a slightly changed drainage pattern, along with the absence of some diversions as well. To use the DAMBRK model, discharges at the apexes of the alluvial fans are required as the inflow hydrograph.

5.3 Description of Fan 4

In the original report, the apex of fan 4 was at the concentration point C27. Later the concentration point was relocated to approximately one-half mile upstream of the previous location. This change was made to reflect the change in the drainage area and channel lengths. According to CBA addendum report, two finger-shaped "active" areas, one starting at a point just upstream of concentration point 19C, and the other at concentration point 22A, come together at a point just upstream of the apex. The combined discharge hydrograph at concentration point C27 was input as the inflow hydrograph to the DAMBRK model. The average width of the fan at the apex

Table 5.1.-Rainfall Amount for 24-Hour Duration for Different Return Periods.

Return Period (1)	Zone 1 (2)	Zone 2 (3)	Zone 3 (4)
2 Year	2.16	1.95	1.90
5 Year	2.81	2.55	2.49
10 Year	3.24	2.96	2.89
25 Year	3.79	3.46	3.38
50 Year	4.29	3.94	3.85
100 Year	4.78	4.39	4.29

Note :

Zone 1 : Basin 1340-1500

Zone 2 : Basin 1-53

Zone 3 : Basin 2005-2051

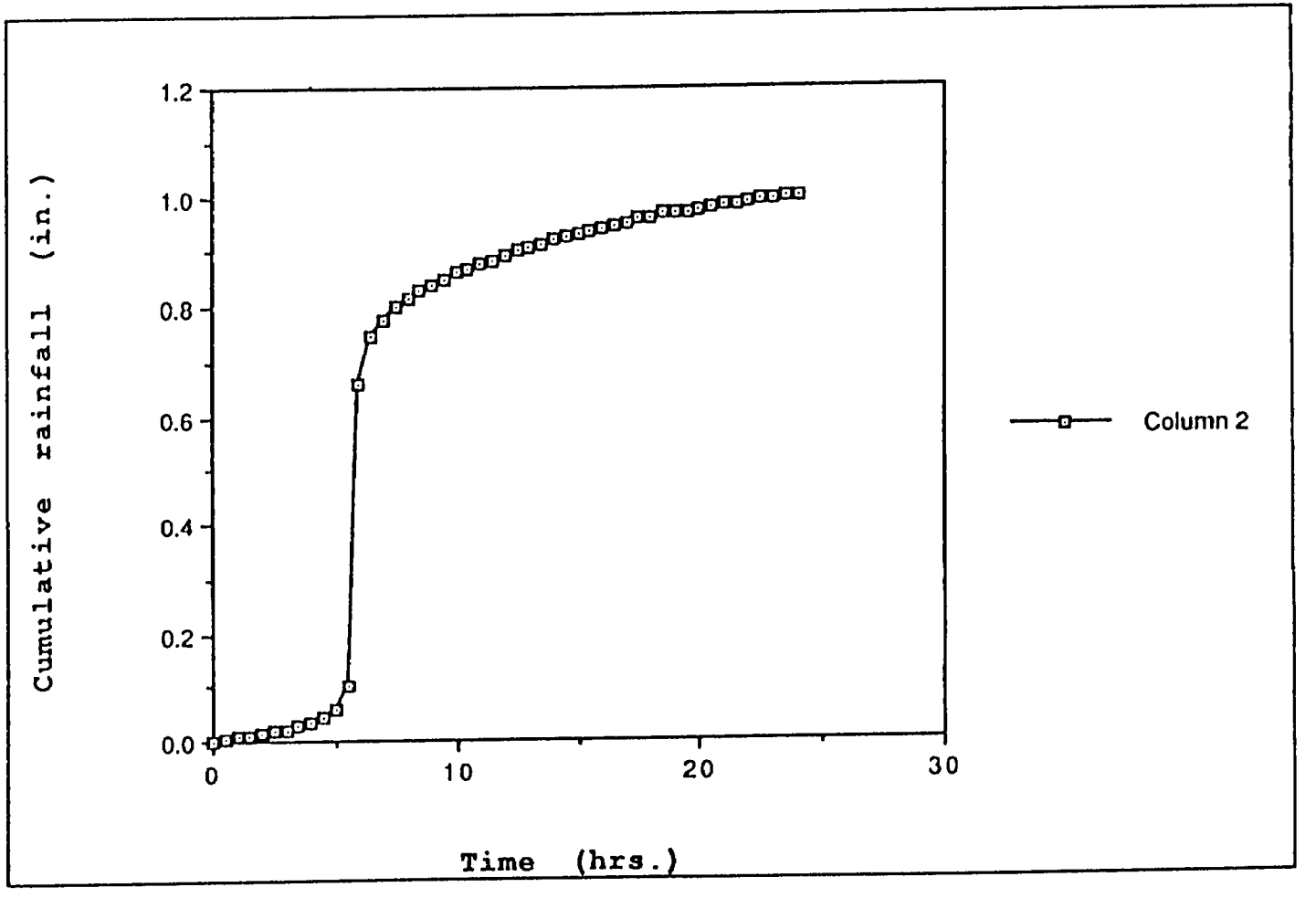

Figure 5.2 SCS type IIA rainfall characteristics.

Table 5.2.- Rainfall Distribution for SCS Type IIA

Time (hr) (1)	Cumulative Rainfall (2)	Time (hr) (3)	Cumulative Rainfall (4)	Time (hr) (5)	Cumulative Rainfall (6)
0.0	0.0	8.5	0.830	17.0	0.950
0.5	0.005	9.0	0.840	17.5	0.958
1.0	0.009	9.5	0.850	18.0	0.961
1.5	0.010	10.0	0.861	18.5	0.968
2.0	0.013	10.5	0.868	19.0	0.969
2.5	0.0.019	11.0	0.878	19.5	0.97
3.0	0.021	11.5	0.884	20.0	0.974
3.5	0.028	12.0	0.891	20.5	0.979
4.0	0.032	12.5	0.900	21.0	0.981
4.5	0.044	13.0	0.905	21.5	0.985
5.0	0.057	13.5	0.912	22.0	0.989
5.5	0.100	14.0	0.919	22.5	0.991
6.0	0.660	14.5	0.923	23.0	0.993
6.5	0.745	15.0	0.930	23.5	0.996
7.0	0.776	15.5	0.934	24.0	1.000
7.5	0.800	16.0	0.939		
8.0	0.816	16.5	0.944		

(C27) was 3000 ft. Increasing width in the downstream direction reached a maximum value of 16,300 ft. at the toe of the fan at section 11. The overall length of the fan, from the apex to the toe, as found from the drainage basin map, was about 5.19 miles. Longitudinal slope of Fan 4 varied from 65.19 ft/mi to 138 ft/mi. Measured average flare angle was about 27.29^{o}. The number of cross-sections used to describe fan 4 was eleven. These sections were taken along the 50 feet contour intervals. Figure 5.3 is the topographic map showing the boundaries of the alluvial fan 4 along with the cross-sections used to define fan 4 in the DAMBRK model.

5.4 Description of Fan 5

In an after field survey of alluvial fan 5, it was revealed that the area between C1481 and halfway through area 1500 to approximately Dynamite Boulevard is old (Pleistocene in age, based on surface soils), is dissected and contains outcropping of granite bedrock one or two feet below the ground surface along the channel banks (CBA, 1989, p. 1). For this reason, the apex of the alluvial fan 5 was relocated at the concentration point C1481. Concentration point C1500A is located at the downstream limit of the "inactive" area of the sub-basin 1500A. In the original report (CBA, 1988, p. 15) the apex of the alluvial fan 5 was at C1500, which may be regarded as C1500B in the new model set-up. The average width of fan 5 at the apex (C1481) was 500 ft. The widths increased in the downstream direction until it reached a maximum value of 20,000 ft. at the toe of the fan. The overall length of the fan, from the apex to the toe, as found from the drainage basin maps, was 8.59 miles. Longitudinal slope of the fan varied from 54.43 ft/mi to 114.78 ft/mi. Measured average flare angle was about 24.26^{o}. Fifteen cross-sections were used to describe the 8.59 mile long fan 5. Again, the cross-sections were taken along the 50 feet contour intervals. Figure 5.4 is the topographic map showing

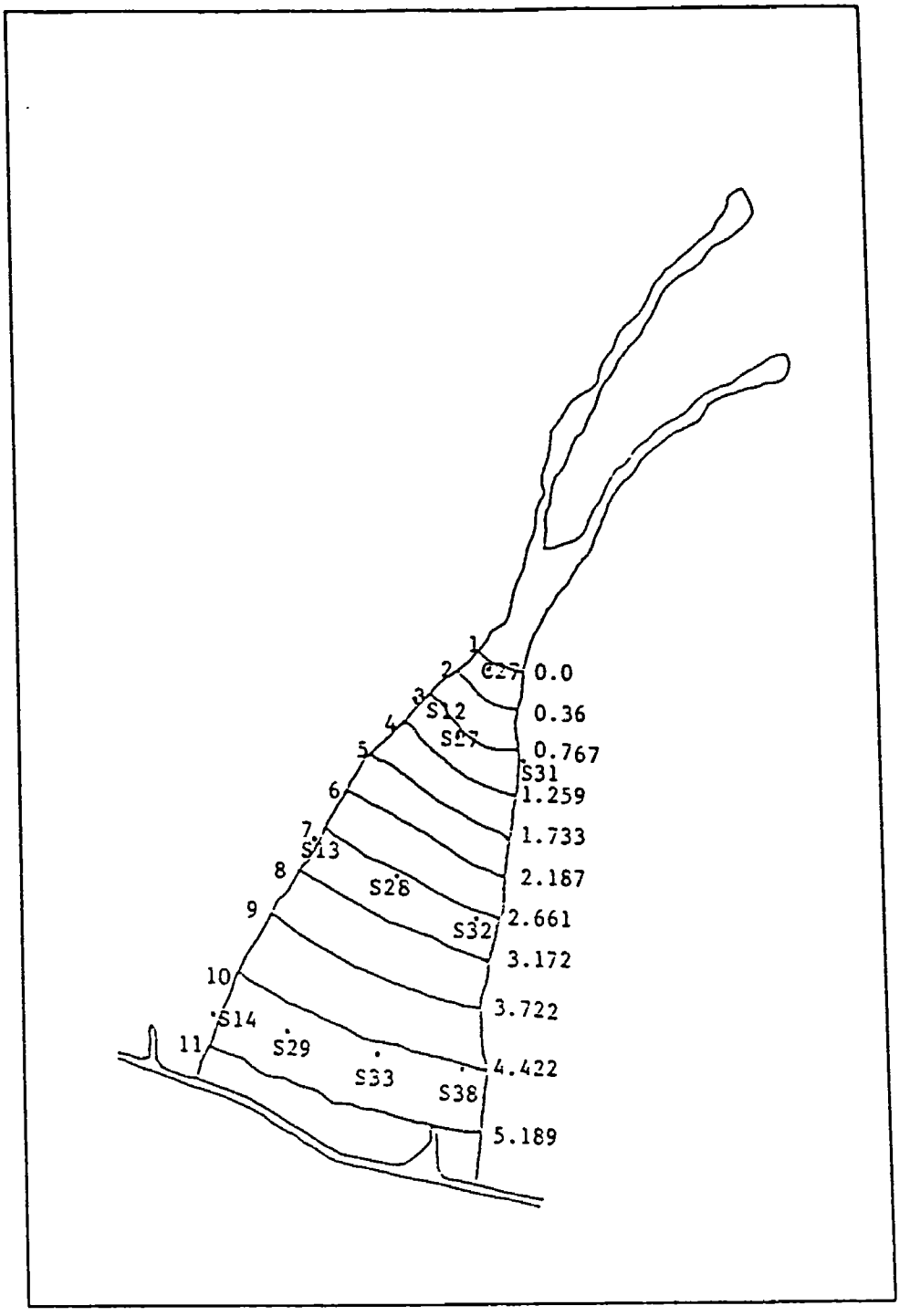

Figure 5.3 Boundaries of alluvial fan 4 with the cross-sections.

the boundaries of the alluvial fan 5 along with the cross-sections used to define fan 5 in the DAMBRK model.

5.5 Hydrology of Fan 4 and Fan 5

The changes in the drainage pattern, within the area of interest, discussed in a previous section, were in corporated in the United States Army Corps of Engineers' HEC-1 Flood Hydrograph Package computer model. The HEC-1 model produces the hydrographs at the apexes, concentration points C27 and C1481 respectively, of fan 4 and fan 5. These hydrographs were used as the inflows to the DAMBRK model. The Manning's roughness coefficient used for fan 4 was 0.045; while a value of 0.050 was used to model fan 5. The width of the flow area was taken as the boundary of the alluvial fans as shown on the drainage basin maps.

The inflow hydrograph at the apex of Fan 4 had a local peak flow of 9,600 cfs. within 20 minutes but attained a peak flow of 12,150 cfs., as can be seen in Figure 5.5(a), within about 50 minutes. Similarly, the inflow at the apex of Fan 5 had a peak flow of 4,822 cfs within only 25 minutes as shown in Figure 5.5(b). The time required for the inflow hydrograph at C27 to recede back to the initial flow (200 cfs.) was about 14 hours; while the inflow hydrograph at C1481 took about only 5 hours to come back to it's initial flow. Table 5.3 lists the two hydrographs at the concentration points C27 and C1481. Fig 5.5 shows the inflow characteristics of the two flood events.

5.6 Approaches

Both fan 4 and fan 5 were modeled with the discharge hydrographs at the apexes only (Table 5.3 and Fig. 5.5). This approach enabled determination of the flow velocities and the depths of flow in different parts of the alluvial fan considering only the inflow at the apex. The second approach adopted to model these fans was to use the discharges from the sub-basins within the

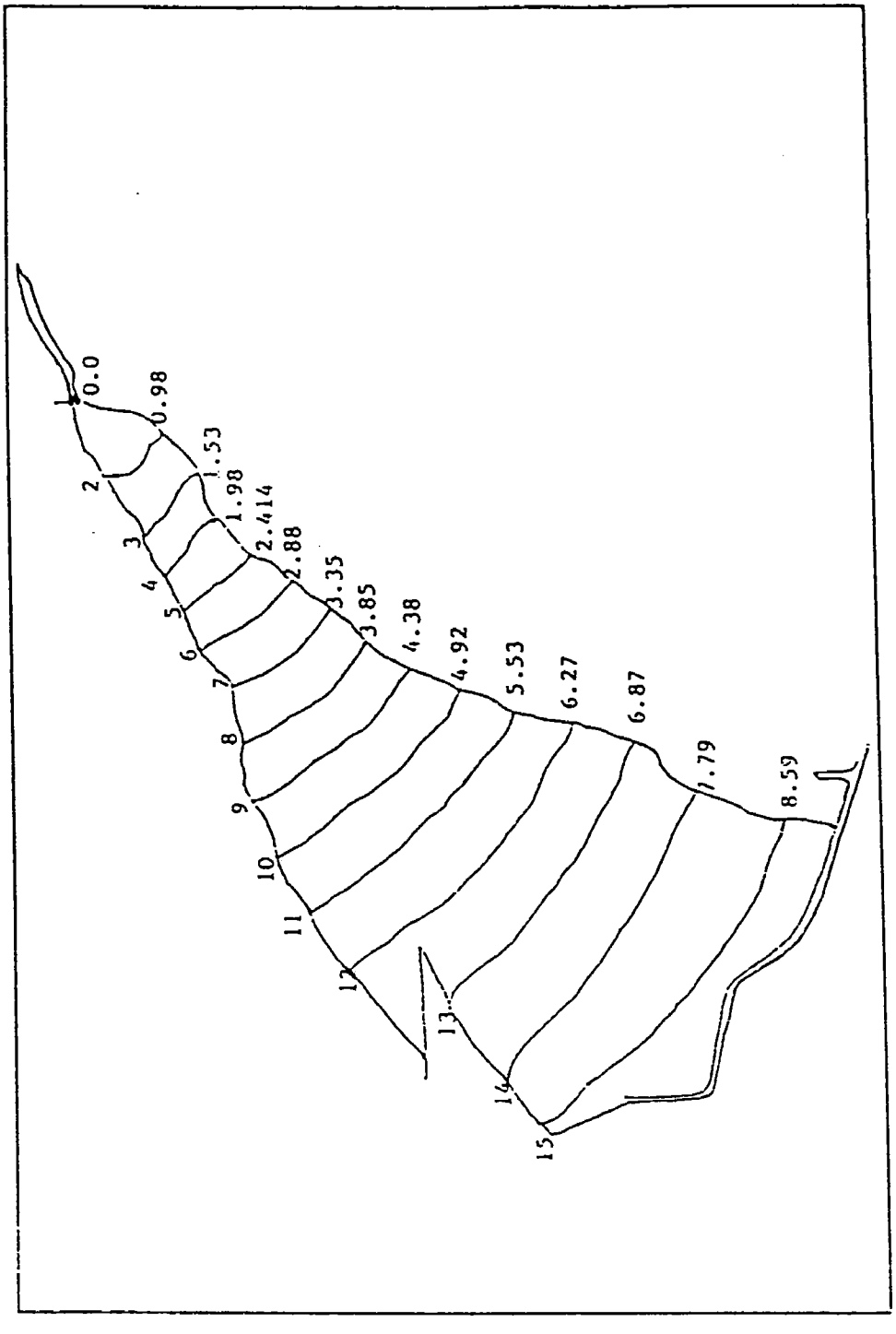

Figure 5.4 Boundaries of alluvial fan 5 with the cross-sections.

Table 5.3.- Discharge Hydrographs at the Apexes.

Fan4 Inflow (CP27)				Fan5 Inflow (CP1481)			
Time (1)	Flow (2)	Time (3)	Flow (4)	Time	Flow	Time	Flow
0	200	120	2400	0	100	120	400
5	600	125	2200	5	400	125	400
10	1200	130	2000	10	1400	130	400
15	6800	135	2000	15	3300	135	400
20	9600	140	1800	20	4500	140	300
25	9000	145	1600	25	4822	145	300
30	8000	155	1600	30	4500	155	300
35	7200	160	1400	35	3800	160	300
40	7800	170	1400	40	3100	170	300
45	11000	175	1200	45	2600	175	275
50	12150	190	1200	50	2200	190	200
55	10600	195	1000	55	1900	195	200
60	9000	215	1000	60	1600	215	200
65	7800	220	800	65	1400	220	200
70	6800	265	800	70	1200	265	200
75	5800	270	600	75	1100	270	200
80	5200	300	600	80	900	300	200
85	4600	305	600	85	800	305	100
90	4000	385	600	90	800	385	100
95	3600	390	400	95	700	390	100
100	3400	815	400	100	600	815	100
105	3000	820	200	105	500	820	100
110	2800	1040	200	110	500	1040	100
115	2600	1080	200	115	500	1080	100

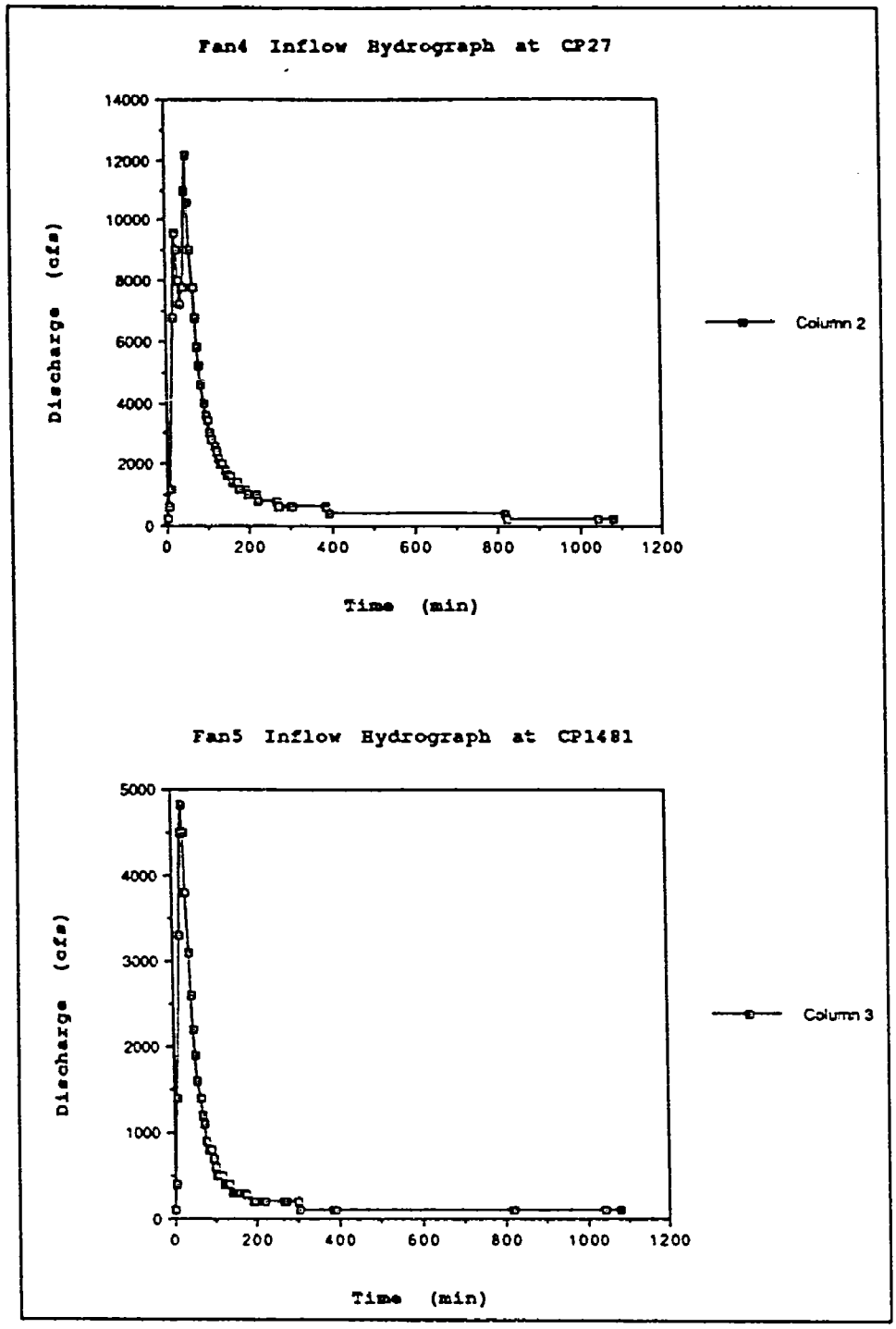

Figure 5.5 Discharge hydrographs at the apexes.

alluvial fan boundary in addition to the hydrographs at the fan apexes. These discharges, from the sub-basins, were used as lateral inflows to the DAMBRK model. The second approach was not possible to apply on fan 5 because of limited availability of drainage maps.

5.7 Flows from the Sub-Basins

Sub areas that are included within fan 4 are sub-basins 12, 13, 14, 27, 28, 29, 31, 32, 33, and 38. All these sub-basins produced individual outflow hydrographs. These hydrographs were combined to produce three different lateral inflow hydrographs to the DAMBRK model. Flows from sub areas 12, 27, and 31 were combined to produce lateral 1, as shown in Table 5.4 and Fig. 5.6, with a peak flow of 3,000 cfs. within 20 minutes. The peak flow from lateral 2, as shown in Table 5.5 and Fig. 5.7, which is a combination of flows from sub areas 13, 28, and 32, was 2,573 cfs. and it was achieved in only 25 minutes. The third lateral inflow hydrograph shown in Table 5.6 and Fig. 5.8, which is the combination of flows from sub areas 14, 29, 33, 38, was 3,770 cfs. in 35 minutes.

5.8 Results

The application the US National Weather Service DAMBRK model to the alluvial fans was possible with different approaches. Both Fan 4 and Fan 5 had to be modeled with the mixed flow algorithm option of the model.

Fan 4 was modeled in two ways. First, only with the inflow hydrograph at the apex, and second, adding the discharges from the sub-basins within the fan boundaries. The velocity and the depth of flow from the DAMBRK model is compared with the same values from the FEMA method. The maximum velocity, found by the FEMA method, within fan 4 was 8.0 ft/sec with a minimum value of 6.0 ft/sec. On the other hand, DAMBRK produces a maximum velocity of 5.18 ft/sec and a minimum value of 0.98 ft/sec. The

Table 5.4.- Inflow Hydrograph for Lateral 1.

	DISCHARGES			
Time (min) (1)	Sub12 Outflow (cfs) (2)	Sub27 Outflow (cfs) (3)	Sub31Outflow (cfs) (4)	Lateral 1 (cfs) (5)
0	200	110	200	510
5	440	280	440	1160
10	740	570	700	2010
15	1000	834	960	2794
20	1120	800	1080	3000
25	1190	620	1137	2947
30	1140	480	1060	2680
35	960	380	920	2260
40	800	320	760	1880
45	660	280	620	1560
50	540	240	520	1300
55	460	210	420	1090
60	400	180	380	960
65	340	160	320	820
70	300	140	280	720
75	260	130	260	650
80	240	120	220	580
85	220	110	200	530
90	200	100	180	480
95	180	90	180	450
100	160	90	160	410
105	160	80	140	380
110	140	80	140	360
115	140	70	140	350
120	140	70	120	330
125	120	70	120	310
130	120	60	120	300
135	120	60	100	280
140	100	60	100	260
145	100	60	100	260
155	100	50	80	230
160	100	50	80	230
170	95	50	80	225
175	90	50	80	220
190	80	40	60	180
195	60	40	60	160
215	60	30	60	150
220	60	30	60	150
265	60	30	60	150
270	60	30	60	150
385	40	20	40	100
390	40	20	40	100
815	20	10	20	50
820	20	10	20	50
1080	20	10	20	50

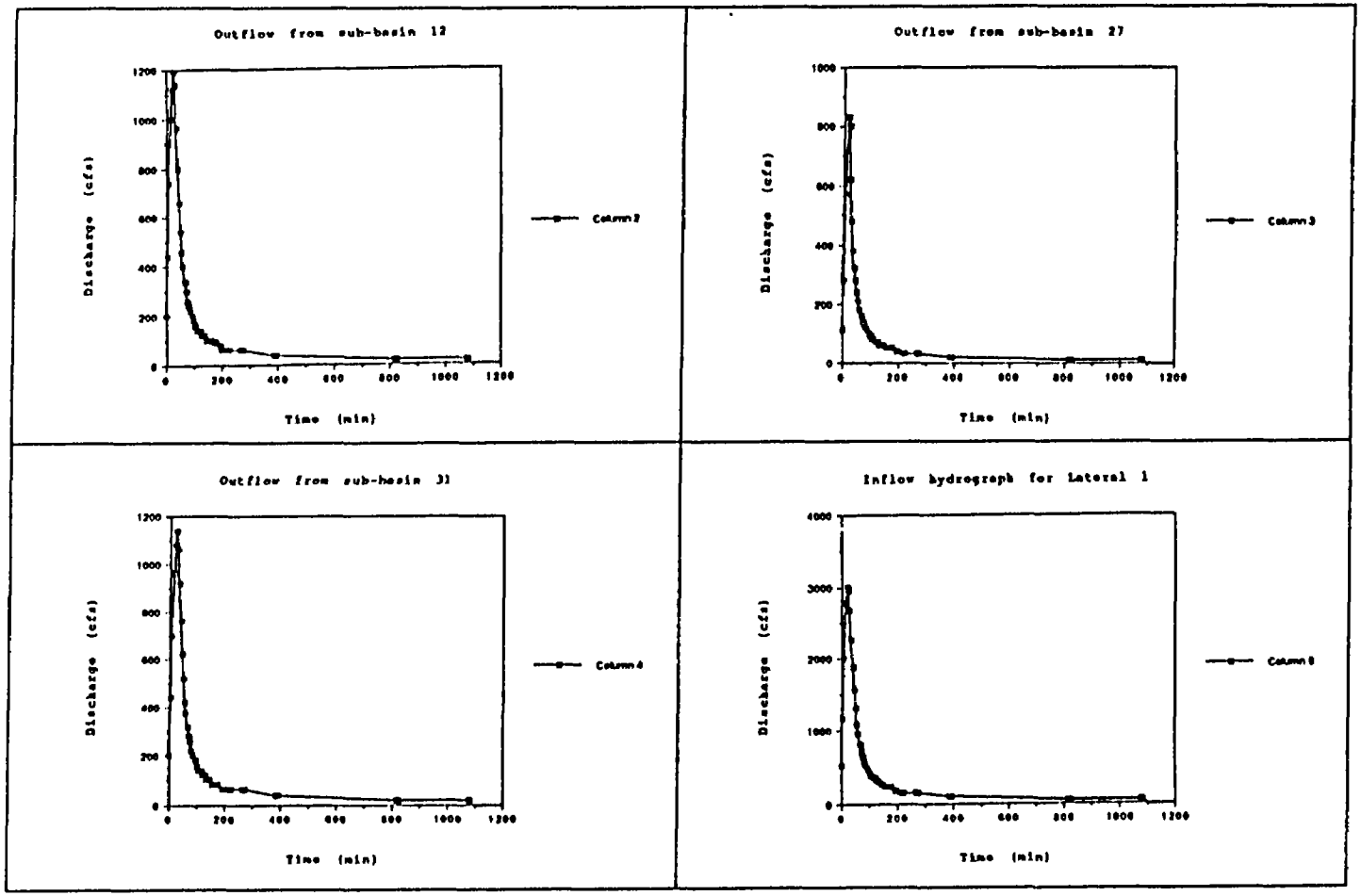

Figure 5.6 Lateral Inflow 1 with sub-basin outflows.

Table 5.5.- Inflow Hydrograph for Lateral 2.

	DISCHARGES			
Time (min) (1)	Sub13 Outflow (cfs) (2)	Sub28 Outflow (cfs) (3)	Sub32 Outflow (cfs) (4)	Lateral 2 (cfs) (5)
0	160	70	310	540
5	300	120	560	980
10	520	240	940	1700
15	680	340	1180	2200
20	780	390	1303	2473
25	840	430	1303	2573
30	880	470	1180	2530
35	912	500	1000	2412
40	840	540	810	2190
45	720	560	630	1910
50	600	590	560	1740
55	500	607	460	1567
60	420	600	400	1420
65	360	580	340	1280
70	320	520	300	1140
75	280	480	280	1040
80	260	420	240	920
85	220	380	220	820
90	200	350	200	750
95	180	320	180	680
100	180	300	180	660
105	160	280	160	660
110	140	260	160	560
115	140	240	140	520
120	120	230	140	490
125	120	210	120	450
130	120	200	120	440
135	100	195	120	415
140	100	190	100	390
145	100	180	100	380
155	100	160	100	360
160	80	150	100	330
170	80	130	80	290
175	80	130	80	290
190	60	110	80	250
195	60	110	80	250
215	60	90	60	210
220	60	90	60	210
265	60	70	60	190
270	60	70	60	190
385	40	50	40	130
390	40	50	40	130
815	20	30	20	70
820	20	30	20	70
1080	20	20	20	60

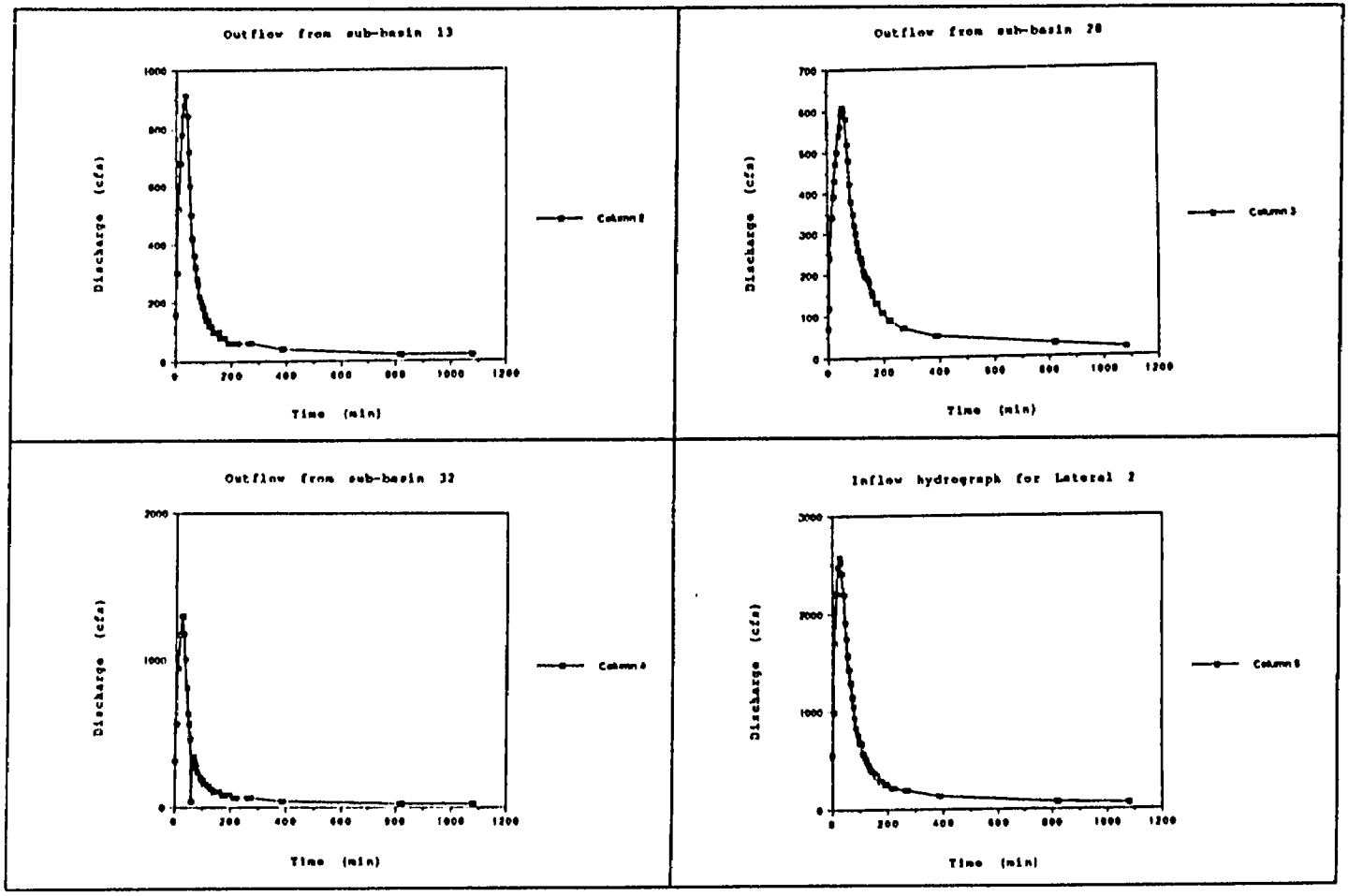

Figure 5.7 Lateral Inflow 2 with sub-basin outflows.

Table 5.6.- Inflow Hydrograph for Lateral 3.

DISCHARGES					
Time (min) (1)	Sub14 Outflow (cfs) (2)	Sub29 Outflow (cfs) (3)	Sub33 Outflow (cfs) (4)	Sub38 Outflow (cfs) (5)	Lateral 3 (7)
0	100	50	200	160	510
5	190	90	400	400	1080
10	330	160	700	700	1890
15	450	240	910	520	2120
20	510	280	1020	1080	2890
25	550	310	1100	1300	3260
30	590	330	1190	1520	3630
35	630	360	1193	1587	3770
40	660	380	1040	1500	3580
45	680	400	900	1480	3460
50	620	420	740	1500	3280
55	590	430	620	1500	3140
60	510	450	520	1400	2880
65	430	460	460	1240	2590
70	380	470	400	1080	2330
75	330	480	360	940	2110
80	290	490	320	820	1920
85	260	500	280	720	1760
90	230	500	260	660	1650
95	210	510	240	600	1560
100	190	522	220	540	1472
105	180	522	200	500	1402
110	160	510	180	440	1290
115	150	480	180	420	1230
120	140	450	160	380	1130
125	130	420	160	360	1070
130	120	390	140	340	990
135	120	370	140	300	930
140	110	350	140	300	900
145	100	330	120	280	830
155	90	280	120	240	730
160	90	270	120	240	720
170	80	250	100	220	650
175	80	240	100	200	620
190	70	210	80	180	540
195	70	200	80	180	530
215	60	180	80	160	480
220	60	170	80	140	450
265	50	130	60	120	360
270	50	120	60	120	350
385	40	80	40	100	260
390	40	80	40	100	260
815	20	40	20	60	140
820	20	40	20	60	140
1080	10	30	20	40	100

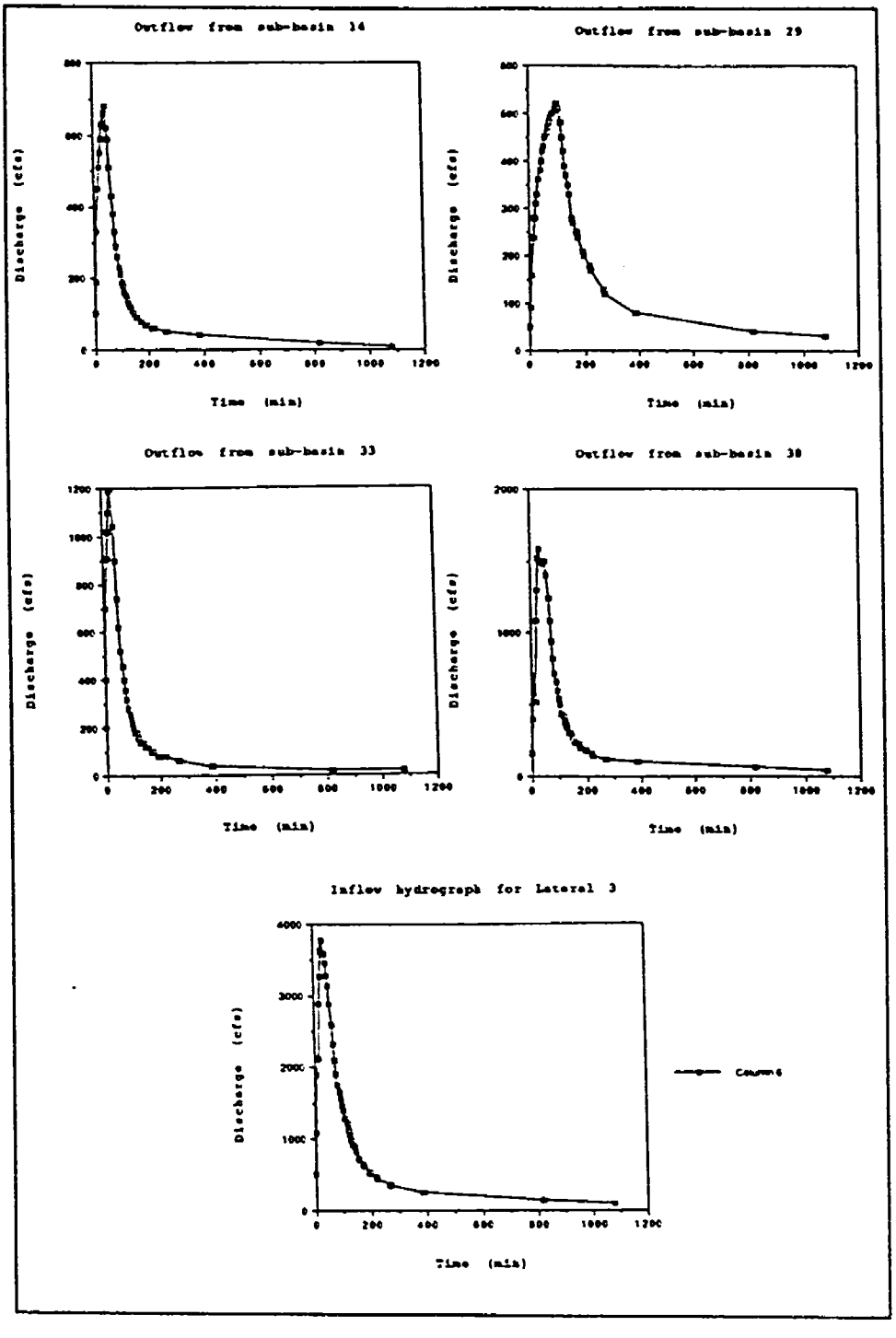

Figure 5.8 Lateral Inflow 3 with sub-basin outflows.

depth of flow found from the DAMBRK model ranged between 20% to 21% of the depth found in the FEMA method. Tables 5.7 and 5.8 show the relative comparison between the two methods.

Fan 5 also experienced both subcritical and supercritical flows. Since fan 5 could not be modeled with the sub-basin discharges, due to lack of drainage basin maps, a sensitivity analysis was performed on this fan as a second approach. The velocity ranges found from the FEMA method was between 3.0 ft/sec and 8.0 ft/sec; while the DAMBRK produces a maximum velocity of 5.62 ft/sec and a minimum velocity of 0.78 ft/sec. Again, the depths of flow found by the use of DAMBRK model was only about 20% of the depths of flow found by the FEMA method. Three different Manning's roughness coefficient values were used to perform the sensitivity analysis on fan 5. As the n value was increased in general the value of velocities also decreased. The flow velocities decreased between 3.5% to 3.7% on the average when n value increased from 0.050 to 0.52, and 0.055. These results are listed in Tables 5.9, 5.10, and 5.11.

Table 5.7.- Comparison of Velocity and Depth between DAMBRK and FEMA Method for Fan 4 (Inflow at the Apex only)

Distance from Apex	Discharge (cfs)	Velocity (ft/sec)		Depth (ft)	
	DAMBRK	DAMBRK	FEMA	DAMBRK	FEMA
0.000	12,150	5.18	8.0	0.88	3.0
0.360	11,487	3.98	8.0	0.66	3.0
0.767	11,160	3.31	7.0	0.52	3.0
2.187	10,734	2.40	7.0	0.43	2.0
2.661	10,603	2.31	7.0	0.42	2.0
4.422	9,489	1.81	6.0	0.35	2.0
5.189	9,097	1.73	6.0	0.32	2.0

Table 5.8.- Comparison of Velocity and Depth between DAMBRK and FEMA Method for Fan 4 (Addition of Lateral Inflow)

Distance from Apex	Discharge (cfs)	Velocity (ft/sec)		Depth (ft)	
	DAMBRK	DAMBRK	FEMA	DAMBRK	FEMA
0.000	12,150	5.20	8.0	0.80	3.0
0.360	11,787	4.42	8.0	0.62	3.0
0.767*	11,670	3.56	7.0	0.50	3.0
2.187	11,897	2.42	7.0	0.47	2.0
2.661*	11,623	2.29	7.0	0.46	2.0
4.422*	11,156	1.92	6.0	0.38	2.0
5.189	11,757	1.91	6.0	0.38	2.0

*Locations of Lateral Inflow Hydrographs.

Table 5.9.- Comparison of Velocity and Depth between DAMBRK and FEMA Method for Fan5 (Inflow at the Apex only) with n=0.050.

Distance from Apex	Discharge (cfs)	Velocity (ft/sec)		Depth (ft)	
		DAMBRK	FEMA	DAMBRK	FEMA
0.000	4,822	5.62	8.0	1.72	3.0
0.98	4,698	2.41	7.5	0.45	3.0
1.53	4,608	2.48	7.0	0.42	3.0
1.98	4,528	2.44	7.0	0.43	2.0
2.89	4,275	2.04	6.0	0.33	2.0
3.35	4,145	1.92	6.0	0.32	2.0
3.85	3,994	1.65	6.0	0.27	1.0
4.38	3,829	1.49	6.0	0.23	1.0
4.92	3,673	1.33	5.0	0.20	1.0
6.28	3,315	1.07	4.0	0.17	1.0
6.88	3,213	1.01	4.0	0.19	1.0
7.79	1,698	0.78	3.0	0.10	<0.50

Table 5.10.- Comparison of Velocity and Depth between DAMBRK and FEMA Method for Fan5 (Inflow at the Apex only) with n=0.052.

Distance from Apex	Discharge (cfs)	Velocity (ft/sec)		Depth (ft)	
		DAMBRK	FEMA	DAMBRK	FEMA
0.000	4,822	5.49	8.0	1.72	3.0
0.98	4,697	2.35	7.5	0.45	3.0
1.53	4,596	2.41	7.0	0.42	3.0
1.98	4,510	2.38	7.0	0.43	2.0
2.89	4,248	1.99	6.0	0.33	2.0
3.35	4,124	1.87	6.0	0.32	2.0
3.85	3,961	1.61	6.0	0.27	1.0
4.38	3,797	1.45	6.0	0.23	1.0
4.92	3,644	1.30	5.0	0.20	1.0
6.28	3,288	1.04	4.0	0.17	1.0
6.88	3,196	0.98	4.0	0.19	1.0
7.79	1,187	0.67	3.0	0.10	<0.50

Table 5.11.- Comparison of Velocity and Depth between DAMBRK and FEMA Method for Fan5 (Inflow at the Apex only) with n=0.055.

Distance from Apex	Discharge (cfs)	Velocity (ft/sec)		Depth (ft)	
		DAMBRK	FEMA	DAMBRK	FEMA
0.000	4,822	5.31	8.0	1.82	3.0
0.98	4,693	2.27	7.5	0.48	3.0
1.53	4,590	2.33	7.0	0.44	3.0
1.98	4,490	1.92	7.0	0.45	2.0
2.89	4,222	1.81	6.0	0.35	2.0
3.35	4,094	1.55	6.0	0.33	2.0
3.85	3,940	1.39	6.0	0.28	1.0
4.38	3,774	1.25	6.0	0.24	1.0
4.92	3,613	1.00	5.0	0.21	1.0
6.28	3,264	0.94	4.0	0.18	1.0
6.88	3,169	0.64	4.0	0.20	1.0
7.79	1,149	0.78	3.0	0.10	<0.50

CHAPTER 6

SUMMARY AND CONCLUSIONS

6.1 Summary

The United States National Weather Service DAMBRK model is based upon a four-point, implicit, finite difference solution of the Saint-Venant equations for one-dimensional unsteady flows. The model was used in several hypothetical cases as well as distributary flow areas. Application of the DAMBRK model to the hypothetical cases enabled determination of the limitations of the model with respect to flare angle, longitudinal slope, fan length, peak inflows, etc. Longitudinal slope is found to have the greatest influence on the performance of all the other parameters; and it was easier to model cases where the slopes were greater. After evaluating the DAMBRK model it was applied to three actual distributary flow areas. Lost Dog Wash was the first alluvial fan that was modeled in order to develop a modeling procedure. Fan 4 and fan 5 (two of the six alluvial fans in North Scottsdale) were modeled accordingly. The 100-year 24-hour rainfall event (used by FEMA) was used for the purpose of modeling these distributary flow areas.

The Federal Emergency Management Agency (FEMA) uses a method for analyzing flood hazards on alluvial fans. The FEMA method assumes an equal probability of flooding across a contour on the alluvial fan. The depths and velocities from the DAMBRK model were compared with those found from FEMA procedure which has been applied in north Scottsdale area to analyze flooding potential. The velocities in fan 4 ranged only between 41% to 43% of the velocities found by the FEMA method. The corresponding depths in the distributary area was found to be only 20%-21% of the depths found by the FEMA method. In fan 5, the DAMBRK model produced velocities which are only about 33% of the velocities that was shown by FEMA procedure. On

the other hand, the depths of flows were only within 20% of the values that were given by FEMA method.

6.2 Limitations of using DAMBRK

The results that were obtained by use of the DAMBRK model were carefully compared with the values that have been suggested applying the FEMA method. A substantial difference exists between the results of the two methods as described above. After reviewing the application of the DAMBRK model to some of the distributary areas in north Scottsdale area the following conclusions are made :

1. In conjunction with a widely used, generally accepted, conventional method for determining the hydrology of an area, DAMBRK can be applied to determine the flooding extent of an alluvial fan considering the following limitations that the DAMBRK model uses the topography of an alluvial fan prior to flooding and as a result ignores erosion, sediment transport, and debris flow.
2. DAMBRK model can determine the flood elevations in the flooded zone; so, the model can also be utilized in delineating flood plains if erosion will not be significant.
3. Infiltration and transmission losses can be accounted for in an indirect and somewhat cumbersome manner as negative lateral inflows.
4. Use of the DAMBRK model only describes a one-dimensional flow. Through the use of defining cross-sections along the contour in a somewhat radial pattern could be thought of as a quasi-two-dimensional framework. When highly two-dimensional flow pattern exist, then this approach may be only very approximate.

More frequent use of the unsteady flow model, DAMBRK, is encouraged to find out more precise applicability. Another way of using the unsteady flow model DAMBRK may be to perform sensitivity analysis on the area of interest. An analysis of this type will produce different ranges for the variable parameters.

6.3 Recommendation

The following are recommendations for further study :

1. An erosion and sediment transport model should be incorporated into the DAMBRK model to account for the effects of erosion and sediment transport on alluvial fans.
2. A model to describe transmission losses and infiltration should be incorporated into the DAMBRK model to define the negative lateral inflows due to these losses.
3. A similar study should be performed using a two-dimensional model to determine the advantages and limitations of these approaches to model flood flows on alluvial fans.

APPENDIX A

DESCRIPTION OF THE THEORETICAL ASPECTS AND LIMITATIONS OF THE DAMBRK MODEL

THEORY

The DAMBRK model is based upon a weighted four-point implicit finite difference solution of the Saint-Venant equations for one dimensional unsteady flow. The combination of the continuity equation and the momentum equation is known as the Saint-Venant equations. The conservation form of the Saint-Venant equations, given below, provides the required versatility to simulate a wide range of flows from gradual long-duration flows in rivers to flood waves caused by dam failure. The continuity equation is

$$\frac{\delta Q}{\delta x} + \frac{\delta\left(A + A_0\right)}{\delta t} - q = 0 \qquad \text{(A-1)}$$

and the momentum equation is

$$\frac{1}{A}\frac{\partial Q}{\partial t} + \frac{1}{A}\frac{\partial\left(\beta Q^2/A\right)}{\partial x} + g\left(\frac{\partial h}{\partial x} + S_f + S_e\right) - \beta q v_x + W_f B = 0 \qquad \text{(A-2)}$$

where, x=longitudinal distance along the channel or river,

t=time,

A=cross-sectional area of flow,

A_0=cross-sectional area of off-channel dead storage,

(contributes to continuity, but not momentum),

q=lateral inflow per unit length along the channel,

h=water surface elevation,

v_x=velocity of lateral flow in the direction of channel flow,

Q=total discharge,

β=momentum correction factor,

g=gravitational acceleration,

S_f=boundary friction slope,

S_e=expansion-contraction slope/eddy loss slope,

W_f=wind shear force,

B=width of the channel at the water surface.

The momentum equation consists of terms for the physical process that govern the flow momentum. The term $g\frac{\partial h}{\partial x}$, defining the change in water surface elevation can also be expressed as $g\left(\frac{\partial y}{\partial x} - S_0\right)$, where y is the depth, and S_0 is the channel bottom slope. The other terms that are contained in the momentum equation are: the **local acceleration** term, $\frac{1}{A}\frac{\delta Q}{\delta t}$, which describes the change in momentum due to change in velocity over time, the **convective acceleration** term, $\frac{1}{A}\frac{\delta\left(\beta Q^2/A\right)}{\delta x}$, which describes the change in momentum due to change in velocity along the channel, the **pressure force** term, $\frac{\partial h}{\partial x}$, is proportional to the change in water depth along the channel, the **gravity force** term, gS_0, is proportional to the bed slope, S_0, and the **friction force** term, gS_f, is proportional to the local and convective acceleration terms.

Derivation of the Saint-Venant equations require the following assumptions (Chow et al., 1988) :

1. The flow is one-dimensional; depth and velocity vary only in the longitudinal direction of the channel which implies that velocity is constant and the water surface is horizontal across any section

perpendicular to the longitudinal axis.

2. Flow is assumed to vary gradually along the channel so that hydrostatic pressure prevails and vertical acceleration can be neglected.

3. The longitudinal axis of the channel, from one cross-section to the next, is approximated as a straight line.

4. The bottom slope is small and the channel bed is fixed so that the effects of scour and deposition are negligible.

5. Resistance coefficients for steady uniform turbulent flow are applicable so that Manning's equation can be used to approximate the resistance effects.

6. The fluid is incompressible and of constant density throughout the flow.

METHODOLOGY

In order to numerically solve the Saint-Venant equations an implicit four-point, nonlinear finite difference solution scheme is used. At first, the finite differences will be defined and later on the solution procedure will be described. A finite-difference grid or x-t solution plane is shown in Figure A-1. The horizontal lines represent different times (time lines) while the vertical lines represent the distance along the river or channel. The spatial derivatives $\frac{\partial Q}{\partial x}$ and $\frac{\partial h}{\partial x}$ are estimated between adjacent time lines using the following four-point finite difference approximations :

$$\frac{\delta Q}{\delta x} = \theta \frac{\left(Q_{i+1}^{j+1} - Q_i^{j+1}\right)}{\Delta x_i} + (1-\theta)\frac{\left(Q_{i+1}^{j} - Q_i^{j}\right)}{\Delta x_i} \quad \text{(A-3)}$$

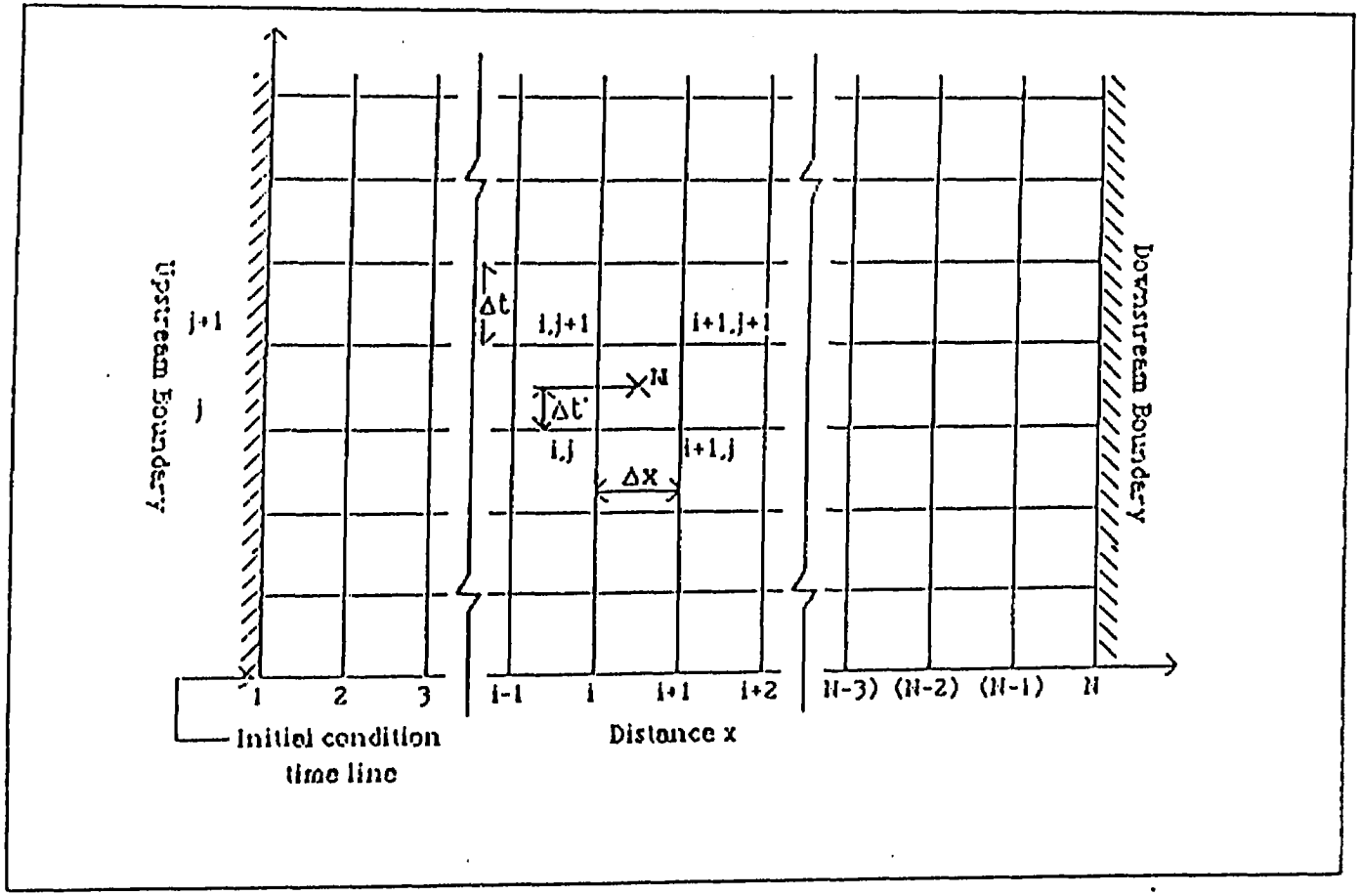

Figure A-1 The x-t solution plane. The finite difference forms of the Saint-Venant equations are solved at a discrete number of points (values of the independent variables x and t) arranged to form the rectangular grid shown. (After Fread, 1974a)

$$\frac{\delta h}{\delta x} = \theta \frac{\left(h_{i+1}^{j+1} - h_i^{j+1}\right)}{\Delta x_i} + (1-\theta)\frac{\left(h_{i+1}^{j} - h_i^{j}\right)}{\Delta x_i} \quad \text{(A-4)}$$

where θ represents a weight between the time lines j and j+1 ($q=\Delta t/Dt'$). This procedure estimates $\frac{\partial Q}{\partial x}$ and $\frac{\partial h}{\partial x}$. Then θ weighs the derivatives $\frac{\partial Q}{\partial x}$ and $\frac{\partial h}{\partial x}$ between the adjacent time lines. For rivers θ has been found to be in the order of 0.55 to 0.60.

The time derivatives are

$$\frac{\partial\left(A + A_0\right)}{\partial t} = \frac{\left(A + A_0\right)_i^{j+1} + \left(A + A_0\right)_{i+1}^{j+1} - \left(A + A_0\right)_i^{j} - \left(A + A_0\right)_{i+1}^{j}}{2\Delta x_i} \quad \text{(A-5)}$$

$$\frac{\partial Q}{\partial t} = \frac{Q_i^{j+1} + Q_{i+1}^{j+1} - Q_i^{j} - Q_{i+1}^{j}}{2\Delta t_i} \quad \text{(A-6)}$$

The nonderivative terms, such as q and A, are estimated between adjacent time lines using

$$q = \theta\frac{q_i^{j+1} + q_{i+1}^{j+1}}{2} + (1 - \theta)\frac{q_i^{j} + q_{i+1}^{j}}{2}$$

$$= \theta\bar{q}_i^{j+1} + (1 - \theta)\bar{q}_i^{j} \quad \text{(A-7)}$$

LIMITATIONS

The following are limitations associated with use of the DAMBRK

model:

1. The governing equations for the unsteady flows (Saint-Venant) are one-dimensional. But in the real life situation flows on an alluvial fan or plain may be near two-dimensional, i.e., the velocity of flow and the water surface elevations vary in x-direction (along the channel/valley) and as well as in a direction perpendicular to x-direction. The problem might become acute when the flow expands onto an extremely wide and flat flood plain after having passed through a severely constricting upstream reach. The two-dimensional effects could be minimized if the cross-sections are defined radially with increasing diameter. This keeps the flow along the channel/valley perpendicular to the sections.

2. A dynamic system, like an alluvial fan, typically is in an unstable state. Which implies that high velocity flows, associated with alluvial fans, can cause significant scour of the alluvial channels. This enlargement of the channel section by degradation is neglected in the DAMBRK model since the equations for sediment transport, sediment continuity, dynamic bed-form friction, and channel bed armoring are not included among the governing equations.

3. There is an uncertainty associated with selecting the Manning's n value. This becomes difficult because floods with very high magnitude may inundate areas that have never been flooded before, or the debris carried by the flow may alter the previous n value. One possible way to get around the uncertainty is to perform a sensitivity test using the DAMBRK model to simulate the flow, first with lower estimated values and then with the higher estimated values. The water surface profiles along channel/valley

will represent an envelope of possible flood peak elevations within the range of uncertainty associated with Manning's n values.

4. The DAMBRK model can handle seepage loss, using an equivalent outflow per unit length of the channel in the governing equation. These losses are very difficult to determine. If there is not sufficient justification to consider seepage losses, a conservative approach would be to neglect them.

APPENDIX B

SUMMARY OF SIMULATED RUNS IN TABLES

Table B-1.1 Variation of Discharge and Depth with Different Slopes.

Channel Section	Slope (ft/mi)	Peak Discharge (cfs)	Depth (ft)	Velocity (fps)	Time (hrs)
6	2.2	12,238	4.92	2.19	3.00
	11.0	13,388	3.95	3.57	2.60
	17.6	14,059	3.63	4.27	2.60
	26.4	14,217	3.38	4.97	2.50
	39.6	14,300	3.14	5.80	2.50
10	2.2	9,605	4.44	1.95	4.00
	11.0	13,387	3.86	3.60	3.20
	17.6	13,753	3.59	4.26	3.10
	26.4	13,967	3.35	4.96	2.90
	39.6	14,117	3.12	5.79	2.80

Note.

Channel Length : 21,600 ft. (or approx. 4.09 miles).

Peak Inflow : 15,000 cfs.

Flare Angle : 11.42 degrees.

Subcritical Flow

Table B-2.1 Variation of Discharge and Depth with Different Flare Angles.

Channel Section	Angle (Degrees)	Peak Discharge (cfs)	Depth (ft)	Velocity (fps)	Time (hrs)
6	4.77	13,142	6.70	2.94	2.60
	6.67	12,908	5.95	2.59	2.70
	8.10	12,731	5.56	2.42	2.80
	9.52	12,518	5.26	2.31	2.90
	11.42	12,238	4.92	2.19	3.00
10	4.77	11,286	6.39	2.63	3.20
	6.67	10,751	5.57	2.33	3.40
	8.10	10,313	5.18	2.14	3.60
	9.52	9,847	4.80	2.03	3.80
	11.42	9,605	4.44	1.95	4.00

Note.

Channel Length : 21,600 ft. (or approx. 4.09 miles).

Peak Inflow : 15,000 cfs.

Slope : 2.2 ft/mi.

Subcritical Flow

Table B-2.2 Variation of Discharge and Depth with Different Flare Angles.

Channel Section	Angle (Degrees)	Peak Discharge (cfs)	Depth (ft)	Velocity (fps)	Time (hrs)
6	4.77	14,482	4.29	7.14	2.30
	6.67	14,409	3.82	6.60	2.40
	8.10	14,393	3.56	6.30	2.40
	9.52	14,335	3.36	6.06	2.40
	11.42	14,300	3.14	5.80	2.50
10	4.77	14,284	4.27	7.13	2.60
	6.67	14,225	3.79	6.59	2.70
	8.10	14,168	3.54	6.29	2.70
	9.52	14,160	3.34	6.05	2.80
	11.42	14,117	3.12	5.79	3.80

Note.

Channel Length : 21,600 ft. (or approx. 4.09 miles).

Peak Inflow : 15,000 cfs.

Slope : 39.6 ft/mi.

Subcritical Flow

Table B-3.1 Variation of Discharge and Depth with Different Angle & Inflow.

Channel Section	Angle (Degrees)	Peak Inflow (cfs)	Peak Discharge (cfs)	Depth (ft)	Velocity (fps)	Time (hrs)
6	11.42	15,000	14,300	3.14	5.80	2.50
	14.25	12,500	11,883	2.70	5.25	2.50
	19.38	10,000	9,477	2.22	4.59	2.60
	28.07	9,000	8,511	1.85	4.07	2.70
	41.11	7,000	6,579	1.45	3.46	2.90
	64.00	6,000	5,628	1.13	2.93	3.00
	87.56	5,000	4,672	0.90	2.50	3.20
10	11.42	15,000	14,117	3.12	5.79	2.80
	14.25	12,500	11,727	2.69	5.23	2.90
	19.38	10,000	9,348	2.20	4.58	3.10
	28.07	9,000	8,379	1.84	4.06	3.20
	41.11	7,000	6,472	1.44	3.44	3.50
	64.00	6,000	5,529	1.12	2.92	3.70
	87.56	5,000	4,585	0.89	2.50	4.00

Note.

Channel Length : 21,600 ft. (or approx. 4.09 miles).

Slope : 39.6 ft/mi.

Subcritical Flow

Table B-3.2 Variation of Discharge and Depth with Different Angle & Inflow.

Channel Section	Angle Degrees	Peak Inflow (cfs)	Peak Discharge (cfs)	Depth (ft)	Velocity (fps)	Time (hrs)
	11.42	15,000	12,238	4.92	2.19	3.00
	14.25	12,500	9,632	4.17	1.92	3.20
	19.38	10,000	7,207	3.36	1.63	3.60
6	28.07	8,000	5,465	2.65	1.36	3.90
	41.11	6,000	4,212	2.07	1.13	4.40
	64.00	4,500	2,710	1.46	0.88	5.10
	87.56	3,500	1,997	1.11	0.72	5.80
	11.42	15,000	9,605	4.44	1.95	4.00
	14.25	12,500	7,617	3.74	1.76	4.40
	19.38	10,000	5,752	3.00	1.53	5.00
10	28.07	8,000	4,341	2.35	1.29	5.70
	41.11	6,500	3,325	1.84	1.09	6.60
	64.00	4,500	2,151	1.31	0.84	8.00
	87.56	3,500	1,608	1.01	0.69	9.30

Note.

Channel Length : 21,600 ft. (or approx. 4.09 miles).

Slope : 2.2 ft/mi.

Subcritical Flow

Table B-4.1 Variation of Discharge and Depth with Different Flare Angles.

Channel Section	Angle (Degrees)	Peak Discharge (cfs)	Depth (ft)	Velocity (fps)	Time (hrs)
6	11.42	4,877	1.36	10.51	2.20
	14.25	4,869	1.26	9.95	2.20
	19.38	4,855	1.12	9.22	2.20
	41.11	4,858	0.84	7.60	2.30
	64.00	4,846	0.69	6.69	2.30
10	11.42	4,823	1.12	15.37	2.30
	14.25	4,869	1.03	14.57	2.40
	19.38	4,855	0.92	13.51	2.40
	41.11	4,858	0.69	11.12	2.50
	64.00	4,846	0.57	9.79	2.50

Note.

Channel Length : 21,600 ft. (or approx. 4.09 miles).

Peak Inflow : 5,000 cfs.

Slope : 1100.0 ft/mi.

Supercritical Flow

Table B-4.2 Variation of Discharge and Depth with Different Flare Angles.

Channel Section	Angle (Degrees)	Peak Discharge (cfs)	Depth (ft)	Velocity (fps)	Time (hrs)
6	11.42	9,764	1.77	12.50	2.20
	14.25	9,764	1.63	11.84	2.20
	19.38	9,758	1.45	10.98	2.20
	41.11	9,695	1.09	9.03	2.20
	64.00	9,701	0.90	7.96	2.30
10	11.42	9,705	1.46	18.30	2.30
	14.25	9,696	1.34	17.34	2.30
	19.38	9,667	0.20	16.06	2.30
	41.11	9,656	0.90	13.23	2.40
	64.00	9,595	0.74	11.64	2.40

Note.

Channel Length : 21,600 ft. (or approx. 4.09 miles).

Peak Inflow : 10,000 cfs.

Slope : 1100.0 ft/mi.

Supercritical Flow

Table B-4.3 Variation of Discharge and Depth with Different Flare Angles.

Channel Section	Angle (Degrees)	Peak Discharge (cfs)	Depth (ft)	Velocity (fps)	Time (hrs)
6	11.42	14,621	2.06	13.82	2.20
	14.25	14,635	1.90	13.11	2.20
	19.38	14,642	1.69	12.15	2.20
	41.11	14,603	1.27	10.00	2.20
	64.00	14,520	1.05	8.80	2.20
10	11.42	14,539	1.69	20.24	2.30
	14.25	14,553	1.56	19.19	2.30
	19.38	14,549	1.40	17.79	2.30
	41.11	14,460	1.04	14.64	2.40
	64.00	14,472	0.86	12.90	2.40

Note.

Channel Length : 21,600 ft. (or approx. 4.09 miles).

Peak Inflow : 15,000 cfs.

Slope : 1100.0 ft/mi.

Supercritical Flow

Table B-5.1 Variation of Discharge and Depth with Flare Angle in a Multislope Channel

Channel section	Angle (degrees)	Peak discharge (cfs)	Depth (ft)	Velocity (fps)	Time (hrs)
6	11.42	14,246	3.14	5.79	2.20
	19.38	14,198	2.24	4.63	2.20
	41.11	14,146	1.93	4.19	2.20
	53.13	14,095	1.73	3.89	2.20
	64.01	14,053	1.59	3.68	2.30
10	11.42	12,807	4.98	2.07	2.70
	19.38	12,471	3.49	1.68	3.00
	41.11	12,299	2.98	1.53	3.10
	53.13	12,213	2.66	1.43	3.20
	64.01	12,117	2.44	1.35	3.30

Note.

Channel Length : 21,600 ft. (or approx. 4.09 miles).

Peak Inflow : 15,000 cfs.

Slope : Varies from 1100 ft/mi to 2.2 ft/mi

Combination of Subcritical and Supercritical Flow

APPENDIX C

SAMPLE INPUT DATA

```
     EXAMPLE-1              OPT:  MIXED SL
              HASAN MUSHTAQ
          9          0          0          3          4          0          0          0
0.         6.
400.       15000.     400.       400.
0.         2.         4.         6.
         10          6          2          1          0          3
          6         10
0.
6150.      6153.      6155.      6155.01    6158.      6162.
0.         60.        100.       100.       100.       100.
0.
0.4545454
5650.      5653.      5655.      5655.01    5658.      5660.
0.         348.       580.       580.       580.       580.
0.
0.9090909
5225.      5228.      5230.      5230.01    5233.      5235.
0.         636.       1060.      1060.      1060.      1060.
0.
1.3636364
4875.      4878.      4880.      4880.01    4883.      4885.
0.         924.       1540.      1540.      1540.      1540.
0.
1.8181818
4575.      4578.      4580.      4580.01    4583.      4585.
0.         1212.      2020.      2020.      2020.      2020.
0.
2.2727273
4325.      4328.      4330.      4330.01    4333.      4335.
0.         1500.      2500.      2500.      2500.      2500.
0.
2.7272727
4307.      4310.      4312.      4312.01    4315.      4317.
0.         1500.      2500.      2500.      2500.      2500.
0.
3.1818182
4295.      4298.      4300.      4300.01    4303.      4305.
0.         1500.      2500.      2500.      2500.      2500.
0.
3.6363636
4290.      4293.      4295.      4295.01    4298.      4300.
0.         1500.      2500.      2500.      2500.      2500.
0.
4.0909091
4289.      4292.      4294.      4294.01    4297.      4299.
0.         1500.      2500.      2500.      2500.      2500.
0.
0.05       0.05       0.05       0.05       0.05       0.05
0.05       0.05       0.05       0.05       0.05       0.05
0.05       0.05       0.05       0.05       0.05       0.05
0.05       0.05       0.05       0.05       0.05       0.05
0.05       0.05       0.05       0.05       0.05       0.05
0.03       0.03       0.03       0.03       0.03       0.03
0.03       0.03       0.03       0.03       0.03       0.03
0.03       0.03       0.03       0.03       0.03       0.03
0.03       0.03       0.03       0.03       0.03       0.03
0.045      0.050      0.038      0.029      0.024      0.022      0.019      0.017
0.017
0.
0.
0.
```

APPENDIX D

INPUT AND OUTPUT FILES FOR THE LOST DOG WASH

```
     EXAMPLE-1              OPT: 8
              HASAN MUSHTAQ
          9          0          0          3          4          0          0          0
0.        6.
1520.     15000.     1520.      1520.
0.        2.         4.         6.
         10          6          3          1          0          1
          3          7         10
0.
1638.     1639.      1640.      1641.      1642.      1644.
90.       90.        90.        90.        90.        90.
0.
0.0378787
1626.     1627.      1628.      1629.      1630.      1631.
220.      220.       220.       220.       220.       220.
0.
0.0776515
1614.     1615.      1616.      1617.      1618.      1619.
430.      430.       430.       430.       430.       430.
0.
0.1155303
1602.     1603.      1604.      1654.      1606.      1607.
580.      580.       580.       580.       580.       580.
0.
0.153409
1590.     1591.      1592.      1593.      1594.      1595.
740.      740.       740.       740.       740.       740.
0.
0.1844697
1578.     1579.      1580.      1581.      1582.      1583.
880.      880.       880.       880.       880.       880.
0.
0.217803
1566.     1567.      1568.      1569.      1570.      1571.
980.      980.       980.       980.       980.       980.
0.
0.248106
1554.     1555.      1556.      1557.      1558.      1559.
1020.     1020.      1020.      1020.      1020.      1020.
0.
0.2821969
1542.     1543.      1544.      1545.      1546.      1547.
990.      990.       990.       990.       990.       990.
0.
0.323106
1530.     1531.      1532.      1533.      1534.      1535.
1040.     1040.      1040.      1040.      1040.      1040.
0.
0.05      0.05       0.05       0.05       0.05       0.05
0.05      0.05       0.05       0.05       0.05       0.05
0.05      0.05       0.05       0.05       0.05       0.05
0.05      0.05       0.05       0.05       0.05       0.05
0.05      0.05       0.05       0.05       0.05       0.05
0.05      0.05       0.05       0.05       0.05       0.05
0.05      0.05       0.05       0.05       0.05       0.05
0.05      0.05       0.05       0.05       0.05       0.05
0.05      0.05       0.05       0.05       0.05       0.05
0.013     0.020      0.001      0.001      1.380      1.312      1.272      1.234
1.196
0.
0.
0.
```

ANALYSIS OF THE DOWNSTREAM FLOOD HYDROGRAPH

PRODUCED BY THE DAM BREAK OF

EXAMPLE-1

ON

OPT: 8

ANALYSIS BY

HASAN MUSHTAQ

BASED ON PROCEDURE DEVELOPED BY
DANNY L. FREAD, PH.D., SR. RESEARCH HYDROLOGIST

QUALITY CONTROL TESTING AND OTHER SUPPORT BY
JANICE M. LEWIS, RESEARCH HYDROLOGIST

HYDROLOGIC RESEARCH LABORATORY
W23, OFFICE OF HYDROLOGY
NOAA, NATIONAL WEATHER SERVICE
SILVER SPRING, MARYLAND 20910

1

```
*****************************
*****************************
***                       ***
***  SUMMARY OF INPUT DATA  ***
***                       ***
*****************************
*****************************
```

INPUT CONTROL PARAMETERS FOR EXAMPLE-1

PARAMETER	VARIABLE	VALUE
NUMBER OF DYNAMIC ROUTING REACHES	KKN	9
TYPE OF RESERVOIR ROUTING	KUI	0
MULTIPLE DAM INDICATOR	MULDAM	0
PRINTING INSTRUCTIONS FOR INPUT SUMMARY	KDMP	3
NO. OF RESERVOIR INFLOW HYDROGRAPH POINTS	ITEH	4
INTERVAL OF CROSS-SECTION INFO PRINTED OUT WHEN JNK=9	NPRT	0
FLOOD-PLAIN MODEL PARAMETER	KFLP	0
METRIC INPUT/OUTPUT OPTION	METRIC	0

DHF(INTERVAL BETWEEN INPUT HYDROGRAPH ORDINATES) = 0.00 HRS.

TEH(TIME AT WHICH COMPUTATIONS TERMINATE)= 6.0000 HRS.

BREX(BREACH EXPONENT) = 0.000

MUD(MUD FLOW OPTION) = 0

IWF(TYPE OF WAVE FRONT TRACKING) = 0

KPRES(WETTED PERIMETER OPTION) = 0

KSL(LANDSLIDE PARAMETER) = 0

INFLOW HYDROGRAPH TO EXAMPLE-1

1520.00 15000.00 1520.00 1520.00

TIME OF INFLOW HYDROGRAPH ORDINATES

0.0000 2.0000 4.0000 6.0000

1

CROSS-SECTIONAL PARAMETERS FOR OPT: 8
BELOW EXAMPLE-1

PARAMETER	VARIABLE	VALUE
NUMBER OF CROSS-SECTIONS	NS	10
MAXIMUM NUMBER OF TOP WIDTHS	NCS	6
NUMBER OF CROSS-SECTIONAL HYDROGRAPHS TO PLOT	NTT	2
TYPE OF OUTPUT OTHER THAN HYDROGRAPH PLOTS	JNK	1
CROSS-SECTIONAL SMOOTHING PARAMETER	KSA	0
DOWNSTREAM SUPERCRITICAL OR NOT	KSUPC	1
NO. OF LATERAL INFLOW HYDROGRAPHS	LQ	0
NO. OF POINTS IN GATE CONTROL CURVE	KCG	0

NUMBER OF CROSS-SECTION WHERE HYDROGRAPH DESIRED
(MAX NUMBER OF HYDROGRAPHS = 6)

6 10

CROSS-SECTIONAL VARIABLES FOR OPT: 8
BELOW EXAMPLE-1

PARAMETER	UNITS	VARIABLE
LOCATION OF CROSS-SECTION	MILE	XS(I)
ELEVATION(MSL) OF FLOODING AT CROSS-SECTION	FEET	FSTG(I)
ELEV CORRESPONDING TO EACH TOP WIDTH	FEET	HS(K,I)
TOP WIDTH CORRESPONDING TO EACH ELEV (ACTIVE FLOW PORTION)	FEET	BS(K,I)
TOP WIDTH CORRESPONDING TO EACH ELEV (OFF-CHANNEL PORTION)	FEET	BSS(K,I)
NUMBER OF CROSS-SECTION		I
NUMBER OF ELEVATION LEVEL		K

1

CROSS-SECTION NUMBER 1

XS(I) = 0.000 FSTG(I) = 0.00

HS ...	1638.0	1639.0	1640.0	1641.0	1642.0	1644.0
BS ...	90.0	90.0	90.0	90.0	90.0	90.0
BSS ...	0.0	0.0	0.0	0.0	0.0	0.0

CROSS-SECTION NUMBER 2
****

XS(I) = 0.038 FSTG(I) = 0.00

HS ...	1626.0	1627.0	1628.0	1629.0	1630.0	1631.0
BS ...	220.0	220.0	220.0	220.0	220.0	220.0
BSS ...	0.0	0.0	0.0	0.0	0.0	0.0

CROSS-SECTION NUMBER 3
****

XS(I) = 0.078 FSTG(I) = 0.00

HS ...	1614.0	1615.0	1616.0	1617.0	1618.0	1619.0
BS ...	430.0	430.0	430.0	430.0	430.0	430.0
BSS ...	0.0	0.0	0.0	0.0	0.0	0.0

CROSS-SECTION NUMBER 4
****

XS(I) = 0.116 FSTG(I) = 0.00

HS ...	1602.0	1603.0	1604.0	1654.0	1606.0	1607.0
BS ...	580.0	580.0	580.0	580.0	580.0	580.0
BSS ...	0.0	0.0	0.0	0.0	0.0	0.0

1

CROSS-SECTION NUMBER 5
****

XS(I) = 0.153 FSTG(I) = 0.00

HS ...	1590.0	1591.0	1592.0	1593.0	1594.0	1595.0
BS ...	740.0	740.0	740.0	740.0	740.0	740.0
BSS ...	0.0	0.0	0.0	0.0	0.0	0.0

CROSS-SECTION NUMBER 6
****

XS(I) = 0.184 FSTG(I) = 0.00

HS ...	1578.0	1579.0	1580.0	1581.0	1582.0	1583.0
BS ...	880.0	880.0	880.0	880.0	880.0	880.0
BSS ...	0.0	0.0	0.0	0.0	0.0	0.0

CROSS-SECTION NUMBER 7
****

XS(I) = 0.218 FSTG(I) = 0.00

HS ...	1566.0	1567.0	1568.0	1569.0	1570.0	1571.0
ES ...	980.0	980.0	980.0	980.0	980.0	980.0
ESS ...	0.0	0.0	0.0	0.0	0.0	0.0

CROSS-SECTION NUMBER 8
****

XS(I) = 0.248 FSTG(I) = 0.00

HS ...	1554.0	1555.0	1556.0	1557.0	1558.0	1559.0
ES ...	1020.0	1020.0	1020.0	1020.0	1020.0	1020.0
ESS ...	0.0	0.0	0.0	0.0	0.0	0.0

1

CROSS-SECTION NUMBER 9
****

XS(I) = 0.282 FSTG(I) = 0.00

HS ...	1542.0	1543.0	1544.0	1545.0	1546.0	1547.0
ES ...	990.0	990.0	990.0	990.0	990.0	990.0
ESS ...	0.0	0.0	0.0	0.0	0.0	0.0

CROSS-SECTION NUMBER 10
****

XS(I) = 0.323 FSTG(I) = 0.00

HS ...	1530.0	1531.0	1532.0	1533.0	1534.0	1535.0
ES ...	1040.0	1040.0	1040.0	1040.0	1040.0	1040.0
ESS ...	0.0	0.0	0.0	0.0	0.0	0.0

1

MANNING N ROUGHNESS COEFFICIENTS FOR THE GIVEN REACHES
(CM(K,I),K=1,NCS) WHERE I = REACH NUMBER

REACH 1 ...	0.050	0.050	0.050	0.050	0.050	0.050
REACH 2 ...	0.050	0.050	0.050	0.050	0.050	0.050
REACH 3 ...	0.050	0.050	0.050	0.050	0.050	0.050
REACH 4 ...	0.050	0.050	0.050	0.050	0.050	0.050
REACH 5 ...	0.050	0.050	0.050	0.050	0.050	0.050
REACH 6 ...	0.050	0.050	0.050	0.050	0.050	0.050
REACH 7 ...	0.050	0.050	0.050	0.050	0.050	0.050
REACH 8 ...	0.050	0.050	0.050	0.050	0.050	0.050
REACH 9 ...	0.050	0.050	0.050	0.050	0.050	0.050

1

CROSS-SECTIONAL VARIABLES FOR OPT: 8
BELOW EXAMPLE-1

PARAMETER	UNITS	VARIABLE
MINIMUM COMPUTATIONAL DISTANCE USED BETWEEN CROSS-SECTIONS	MILE	DXM(I)
CONTRACTION - EXPANSION COEFFICIENTS BETWEEN CROSS-SECTIONS		FKC(I)

REACH NUMBER	DXM(I)	FKC(I)
1	0.013	0.000
2	0.020	0.000
3	0.001	0.000
4	0.001	0.000
5	1.380	0.000
6	1.312	0.000
7	1.272	0.000
8	1.234	0.000
9	1.196	0.000

1 DOWNSTREAM FLOW PARAMETERS FOR OPT: 8
BELOW EXAMPLE-1

PARAMETER	UNITS	VARIABLE	VALUE
MAX DISCHARGE AT DOWNSTREAM EXTREMITY	CFS	QMAXD	0.0
MAX LATERAL OUTFLOW PRODUCING LOSSES	CFS /FEET	QLL	0.000
INITIAL SIZE OF TIME STEP	HOUR	DTHM	0.0000
DOWNSTREAM BOUNDARY PARAMETER	FEET	YDN	0.000000
SLOPE OF CHANNEL DOWNSTREAM OF DAM	FPM	SOM	0.00
THETA WEIGHTING FACTOR		THETA	0.00
CONVERGENCE CRITERION FOR STAGE	FEET	EPSY	0.000
TIME AT WHICH DAM STARTS TO FAIL	HOUR	TFI	0.00

AT REACH= 1 DXM SHOULD BE CHANGED TO 0.013 DUE TO EXP/CONTRACT CRITERIA

AT REACH= 2 DXM SHOULD BE CHANGED TO 0.020 DUE TO EXP/CONTRACT CRITERIA

AT REACH= 3 DXM SHOULD BE CHANGED TO 0.001 DUE TO EXP/CONTRACT CRITERIA

AT REACH= 6 DXM SHOULD BE CHANGED TO 1.312 DUE TO (WAVE SPEED * DT) CRITERI
A

AT REACH= 8 DXM SHOULD BE CHANGED TO 1.234 DUE TO (WAVE SPEED * DT) CRITERI
A

AT REACH= 9 DXM SHOULD BE CHANGED TO 1.196 DUE TO (WAVE SPEED * DT) CRITERI
A

COMPUTATIONS WILL USE THE FOLLOWING DXM VALUES

0.013 0.020 0.001 0.001 1.380 1.312 1.272 1.234 1.196

TOTAL NUMBER OF CROSS SECTIONS (ORIGINAL+INTERPOLATED) (N) = 84 (MAXIMUM
ALLOWABLE = 200

```
*****************************
*****************************
***                       ***
***  SUMMARY OF OUTPUT DATA ***
***                       ***
*****************************
*****************************
```

1

CROSS-SECTION NO. MESAGE	MILE	BOTTOM ELEVATION FEET	REACH NO.	REACH LENGTH MILE	SLOPE FPM
1	0.00	1638.00			
2	0.04	1626.00	1	0.04	316.80
3	0.08	1614.00	2	0.04	301.71
4	0.12	1602.00	3	0.04	316.80
5	0.15	1590.00	4	0.04	316.80
6	0.18	1578.00	5	0.03	386.34
7	0.22	1566.00	6	0.03	360.00
8	0.25	1554.00	7	0.03	396.00
9	0.28	1542.00	8	0.03	352.00
10	0.32	1530.00	9	0.04	293.33

INITIAL CONDITIONS

INITIAL CONDITIONS

(QDI(I),I=1,N)

1520.	1520.	1520.	1520.	1520.	1520.	1520.	1520.
1520.	1520.	1520.	1520.	1520.	1520.	1520.	1520.
1520.	1520.	1520.	1520.	1520.	1520.	1520.	1520.
1520.	1520.	1520.	1520.	1520.	1520.	1520.	1520.
1520.	1520.	1520.	1520.	1520.	1520.	1520.	1520.
1520.	1520.	1520.	1520.	1520.	1520.	1520.	1520.
1520.	1520.	1520.	1520.	1520.	1520.	1520.	1520.
1520.	1520.	1520.	1520.	1520.	1520.	1520.	1520.
1520.	1520.	1520.	1520.	1520.	1520.	1520.	1520.
1520.	1520.	1520.	1520.	1520.	1520.	1520.	1520.
1520.	1520.	1520.	1520.	1520.	1520.	1520.	1520.

(YI(I),I=1,N)

1639.66	1633.12	1626.97	1620.76	1614.66	1614.31	1613.99	1613.66
1613.33	1613.01	1612.67	1612.35	1612.02	1611.69	1611.37	1611.04
1610.71	1610.39	1610.05	1609.73	1609.41	1609.07	1608.75	1608.43
1608.09	1607.77	1607.45	1607.11	1606.78	1606.46	1606.13	1605.81
1605.49	1605.14	1604.84	1604.49	1604.17	1603.85	1603.52	1603.20
1602.85	1602.55	1602.21	1601.88	1601.56	1601.23	1600.91	1600.59
1600.24	1599.94	1599.59	1599.27	1598.95	1598.62	1598.30	1597.97
1597.63	1597.32	1596.98	1596.66	1596.33	1596.01	1595.68	1595.36
1595.04	1594.71	1594.37	1594.06	1593.72	1593.40	1593.07	1592.75
1592.42	1592.10	1591.77	1591.45	1591.11	1590.80	1590.46	1578.38
1566.40	1554.33	1542.43	1530.36				

1

TIME PARAMETERS OF OUTFLOW HYDROGRAPH IMMEDIATELY DOWNSTREAM OF DAM

PARAMETER	UNITS	VARIABLE	VALUE
TIME TO FAILURE	HR	TFH	2.000
TIME TO START OF RISING LIMB OF HYDROGRAPH	HR	TFO	0.000
TIME TO PEAK	HR	TP	2.000
TIME STEP SIZE	HR	DTHI	0.100

ROUTING COMPLETED.

KTIME= 58 ALLOWABLE KTIME= 699 TT= 6.1

1

PROFILE OF CRESTS AND TIMES FOR OPT: 8
BELOW EXAMPLE-1

DISTANCE FROM DAM MILE	MAX ELEV FEET	MAX FLOW CFS	TIME MAX ELEV-HRS	MAX VEL FPS	FLOOD ELEV FEET	TIME FLOOD ELEV-HRS
0.000	1643.98	14999	2.000	27.89	0.00	0.00
0.019	1635.82	14996	2.000	25.32	0.00	0.00
0.038	1629.41	14992	2.000	19.99	0.00	0.00
0.058	1622.81	14986	2.000	16.41	0.00	0.00
0.078	1616.48	14979	2.000	14.02	0.00	0.00
0.079	1616.14	14979	2.000	13.99	0.00	0.00
0.080	1615.80	14978	2.000	13.94	0.00	0.00
0.081	1615.46	14978	2.000	13.90	0.00	0.00
0.082	1615.13	14978	2.000	13.85	0.00	0.00
0.083	1614.79	14977	2.000	13.80	0.00	0.00
0.084	1614.45	14977	2.000	13.75	0.00	0.00
0.085	1614.12	14976	2.000	13.69	0.00	0.00
0.086	1613.78	14976	2.000	13.64	0.00	0.00
0.087	1613.44	14975	2.000	13.59	0.00	0.00
0.088	1613.11	14975	2.000	13.54	0.00	0.00
0.089	1612.77	14975	2.000	13.48	0.00	0.00
0.090	1612.44	14974	2.000	13.43	0.00	0.00
0.091	1612.10	14974	2.000	13.38	0.00	0.00
0.092	1611.77	14973	2.000	13.33	0.00	0.00
0.093	1611.43	14973	2.000	13.28	0.00	0.00
0.094	1611.10	14972	2.000	13.23	0.00	0.00
0.095	1610.76	14972	2.000	13.18	0.00	0.00
0.096	1610.43	14972	2.000	13.14	0.00	0.00
0.097	1610.09	14971	2.000	13.09	0.00	0.00
0.098	1609.76	14971	2.000	13.04	0.00	0.00
0.099	1609.43	14970	2.000	13.00	0.00	0.00
0.100	1609.09	14970	2.000	12.95	0.00	0.00
0.101	1608.76	14969	2.000	12.91	0.00	0.00
0.102	1608.42	14969	2.000	12.86	0.00	0.00
0.103	1608.09	14968	2.000	12.82	0.00	0.00
0.104	1607.76	14968	2.000	12.78	0.00	0.00
0.105	1607.42	14967	2.000	12.73	0.00	0.00
0.106	1607.09	14967	2.000	12.69	0.00	0.00
0.107	1606.76	14966	2.000	12.65	0.00	0.00
0.108	1606.42	14966	2.000	12.61	0.00	0.00
0.109	1606.09	14966	2.000	12.57	0.00	0.00
0.110	1605.76	14965	2.000	12.53	0.00	0.00
0.111	1605.42	14965	2.000	12.49	0.00	0.00
0.112	1605.09	14964	2.000	12.45	0.00	0.00
0.113	1604.76	14964	2.000	12.41	0.00	0.00
0.115	1604.42	14963	2.000	12.37	0.00	0.00
0.116	1604.09	14963	2.000	12.33	0.00	0.00
0.117	1603.76	14962	2.000	12.30	0.00	0.00
0.118	1603.42	14962	2.000	12.26	0.00	0.00
0.119	1603.09	14961	2.000	12.22	0.00	0.00
0.120	1602.76	14961	2.000	12.19	0.00	0.00
0.121	1602.43	14960	2.000	12.15	0.00	0.00
0.122	1602.09	14960	2.000	12.11	0.00	0.00

1

PROFILE OF CRESTS AND TIMES FOR OPT: 8
BELOW EXAMPLE-1

DISTANCE FROM DAM MILE	MAX ELEV FEET	MAX FLOW CFS	TIME MAX ELEV-HRS	MAX VEL FPS	FLOOD ELEV FEET	TIME FLOOD ELEV-HRS
0.123	1601.76	14959	2.000	12.08	0.00	0.00
0.124	1601.43	14959	2.000	12.04	0.00	0.00
0.125	1601.09	14958	2.000	12.00	0.00	0.00
0.126	1600.76	14958	2.000	11.97	0.00	0.00
0.127	1600.43	14957	2.000	11.93	0.00	0.00
0.128	1600.10	14957	2.000	11.89	0.00	0.00
0.129	1599.77	14956	2.000	11.86	0.00	0.00
0.130	1599.43	14956	2.000	11.82	0.00	0.00
0.131	1599.10	14955	2.000	11.79	0.00	0.00
0.132	1598.77	14955	2.000	11.76	0.00	0.00
0.133	1598.44	14954	2.000	11.72	0.00	0.00
0.134	1598.11	14954	2.000	11.69	0.00	0.00
0.135	1597.78	14953	2.000	11.66	0.00	0.00
0.136	1597.44	14953	2.000	11.62	0.00	0.00
0.137	1597.11	14952	2.000	11.59	0.00	0.00
0.138	1596.78	14952	2.000	11.56	0.00	0.00
0.139	1596.45	14951	2.000	11.53	0.00	0.00
0.140	1596.12	14951	2.000	11.49	0.00	0.00
0.141	1595.79	14950	2.000	11.46	0.00	0.00
0.142	1595.46	14950	2.000	11.43	0.00	0.00
0.143	1595.13	14949	2.000	11.40	0.00	0.00
0.144	1594.79	14949	2.000	11.37	0.00	0.00
0.145	1594.46	14948	2.000	11.34	0.00	0.00
0.146	1594.13	14948	2.000	11.31	0.00	0.00
0.147	1593.80	14947	2.000	11.28	0.00	0.00
0.148	1593.47	14946	2.000	11.25	0.00	0.00
0.149	1593.14	14946	2.000	11.22	0.00	0.00
0.150	1592.81	14945	2.000	11.20	0.00	0.00
0.151	1592.48	14945	2.000	11.17	0.00	0.00
0.152	1592.15	14944	2.000	11.14	0.00	0.00
0.153	1591.82	14944	2.000	11.11	0.00	0.00
0.184	1579.48	14927	2.000	11.42	0.00	0.00
0.218	1567.56	14909	2.000	9.72	0.00	0.00
0.248	1555.33	14891	2.000	10.99	0.00	0.00
0.282	1543.62	14871	2.000	9.26	0.00	0.00
0.323	1531.49	14845	2.000	9.57	0.00	0.00

APPENDIX E

BRIEF DESCRIPTION OF FEMA METHOD

FEMA approaches the alluvial fan flooding problem in two ways. These are, 1) Single channel region, and 2) Multiple channel region. The single channel region is defined as following (FEMA, 1985, p. A5-5) :

> "the length of the single channel measured from the mouth of the canyon to the point where the flood channel splits."

In the event of insufficient information from the field data, for specifying the length of the single channel, FEMA uses a relationship between the length of a single single channel and the ratio of Canyon slope to Fan slope (Figure E-1). The set of equations that are used in the FEMA procedure are as following.

SINGLE CHANNEL REGION

$$Q = 280\ D^{2.5} \qquad \text{(E-1)}$$

Discharges and their depth zone boundaies.

Q	49.5	772	2,770	6,420	12,000
D	0.5	1.5	2.5	3.5	4.5

$$Q = 0.13\ V^{5} \qquad \text{(E-2)}$$

Discharges and their velocity zone boundaries.

Q	68	240	654	1,510	3,080	5,770
V	3.5	4.5	5.5	6.5	7.5	8.5

$$\text{Fan width} = 950\ ACP\ (Z \geq \log Q) \qquad \text{(E-3)}$$

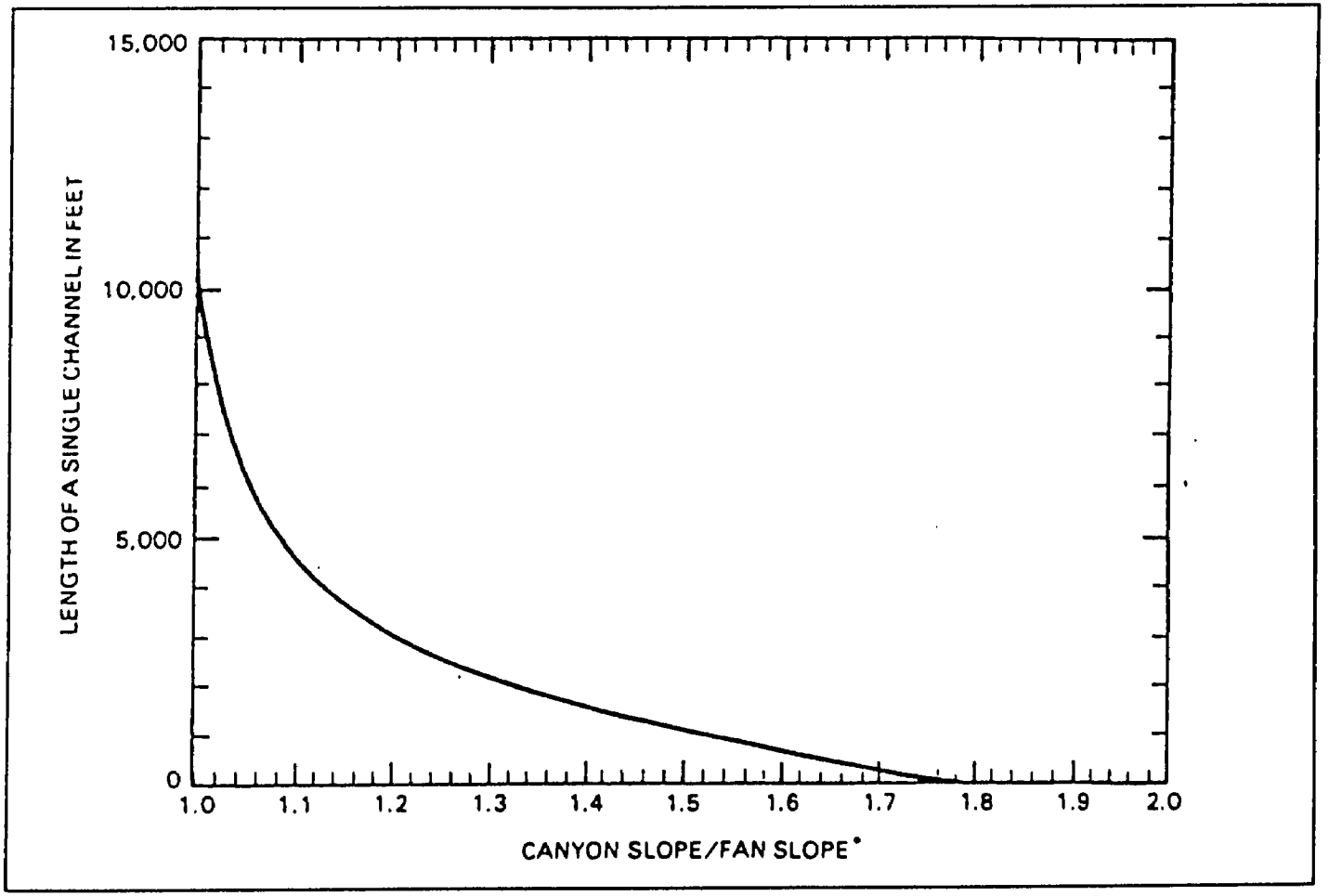

Figure E-1. Relationship between length of a single channel and ratio of Canyon slope to Fan slope (After FEMA, 1985, p. A5-6)

MULTIPLE CHANNEL REGION

$$Q = 145\, n^{2.5}\, S^{-1.25}\, V^{4.17} \qquad \text{(E-4)}$$

$$D = 0.0917\, n^{0.6}\, S^{-0.3}\, Q^{0.36} + 0.001426\, n^{-1.2}\, S^{0.6}\, Q^{0.48} \qquad \text{(E-5)}$$

$$\text{Fan width} = 3610\ ACP\ (Z \geq \log Q) \qquad \text{(E-6)}$$

Definition of terms

Q = discharges in cubic feet, D = total depth in feet due to pressure head and velocity head, V = velocity in feet per second, S = fan slope, n = Manning's roughness coefficient for the alluvial fan flood channel, A = avulsion coefficient (default value 1.5), C = transformation constant for the log-Pearson type III distribution, P = probability of the discharge for the corresponding depth or velocity zone boundary.

* Equations (E-3), (E-4), (E-6) are the modified equations (Official letter from FEMA, 1989)

APPENDIX F

METHOD FOR HAND CALCULATION

There is no analytical solution to Manning's equation for determining the flow depth given the flow rate because the area A and hydraulic radius R may be complicated functions of the depth. Newton's method can be applied iteratively to give a numerical solution. For example, if Q_j is the computed discharge at jth iteration, for a selected depth of y_j, and Q is the actual flow, then the error is

$$f(y_j) = Q_j - Q \qquad \text{(F-1)}$$

The objective is to select y in such a way, so that the error becomes acceptably small. The gradient of f with respect to y is

$$\frac{df}{dy_j} = \frac{dQ_j}{dy_j} \qquad \text{(F-2)}$$

because Q is a constant. Hence, assuming Manning's n is constant,

$$\left(\frac{dy}{df}\right)_j = \left(\frac{1.49}{n} S_0^{\frac{1}{2}} A_j R_j^{\frac{2}{3}}\right) \qquad \text{(F-3)}$$

After going through some manipulation, the gradient becomes

$$\left(\frac{df}{dy}\right)_j = Q_j \left(\frac{2}{3R}\frac{dR}{dy} + \frac{1}{A}\frac{dA}{dy}\right)_j \qquad \text{(F-4)}$$

where the subscript j outside the parentheses indicates that the contents are evaluated for $y = y_j$.

This expression for the gradient is useful for Newton's method, where, given a choice of y_j, y_{j+1} is chosen to satisfy

$$\left(\frac{df}{dy}\right)_j = \frac{0 - f(y)_j}{y_{j+1} - y_j} \qquad \text{(F-5)}$$

This y_{j+1} is the value of y, in a plot of f vs. y, where the tangent to the curve at $y = y_j$ intersects the horizontal axis, as illustrated in Figure (F-1).

Solving equation F-5 for y_{j+1},

$$y_{j+1} = y_j - \frac{f(y_j)}{\left(\frac{df}{dy_j}\right)} \qquad \text{(F-6)}$$

which is the fundamental equation of the Newton's method. Iterations are continued until there is no significant change in y; this will hapen when the error f(y) is very close to zero.

Substituting into equation (F-6) from equations (F-1) and (F-4) gives the Newton's-method equation for solving Manning's equation:

$$y_{j+1} = y_j - \frac{1 - Q/Q_j}{\left(\frac{2}{3R}\frac{dR}{dy} + \frac{1}{A}\frac{dA}{dy}\right)_j} \qquad \text{(F-7)}$$

For a rectangular channel $A = B_W y$ and $R = B_W y/(B_W + 2y)$ where B_W is the channel width; after some manipulation, equation (F-7) becomes

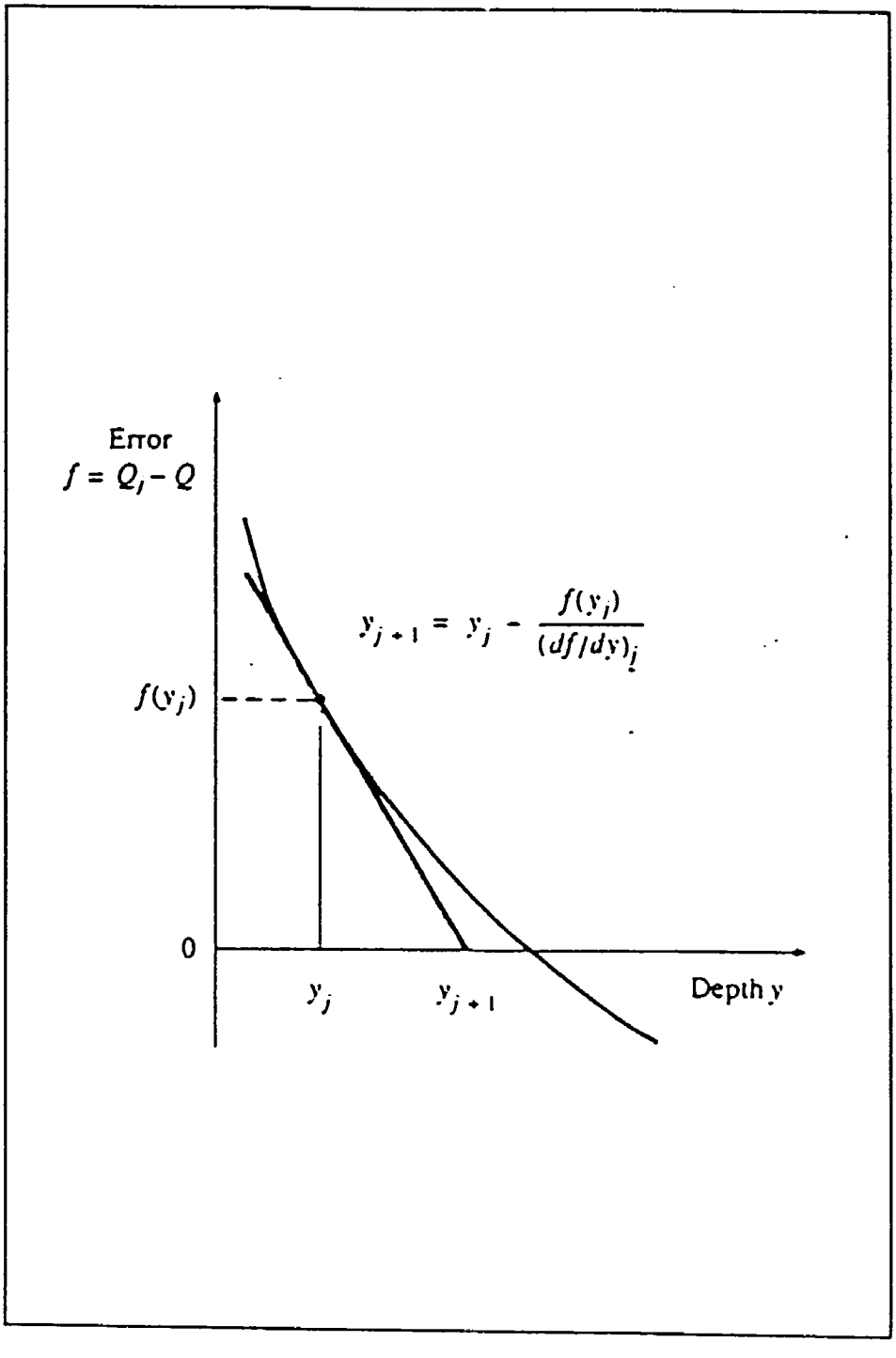

Figure F-1. Graphical representation of Newton's-method (After Chow, 1988, p. 161)

$$y_{j+1} = y_j - \frac{1 - Q\backslash Q_j}{\left\{ \frac{5B_w + 6y_j}{3y_j\left(B_w + 2y_j\right)} \right\}} \qquad \text{(F-8)}$$

The above described procedure cab be used to check the discharge at any particular section. Now, this method was employed to several sections in the alluvial fans. Table F-1 lists the results of the method used.

Table F-1 Results of the Hand Calculation using Newton's Method.

Distance from Apex (mile)	B_W (ft)	S_o (ft/ft)	n	Q (cfs)	y_j (DAMBRK) (ft)	y_j (Newton) (ft)
Lost Dog Wash						
0.078	430	0.058571	0.050	14,979	2.48	2.59
0.218	980	0.0715909	0.050	14,909	1.56	1.48
0.323	1,040	0.055549	0.050	14,845	1.49	1.53
Fan 4						
0.767	6,500	0.0212575	0.045	11,160	0.52	0.54
2.661	11,100	0.0192556	0.045	10,603	0.42	0.39
5.189	16,300	0.0123465	0.045	9,096	0.32	0.34
Fan 5						
0.98	4,400	0.0163125	0.050	4,698	0.52	0.47
3.85	9,000	0.0196382	0.050	3,994	0.27	0.26
7.79	18,100	0.0130909	0.50	1,698	0.10	0.12

GLOSSARY

Alluvial Fan : A deposit whose surface forms a segment of a cone that radiates downslope from the point where the stream leaves the source area (Bull, 1977, p.222)

Alluvial Slope : An alluvial fan that lacks the form of coalescing alluvial fans is best called an alluvial slope (Hawley and Wilson, 1965).

Apex : The point of highest elevation on an alluvial fan, which on undisturbed fan is generally the point the major stream that formed the fan emerges from the mountain front (Federal Register, 1989, p. 9528).

Avulsions : On active alluvial fas, peak flows may abruptly abandon one channel that had been formed during the flood, and form a new channel; this phenomenon is termed as avulsion (FEMA, 1985, p. A5-2).

Bajada : A blanket deposit of alluvium at the base of desert mountain slopes formed by the coalescing of alluvial fans. A bajada can also be termed an alluvial apron or a piedmont plain (French, 1987, p. 222).

Debris Flow : Moving rampart or wall of boulders and mud, a few meters in height without visible water that moves forward in a series of surges or waves along an alluvial fan. Also, a debris is a flowage of a mixture of all sizes of sediment (French, 1987, p. 223).

Flare angle : The angle of widening of the alluvial fan as it moves downslope from the apex.

Pediment : Pediments are formed in an erosional environment (Bull, 1977, p. 222)

Primary diffluence : Primary diffluence or bifurcation is the point below which flow is distributaryand above which the 100-year flood is contained and the flow is tribitary (with possible exception of relatively minor diffluences in the drainage basin). For actively aggrading alluvial fans, the primary diffluence is the same as the apex (Kemna, 1990, p. 167).

Mud flow : A mud flow is a type of debris flow that consists mainly of sand or finer sediment (Bull, 1972)

Regolith : Regolith is the layer of loose rock and mineral material that covers almost all land surfaces (Encyclopedia - on line catalog in Noble Science Library)

REFERENCES

Akan, A. O., and Yen, B. C. (1981). "Diffusion-wave flood routing in channel networks." *Journal of Hydraulics Divisions,* ASCE, 107(6), 719-932.

Blackwelder, E. (1931). "Desert plains." *Journal of Geology,* 39, 134-40.

Brion, L., and Mays, L. W. (1987). "Two-dimensional analysis of backwater at bridges." *Research report 466-1F,* Center for Transportation Research, The University of Texas at Austin, November, 1987.

Bull, W. B. (1977). "The alluvial-fan environment." *Progress in Physical Geography,* 1(2), 222-270.

Bull, W. B. (1988). *Geomorphic responses to climatic change.* Oxford University Press, New York, N.Y.

Cella Barr Associates. (1988). "Hydrologic analysis of Scottsdale alluvial fans 1-6, Maricopa County, Arizona." *CBA File No. 04856-02-74, BAT-108.*

Cella Barr Associates. (1989). "Addendum to hydrologic analysis of Scottsdale alluvial fans 1-6, Maricopa County, Arizona." *CBA File No. 04856-02 74, BAT-120.*

Chow, V. T. (1959). *Open channel hydraulics.* McGraw-Hill Book Company, New York, N. Y.

Chow, V. T., Maidment, D. R., and Mays, L. W. (1988). *Applied hydrology.* McGraw-Hill Book Company, New York, N. Y.

Dawdy, D. R. (1979). "Flood-frequency estimates on alluvial fans." *Journal of the Hydraulics Division,* ASCE, 105(HY 11), 1407-1413.

DMA Consulting Engineers. (1985). "Alluvial fan flooding methodology an analysis." Prepared for FEMA by DMA, Rey, CA, October.

Federal Emergency Management Agency. (1985). "Flood insurance study : Guidelines and specifications for study contractors, Federal emergency management agency, Federal insurance administration." *Report 37,* Appendix 5, p. 1-14.

Federal Register. (1989). "Federal emergency management agency - National flood insurance program : Federal register." 54(43), Tuesday, March 7, 1989, p. 9528.

Fread, D. L. (1974a). "Numerical properties of implicit four-point finite difference equations of unsteady flow." *NOAA Technical Memorandum NWS HYDRO-18,* U.S. Dept. of Commerce, NOAA, NWS, Silver Spring, Maryland.

Fread, D. L. (1988). "The NWS DAMBRK model: Theoretical background/ user documentation." U.S. National Weather Service, NOAA, Silver Spring, Maryland.

French, R. H. (1984). "Flood hazard assessment on alluvial fans - An examination of the methodology." University of Nevada, *Desert Research Institute Publication 45040*, 40p.

French, R. H. (1987). "Hydraulic processes on alluvial fans : Elsevier, Amsterdam." *Development in Water Science*, 31, 244 p.

Grindeland, T. R., O'Brien, J. S., and Li, R. M. (1990). "Hydraulics/Hydrology of arid lands (H^2AL)." Proceedings of the international symposium, San Diego, California, July 30 - Aug 2.

Hawley, J. W., and Wilson, W. E. (1965). "Quaternary geology of the Winnemuca area." Nevada. University of Nevada, *Desert Research Institute Technical Report no. 5*, 66 pp.

Hoggan, D. H. (1989). *Computer assisted floodplain hydrology & hydraulics.* McGraw-Hill Book Company, New York, N. Y.

Hooke, R. LeB. (1967). "Processes on arid-region alluvial fans." *Journal of Geology*, 75, 438-460.

Hromadka, T. V. (1988). "Kinematic wave routing and computational error." *Journal of Hydraulic Engineering*, ASCE, 114(2), 207-217.

Hydrologic Engineering Center. (1981). HEC-1 flood hydrograph package, Users manual. U.S. Army, Corps of Engineers, Davis, California.

Innes, J. L. (1983). "Debris flows." *Progress in Physical Geography*, 7(4), 469-501.

Katopodes, N. D., and Schamber, D. R. (1983). "Applicability of Dam-Break flood wave models." *Journal of Hydraulic Engineering*, ASCE, 109(5), 702-721.

Kemna, S. P. (1990). "Some geomorphic models of flood hazards on distributary flow areas in southern Arizona." M.S. Thesis, University of Arizona, Tucson, Arizona.

Lewin, J. (1978). "Floodplain geomorphology." *Progress in Physical Geography*, 2(3), 408-437.

Mays, L. W. and Tung Y.K. (1991). *Hydrosystems modeling for engineering and management.* to be published by McGraw-Hill Book Company, New York, N. Y.

McGinn, R. A. (1980). "Flood-frequency estimates on alluvial fans - discussion." *Journal of Hydraulic Engineering*, ASCE, 106(HY 10), 1718-1719.

Melton, M. A. (1965). "The geomorphic and paleoclimatic significance of alluvial deposits in southern Arizona." *Journal of Geology*, 73(1), 1-38.

Menges, C. M., and Pearthree, P. A. (1983). "Map of neotic (latest pliocene quarternary) deformation of Arizona." *Arizona Bureau of Geol. and Min. Tech. Open-file Report 83-22*, scale 1:500,000, text 48 p.

Pearthree, P. A. (1988). "A geomorphic analysis of flooding potential associated with a desert stream system - Dead dog wash." Scottsdale, Arizona.

Pearthree, P. A., and Scarborough, R. B. (1985). "Reconnaissance analysis of possible quarternary faulting in central Arizona." *Arizona Bar. Geo. and Min. Tech. Open-file Report 85-4*, scale 1:250,000, text 75 p.

Peterson, F. F. (1981). "Landforms of the basin and range province - defined for soil survey." Reno, Nevada, University of Nevada, *Agricultural Experiment Station Technical Bulletin 28*, 52 p.

Ponce, V. M., and Li, R.M. (1978). "Applicability of kinematic and diffusion models." *Journal of Hydraulics Divisions*, ASCE, 104(3), 353-360.

Simons, Li & Associates, and O'Brien, J. S. (1989). "Flood-hazard delineation for Cornet Creek, Telluride, Colorado." Submitted to FEMA, March.

Simons, Li & Associates. (1987). "Final hydrology report : Outer loop freeway, north of central arizona project aqueduct."

Soil Conservation Service. (1986). "Soil survey of Aguila-Carefree area, parts of Maricopa and Pinal counties, Arizona." Soil Conservation Service, Dept. of Agriculture, 306 p.

Tingsanchali, T., and Manandhar, S. K. (1985). "Analytical diffusion models for flood routing." *Journal of Hydraulic Engineering*, ASCE, 111(3), 435-454.

Viessman, W. Jr., Lewis, G L. and Knapp, J.W. (1989). *Introduction to hydrology (third edition)*. Harper & Row, Publishers, New York, N. Y.

Ward, R. L. (1988). "Present status of managment and technical practices on alluvial fan areas in Arizona : State of the art." Arizona Department of Transportation, Final Report, *Report no. FHWA-AZ88-278*.

Weinmann, P. E., and Laurenson, E. M. (1979). "Approximate flood routing methods : A review." *Journal of the Hydraulics Division*, ASCE, 105(12), 1521-1536.